COASTAL WAVE PATTERNS IN THE HAWAIIAN ISLANDS IN RELATION TO SIGNIFICANT CLIMATE EVENTS

A THESIS SUBMITTED FOR PARTIAL FULFILLMENT OF THE REQUIREMENTS

FOR THE DEGREE OF

BACHELOR OF SCIENCE

IN

GLOBAL ENVIRONMENTAL SCIENCE

DECEMBER 2021

By

Olivia Makai Hughes

Thesis Advisor

Margaret Anne McManus

I certify that I have read this thesis and that, in my opinion, it is satisfactory in scope and quality as a thesis for the degree of Bachelor of Science in Global Environmental Science

THESIS ADVISOR

Margaret Anne McManus

Department of Oceanography

ACKNOWLEDGEMENTS

For, Kimball Millikan, Andreia Quiema, and Christina Comfort, for teaching and advising me as a member of the PacIOOS team for four years. And for my family who always encouraged me to persevere through everything.

ABSTRACT

The Pacific Islands Ocean Observing System (PacIOOS) collects valuable information for recreational ocean users, researchers, industry partners, and ocean managers. Researchers at PacIOOS maintain a network of wave buoys across the Pacific Ocean - ten of which are deployed throughout the waters of the Hawaiian Islands. Waverider buoys measure five wave parameters: significant wave height, peak wave period, peak wave direction, average wave period, and temperature.

Each wavebuoy recorded waves incoming from consistent directions all year, with the exception of the Pearl Harbor buoy. In this contributions seasons are described as Kau and Hoʻoilo. Kau, the hot and dry season, runs from May to October, and Hoʻoilo, the cool and rainy season, runs from November to April. Data from the north shore buoys revealed a seasonal shift of direction for the majority of waves, occurring more frequently from the north during the winter months of Ho`oilo. The majority of waves occurred from a wider range of directions during the summer months of Kau.

The Mokapu, Waimea, Pauwela, and Kaneohe buoys all recorded a maximum sea surface temperature within the first two weeks of September 2015. These trends in sea surface temperature coincide with the El Niño event of 2015-2016. These elevated temperatures may also be the effect of a marine heat wave, as 2015 was also known to have multiple marine heat waves across the globe.

The Waimea, Pauwela, Barber's Point, and Lanai buoys all recorded their maximum wave height on February 11, 2019. This is due to a large weather system that affected areas from northwest America to the Hawaiian Islands.

The analysis shows that the data collected by PacIOOS wavebuoys reflects significant climate events and large storm systems. Continuing to observe and catalog these data will allow us to predict future wave activity as our climate changes and during storm events. This enhanced understanding will allow the public to be informed on how waves will impact their daily activities. Ultimately, the value of these data will increase with time as more data are collected.

TABLE OF CONTENTS

LIST OF TABLES

LIST OF FIGURES

INTRODUCTION

The Pacific Islands Ocean Observing System (https://www.pacioos.hawaii.edu) collects real-time data on ocean conditions and forecasts future events through modeling studies, as a part of their mission to make ocean data available and easily accessible to recreational ocean users, researchers, industry partners, and ocean managers.

The ocean has always been central to life in Hawai‘i, whether for resources, navigation, or recreation, and has been the subject of extensive scientific research. The long term measurements of waves in Hawai’i’s coastal waters are a critical resource for understanding how the ocean waves respond to storm events, and how waves may behave in the future as a consequence of global climate change. The Hawai’ian Islands are experiencing sea level rise. As the sea level rises, the coastline will be more vulnerable to coastal waves. It is predicted that the damage from waves will be most extensive in areas facing accelerated coastal erosion, such as hotels and other privately-owned shoreline properties that have built seawalls and other hardened shoreline structures (Fletcher et al. 2003).

An understanding of the response of waves to climate fluctuations and storm systems in the Hawaiian Islands will allow our community to better prepare for potential impacts. The measurements from the PacIOOS buoys have the historical and real-time information about what directions waves are coming from and when waves are typically higher in amplitude or energy. Moreover, these data are the starting point for calculating wave refraction, steering, reflection, breaking depth and surf height as the waves move toward shore. Long-term data on Hawaiian waves are critical information for researchers who forecast future wave conditions for Hawai‘i. PacIOOS has teams of people already making these forecasts publicly available online. This information allows the community to prepare for the impacts waves will have on the coastlines.

METHODS

Researchers at PacIOOS maintain a network of wave buoys across the Pacific Ocean; ten deployed throughout the Hawaiian Island waters, two deployed at Guam, and one deployed at Saipan, Majuro, and American Sāmoa, respectively. The focus of this report will be on data from all Hawai`i deployed PacIOOS buoys, excluding the Kaneohe WETS Waverider Buoy (225), which is in close proximity to Kaneohe Bay Waverider Buoy (198). The PacIOOS buoys are moored offshore at nine locations between ~2 and 11 km from shore in water depths between ~30 and 350 m; the coordinates of each of these buoys are provided in Table 1.

Waverider buoys measure wave parameters: Significant wave height (H_s) in m, peak wave period (T_p) in s, peak wave direction (D_p) in degrees, average wave period (T_a) in s, and temperature in °C. These wave buoys collect data every 0.78 seconds, which is then averaged over 30 minutes. The Coastal Data Information Program (CDIP) of Scripps Institution of Oceanography at the University of California San Diego reports data based on the beginning of the data acquisition period. These data sets are made publicly available on the PacIOOS website in increments of up to 30 days (https://www.pacioos.hawaii.edu). Long-term data are archived and publicly available on the CDIP website (https://cdip.ucsd.edu/m/).

Table 1: Table of Buoy location, number, and coordinates as of 7/25/2021.

Buoy Location Hawai'i	Buoy Number	Latitude	Longitude
Mokapu, O'ahu	098	21° 24.85'	-157° 40.73'
Waimea Bay, O'ahu	106	21° 40.23'	-158° 7.03'
Pauwela, Maui	187	21° 1.17'	-156° 25.63'
Hilo, Hawai'i	188	19° 46.89'	-154° 58.08'
Kaneohe Bay, O'ahu	198	21° 28.62'	-157° 45.36'
Hanalei, Kauai	202	20° 45.01'	-157° 0.21'
Pearl Harbor, O'ahu	233	21° 17.84'	-157° 57.54'
Barber's Point, O'ahu	238	21° 19.40'	-158° 8.98'
Lanai Southwest	239	20° 45.01'	-157° 0.21'

Waverider Wavebuoy

The hull of the Waverider wavebuoy holds a ring of batteries surrounding an aluminum can, which houses the motion sensors and water temperature sensor. The motion sensors include a stable platform with a vertical accelerometer (A_v), two horizontal accelerometers (A_x and A_y), a three-axial fluxgate compass (H_x, H_y, and H_z), and two pick-up coils on the platforms inside and outside of the vertical accelerometer sphere that measure wave pitch and roll (Datawell BV 2009) (Figures 1 and 2).

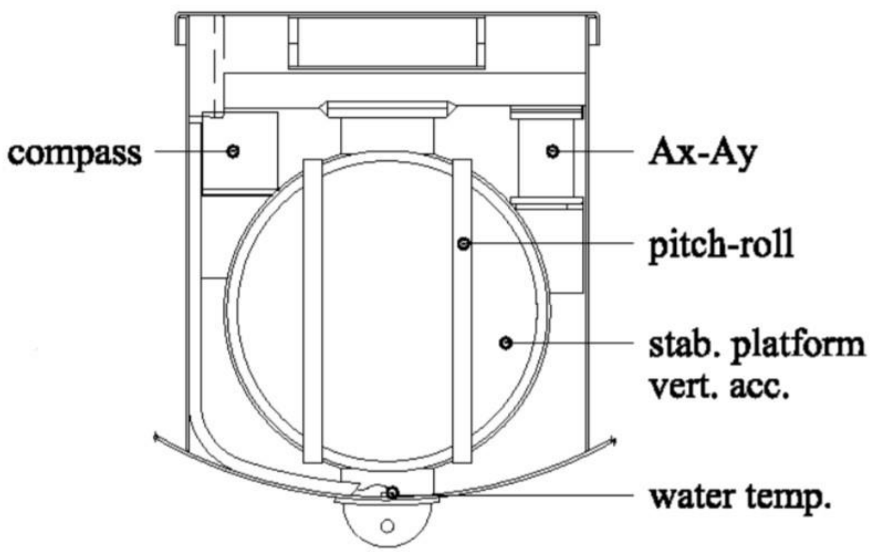

Figure 1: Contents of the aluminum can housing the waverider buoy instruments (Figure from Datawell BV 2009).

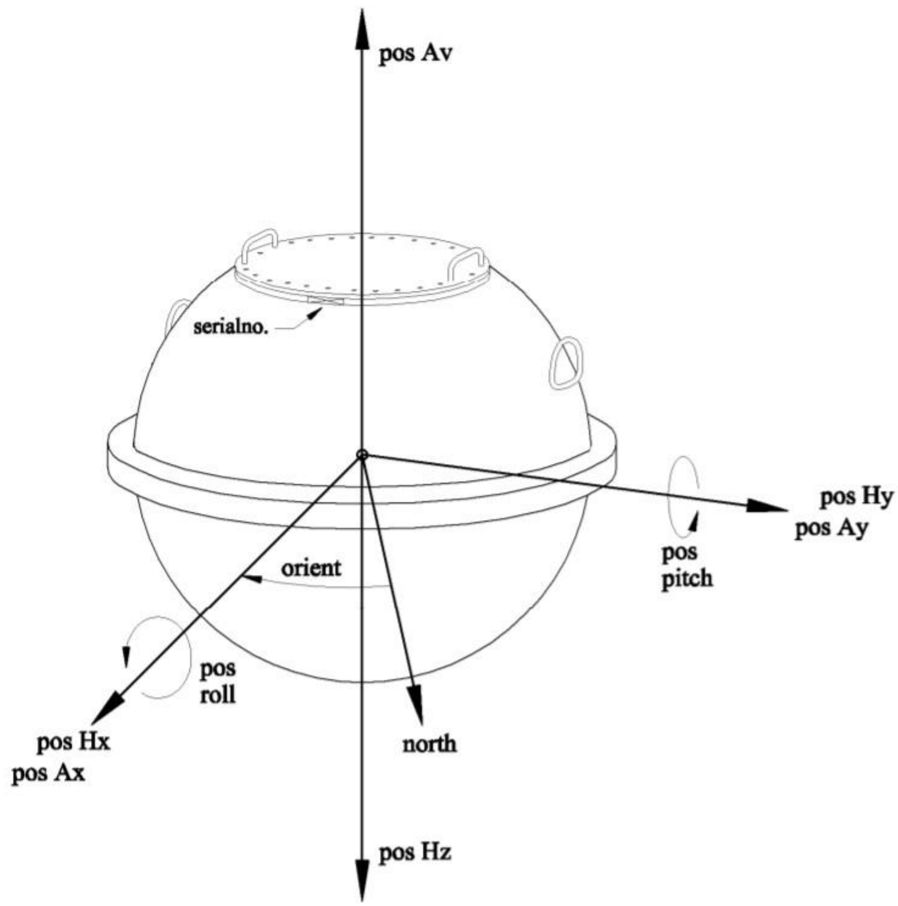

Figure 2: Schematic of the buoy hull with definitions of the axes and signs of the waverider buoy motion sensors (Figure from Datawell BV 2009).

Waverider Wavebuoy Mooring

Wavebuoys have a standard mooring setup with cord and line lengths that may vary depending on seafloor depth at the deployment site of the buoy. From bottom to top, the mooring starts with an anchor weight on the sea floor that is typically made of scrap chain. This is attached to a chain and then a nylon line approximately three m long that connect to an acoustic release. The acoustic release is utilized in order to recover and re-use as much of the mooring as possible to minimize ocean waste. The top of the acoustic release is attached to a long high modulus polyethylene fiber (HMPE) line (at least 100 m). At the bottom of this line is at least one small inline trawl float in order to keep the first few meters of the mooring clear of the seabed. For deeper seafloor depths, a 1.5 kg sinker weight is needed for the HMPE line to keep clear of the sea surface. The HMPE line is connected to a 30 m long rubber cord, 35 mm in diameter. Finally, the rubber cord is attached to a short HMPE line, with a swivel attached to the other end. This swivel connects the rest of the wavebuoy mooring with a stabilizing chain on the bottom center point of the buoy hull. By design, the mooring force acts on the pivotal point of the wavebuoy, and in this way, do not affect the tilt of the buoy (Datawell BV 2009).

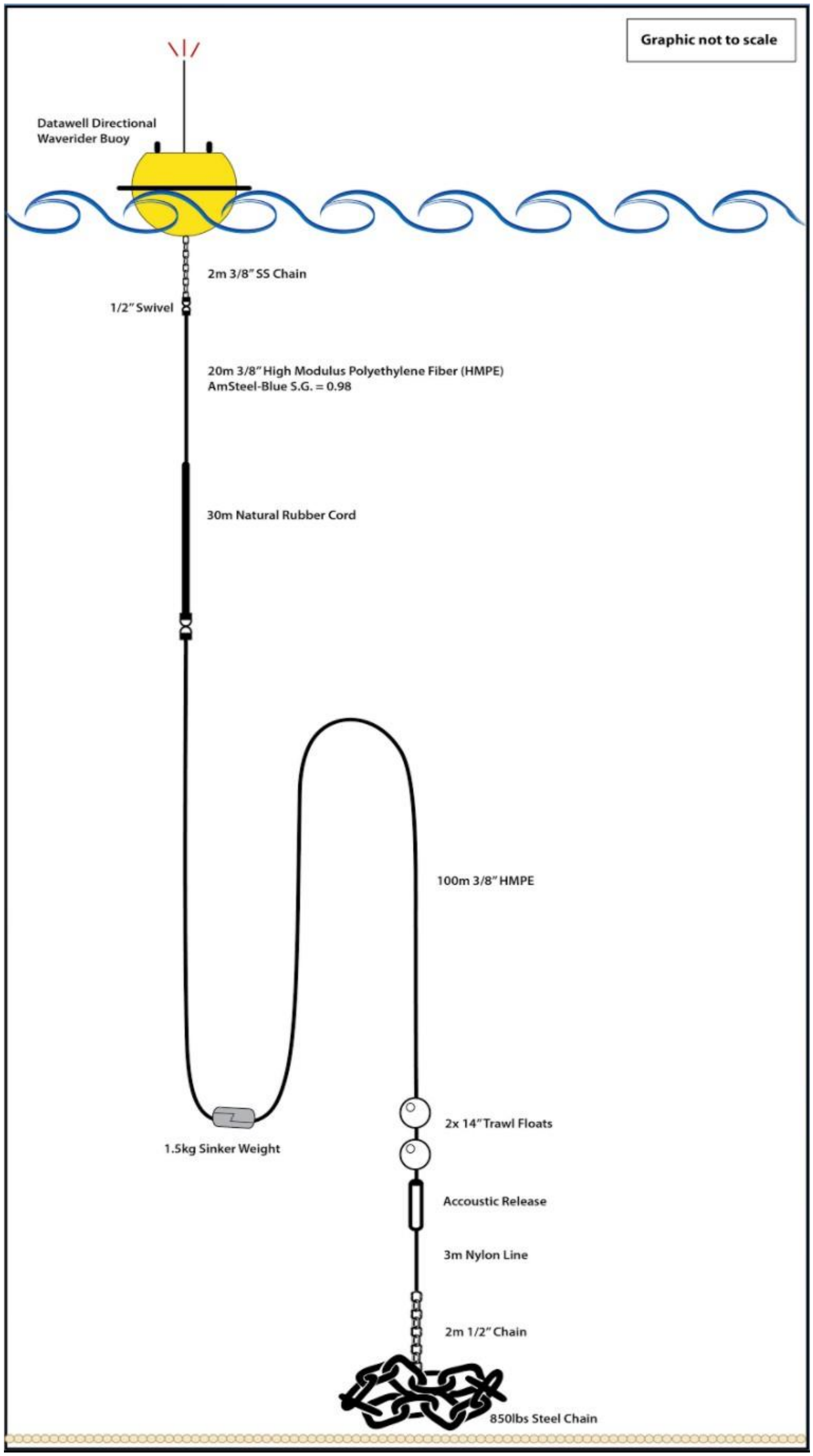

Figure 3: Schematic drawing of wavebuoy mooring. Figure courtesy of Kimball Millikan.

Waverider Wavebuoy Measurements

Significant wave height (H_s or $H_{1/3}$) is defined traditionally as the mean wave height (trough to crest) of the highest 1/3 (or 33%) of all waves passing a particular point. Significant wave height (H_s) is commonly used as a measure of the height of ocean waves. However, it is critical to note that all wave groups in the ocean consist of an entire spectrum of wave heights: significant wave height (H_s) is only part of this spectrum. A wave forecast focused only on significant wave height (H_s) may not account for much larger waves naturally occurring within the entire swell event (i.e. wave group). Wave height measurements have an accuracy of 1cm.

Peak wave direction (D_p) refers to the direction from which the dominant sea surface waves are travelling. This variable is associated with only the highest waves in the total wave spectrum over a sample period. Wave direction is expressed in compass degrees from True North. 0° indicates waves coming directly from the north, 90° are waves coming from the east, 180° are waves from the south, 270° are waves from the west, and 360° are again waves coming from the north. Wave direction measurements have an accuracy of 1.5°.

Peak wave period (T_p) is defined as the duration in seconds between the arrival of the highest energy sea surface waves in the total wave spectrum over a sample period. One period is the duration of time for one full wavelength to pass the buoy site (i.e., crest to crest). In contrast, average wave period (T_a) is defined as the duration in seconds between the arrival of the mean sea surface waves, or waves of average energy levels, over a sample period. Generally, areas dominated by "wind waves" have shorter wave periods, while areas dominated by ocean swell have longer wave periods. Wind waves are locally-formed waves generated by wind and swell are waves created by large storms distant from the observation site. Swell exhibits more regular and longer periods.

Sea surface temperature is defined as the temperature of the sea surface water in degrees Celcius, with an accuracy of 0.2°C.

Wavebuoy Locations and Duration of Deployments

A map of buoy locations with their respective buoy numbers and locations is given in Figure 4, and a timeline of all buoy data illustrating the availability of data for each respective buoy is given in Figure 5.

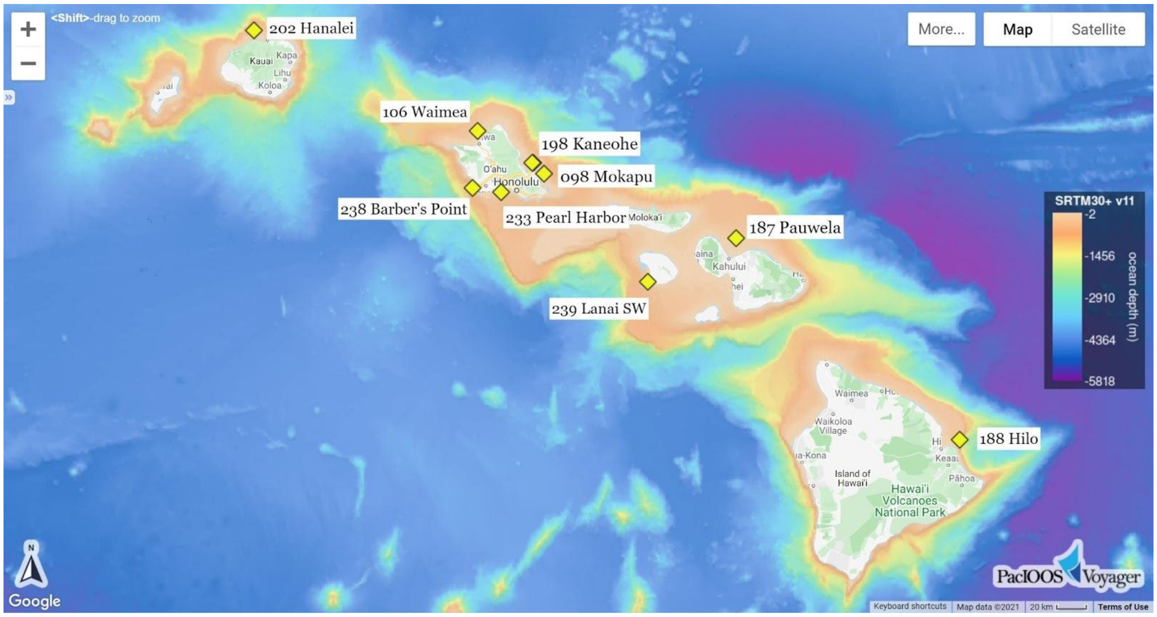

Figure 4: Bathymetric map of wave buoy locations created with Voyager.

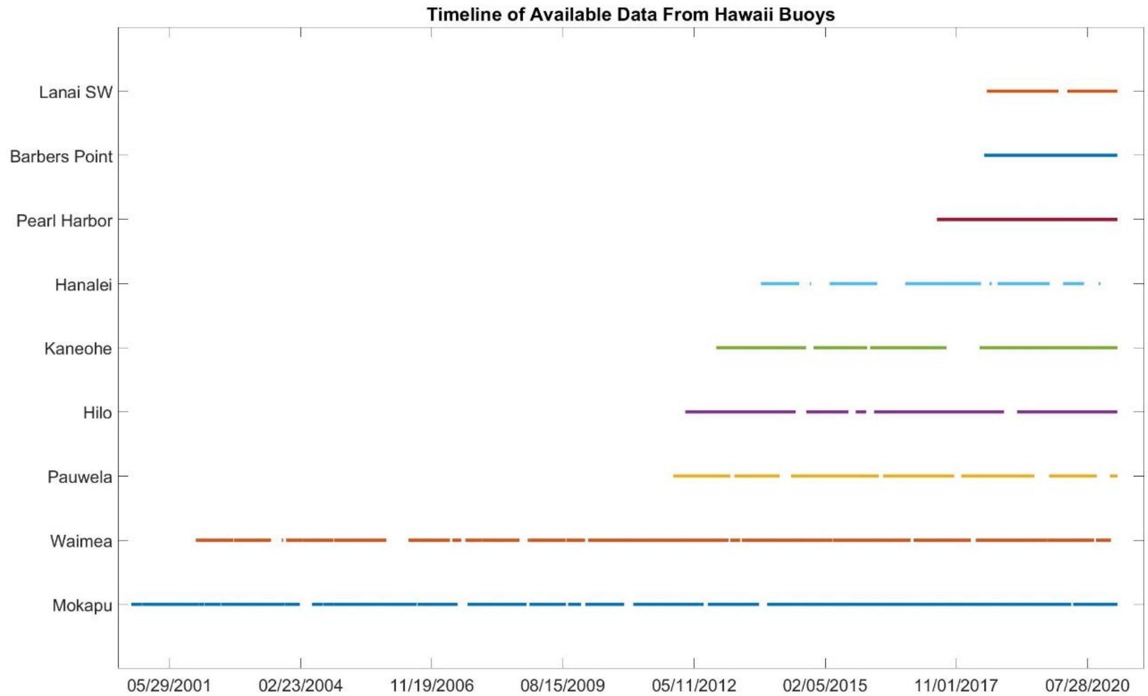

Figure 5: Deployment timeline for seven wave buoys deployed offshore of Hawai`i between 2001 and 2021.

Waverider Wavebuoy Analysis

For each wavebuoy, five plots were created using MATLAB: four time series plots of; surface water temperature (°C), peak wave period (T_p), average wave period (T_a), significant wave height (H_s), and one compass rose plot of peak wave direction (D_p) vs. Significant wave height (H_s).

For the purpose of analyzing long-term sea surface temperature trends, a time-series plot of the mean temperature (°C) was created using Google Sheets for each wavebuoy. A time series plot of monthly mean wave height (m) was also created for each wavebuoy in Google Sheets. Finally, to analyze seasonal wave direction patterns, two histograms were created for each wavebuoy in MATLAB of wave direction in compass degrees versus wave frequency.

When considering seasonality, the traditional Hawai`ian seasons of Kau and Ho`oilo were used to more accurately describe changes in wave patterns (Fletcher et al. 2003). The Ho`oilo months of November through April are the cool and wet season, and are dominated by high winter swell generated by severe storms in the North Pacific and mid-latitude low-pressure areas. The Kau months of May to October are the hot and dry season, and are dominated by southern swell caused by storms in the southern hemisphere (Fletcher et al. 2003).

To analyze seasonal patterns in peak wave direction, two histograms (one fore Kau and one for Hoʻoilo) were plotted for each buoy of direction vs. frequency of waves that occurred.

In order to analyze seasonal patterns in significant wave height, the average value was calculated for each month of data collected, and plotted in a time series plot for each wave buoy.

RESULTS

Waverider Buoy Figures:

The following section of this thesis shows the five plots created in MATLAB of total data collected for each respective buoy. Four time series plots of; surface water temperature (°C), peak wave period (T_p), average wave period (T_a), significant wave height (H_s), and one compass rose plot of peak wave direction (D_p) vs. Significant wave height (H_s).

Mokapu Waverider Buoy 098

The following figures are the five plots created in MATLAB of total data collected for the Mokapu, O‘ahu Waverider Buoy (098). Four time series plots of; surface water temperature (°C) (Figure 6), peak wave period (T_p) (Figure 7), average wave period (T_a) (Figure 8), significant wave height (H_s) (Figure 9), and the compass rose plot of peak wave direction (D_p) vs. Significant wave height (H_s) (Figure 10).

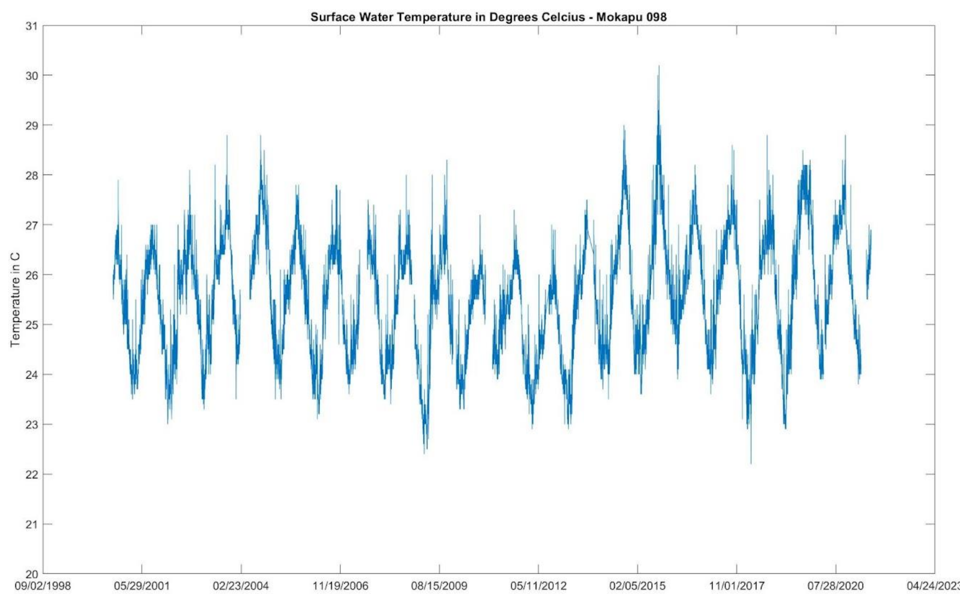

Figure 6: Surface water temperature (°C) vs. time at Mokapu Buoy 098

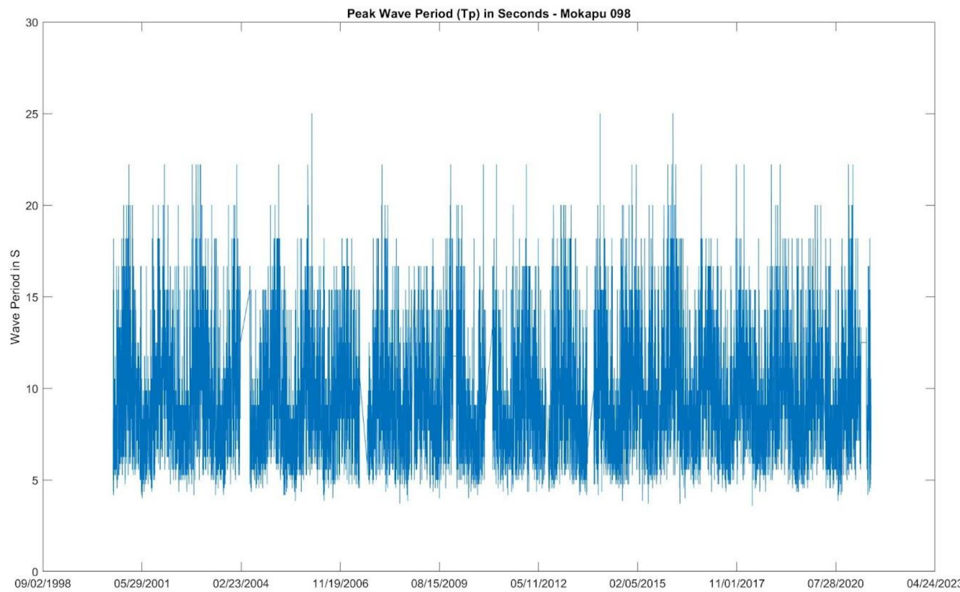

Figure 7: Peak wave period (s) vs. time at Mokapu Buoy 098

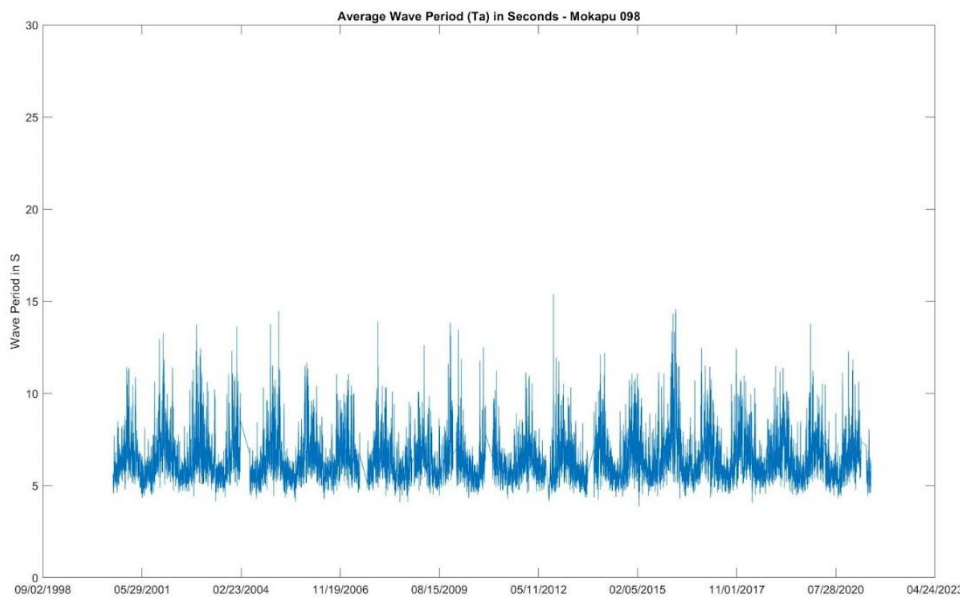

Figure 8: Average wave period (s) vs. time at Mokapu Buoy 098

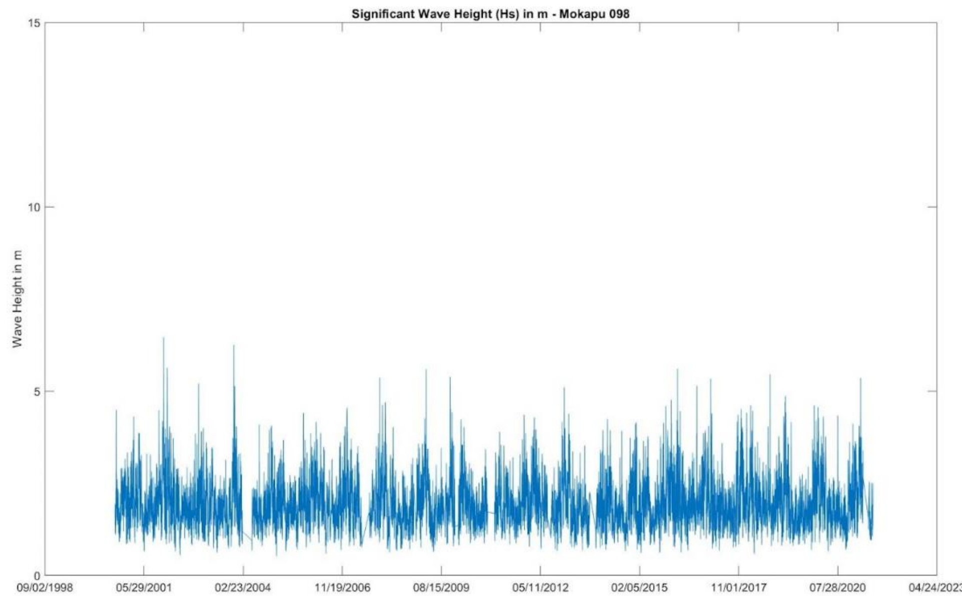

Figure 9: Significant wave height (Hs) (m) vs. time at Mokapu Buoy 098

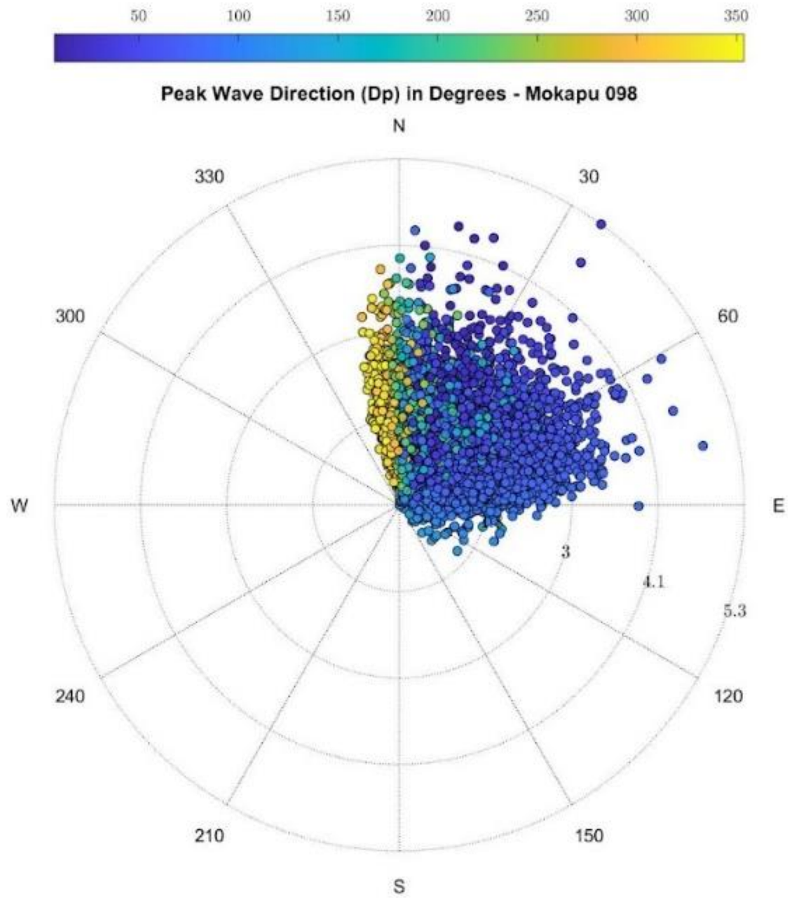

Figure 10: Peak wave direction (°) vs. significant wave height (Hs) (m) at Mokapu Buoy 098. Peak wave direction is the direction from which the waves at the dominant period are coming. The units are degrees from true north, increasing clockwise, with north as 0°, east as 90°, south as 180°, and west as 270°.

Waimea Waverider Buoy 106

The following figures are the five plots created in MATLAB of total data collected for the Waimea, O‘ahu Waverider Buoy (106). Four time series plots of; surface water temperature (°C) (Figure 11), peak wave period (T_p) (Figure 12), average wave period (T_a) (Figure 13), significant wave height (H_s) (Figure 14), and the compass rose plot of peak wave direction (D_p) vs. Significant wave height (H_s) (Figure 15).

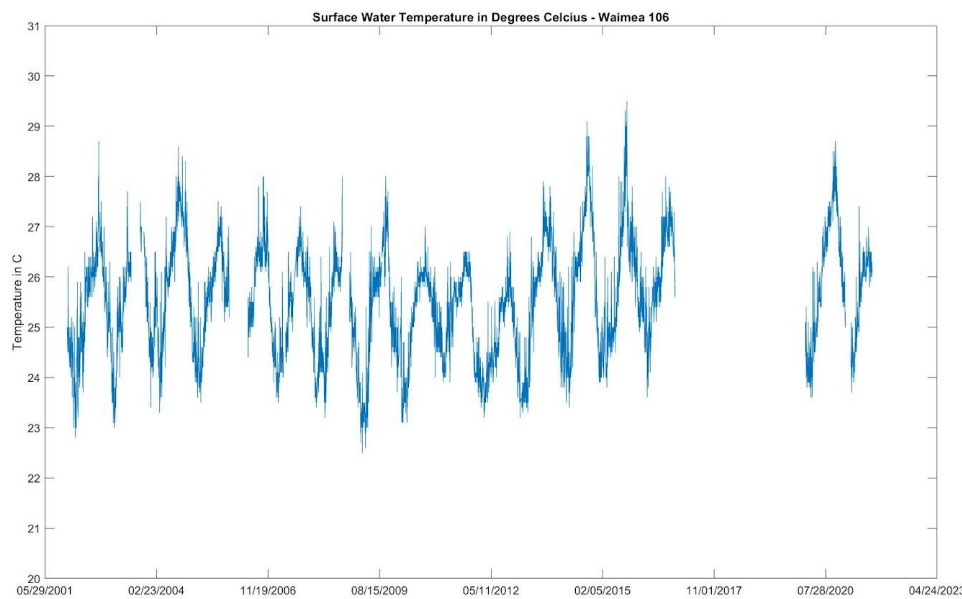

Figure 11: Surface water temperature (°C) vs. time at Waimea Buoy 106

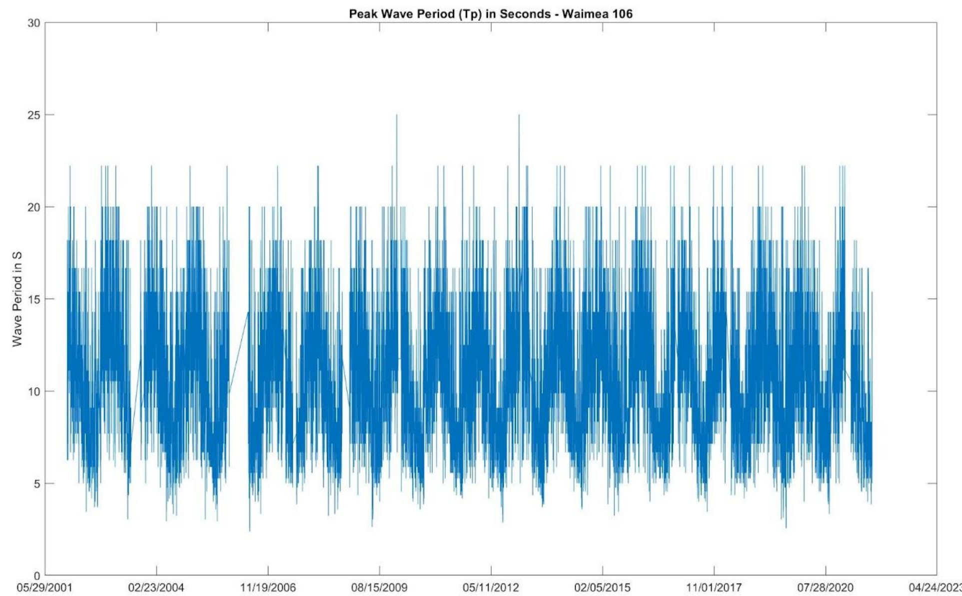

Figure 12: Peak wave period (s) vs. time at Waimea Buoy 106

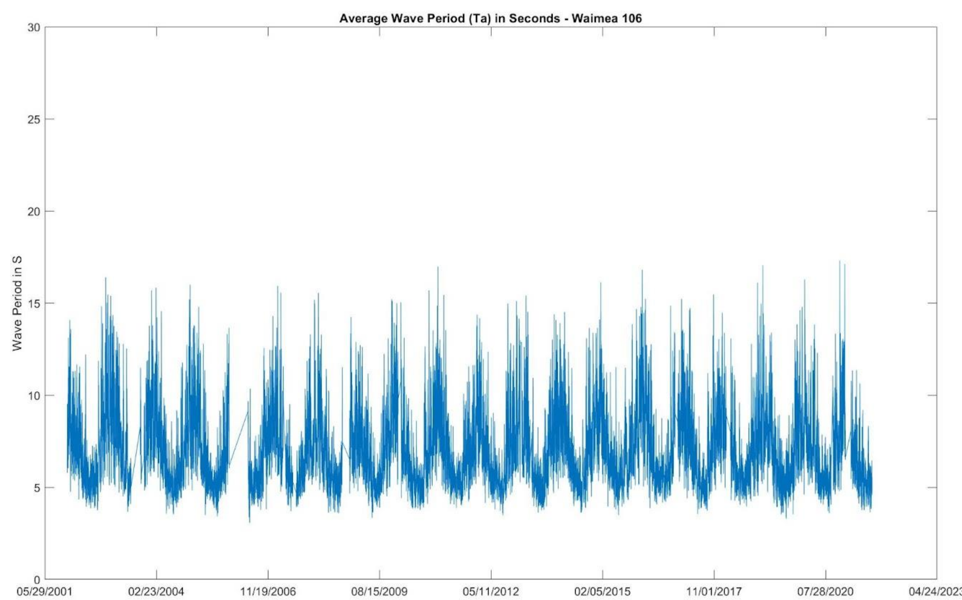

Figure 13: Average wave period (s) vs. time at Waimea Buoy 106

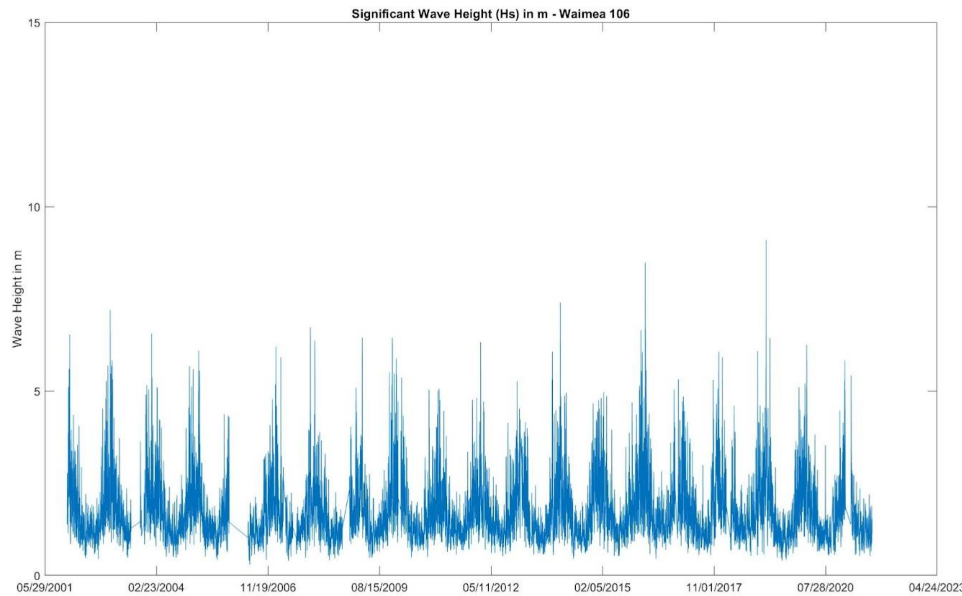

Figure 14: Significant wave height (Hs) (m) vs. time at Waimea Buoy 106

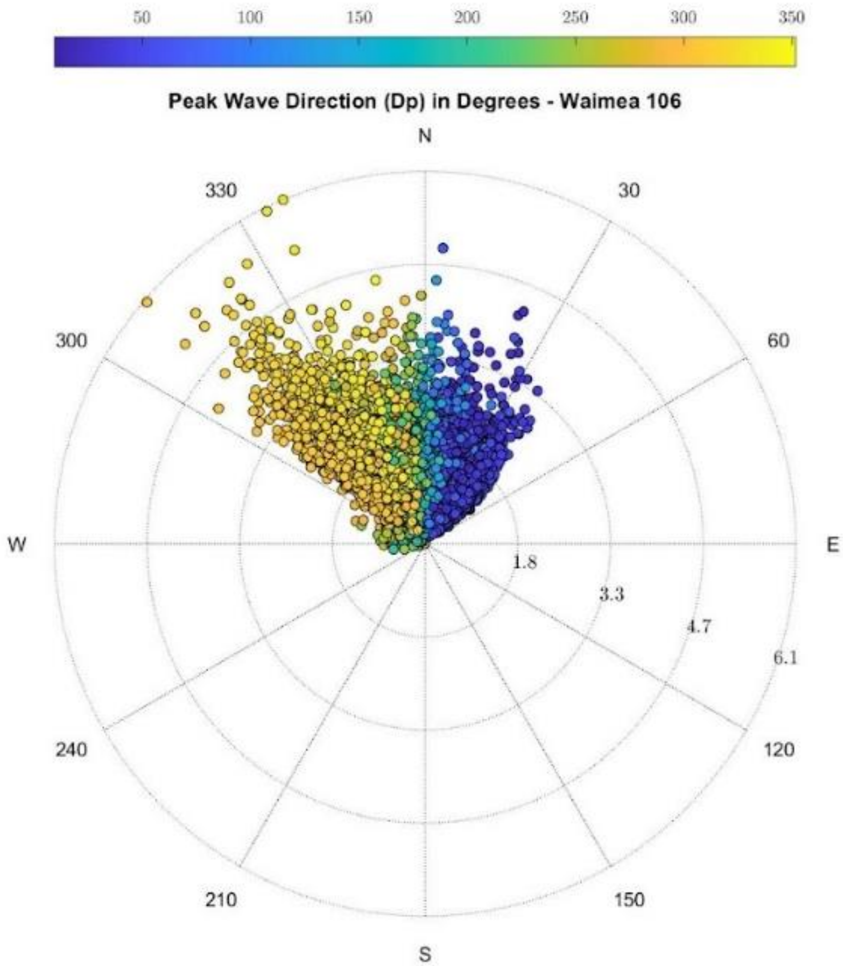

Figure 15: Peak wave direction (°) vs. significant wave height (Hs) (m) at Waimea Buoy 106. Peak wave direction is the direction from which the waves at the dominant period are coming. The units are degrees from true north, increasing clockwise, with north as 0°, east as 90°, south as 180°, and west as 270°.

Pauwela Waverider Buoy 187

The following figures are the five plots created in MATLAB of total data collected for the Pauwela, Maui Waverider Buoy (187). Four time series plots of; surface water temperature (°C) (Figure 16), peak wave period (T_p) (Figure 17), average wave period (T_a) (Figure 18), significant wave height (H_s) (Figure 19), and the compass rose plot of peak wave direction (D_p) vs. Significant wave height (H_s) (Figure 20).

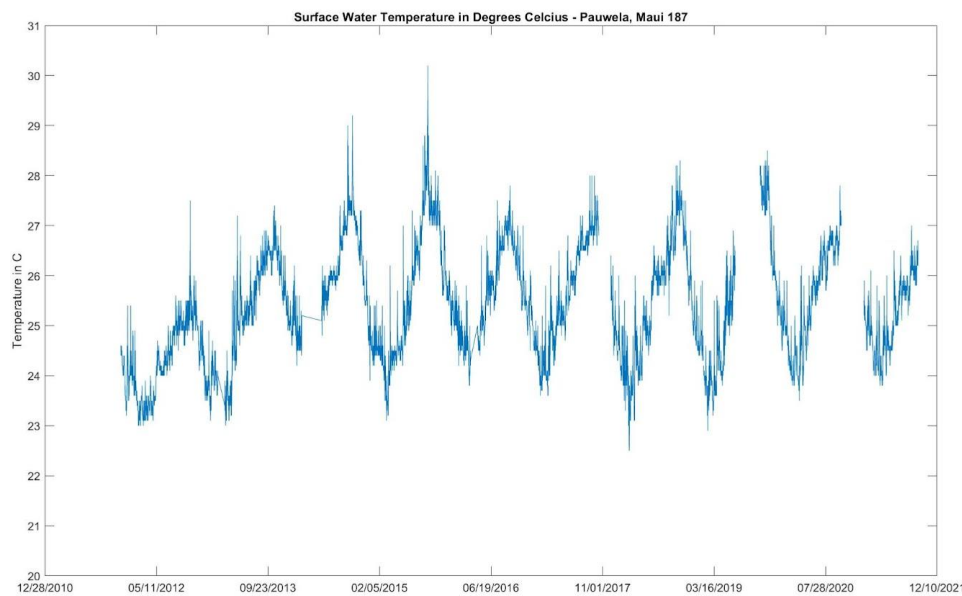

Figure 16: Surface water temperature (°C) vs. time at Pauwela Buoy 187

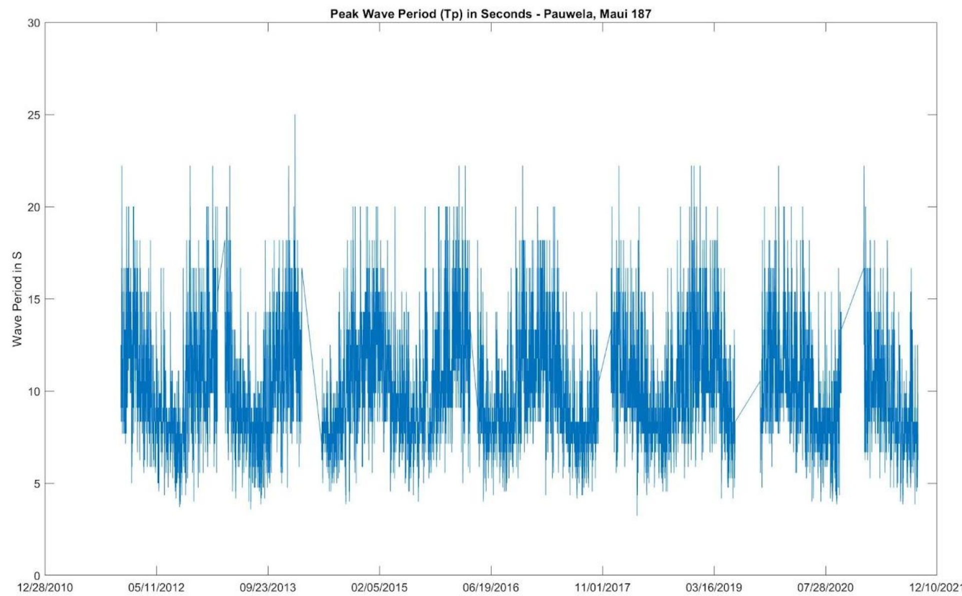

Figure 17: Peak wave period (s) vs. time at Pauwela Buoy 187

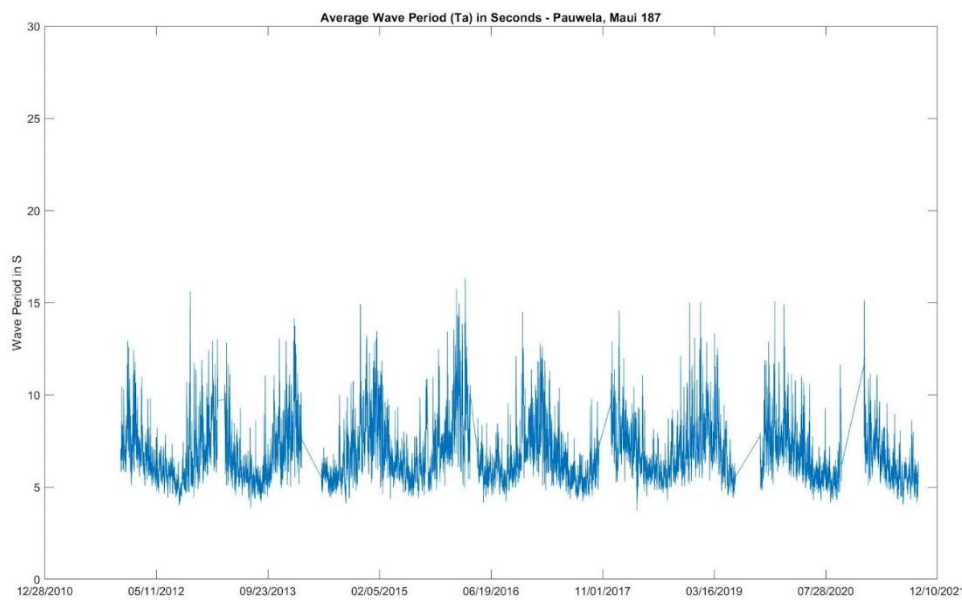

Figure 18: Average wave period (s) vs. time at Pauwela Buoy 187

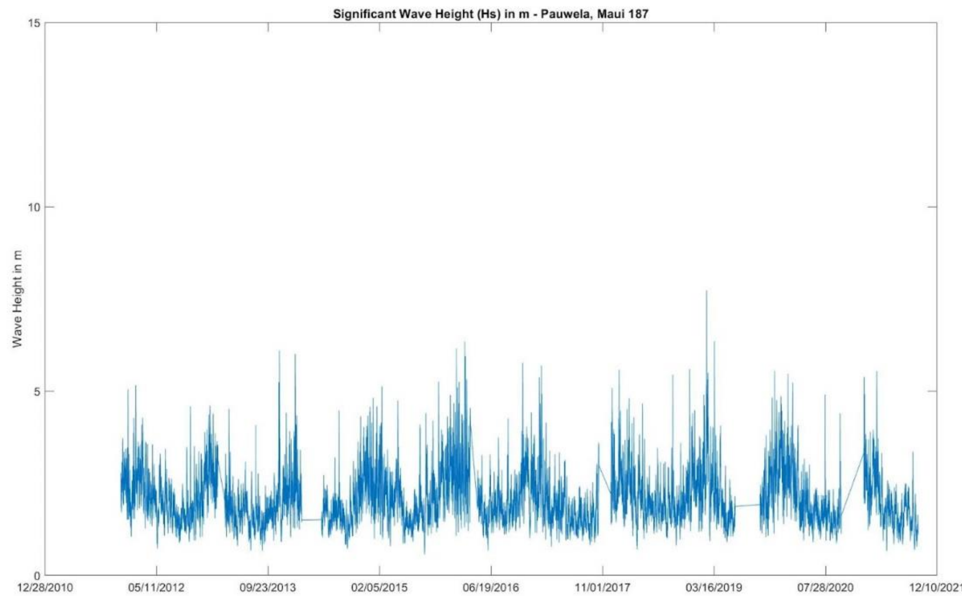

Figure 19: Significant wave height (Hs) (m) vs. time at Pauwela Buoy 187

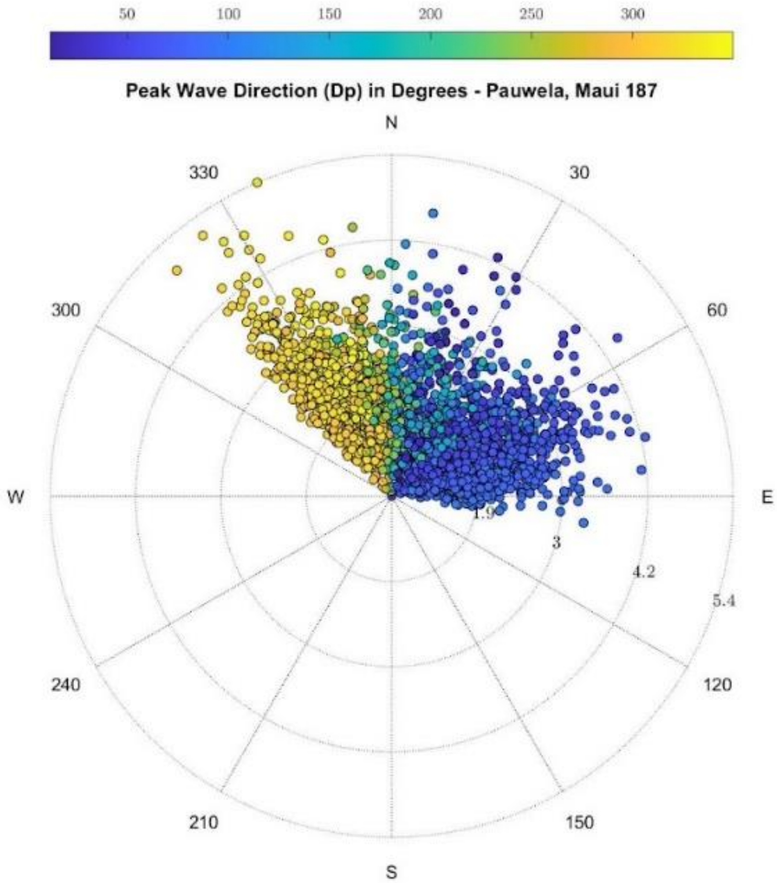

Figure 20: Peak wave direction (°) vs. significant wave height (Hs) (m) at Pauwela Buoy 187. Peak wave direction is the direction from which the waves at the dominant period are coming. The units are degrees from true north, increasing clockwise, with north as 0°, east as 90°, south as 180°, and west as 270°.

Hilo Waverider Buoy 188

The following figures are the five plots created in MATLAB of total data collected for the Hilo, Hawaiʻi Waverider Buoy (188). Four time series plots of; surface water temperature (°C) (Figure 21), peak wave period (T_p) (Figure 22), average wave period (T_a) (Figure 23), significant wave height (H_s) (Figure 24), and the compass rose plot of peak wave direction (D_p) vs. Significant wave height (H_s) (Figure 25).

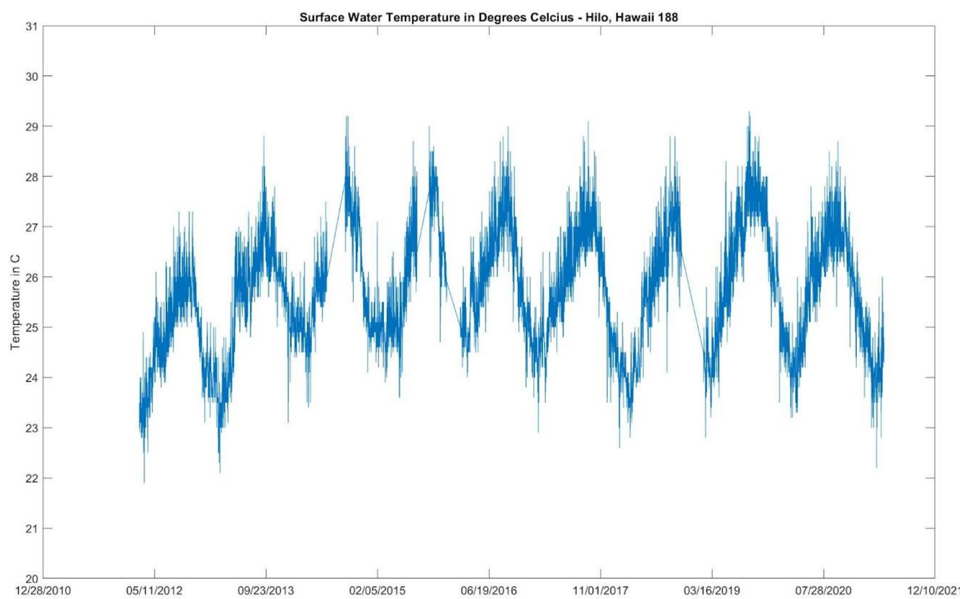

Figure 21: Surface water temperature (°C) vs. time at Hilo Buoy 188

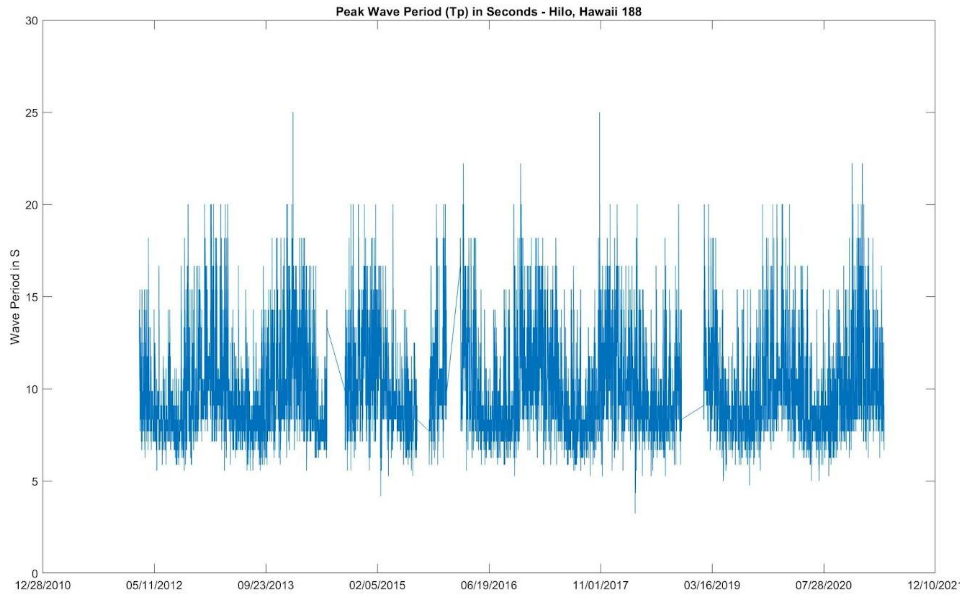

Figure 22: Peak wave period (s) vs. time at Hilo Buoy 188

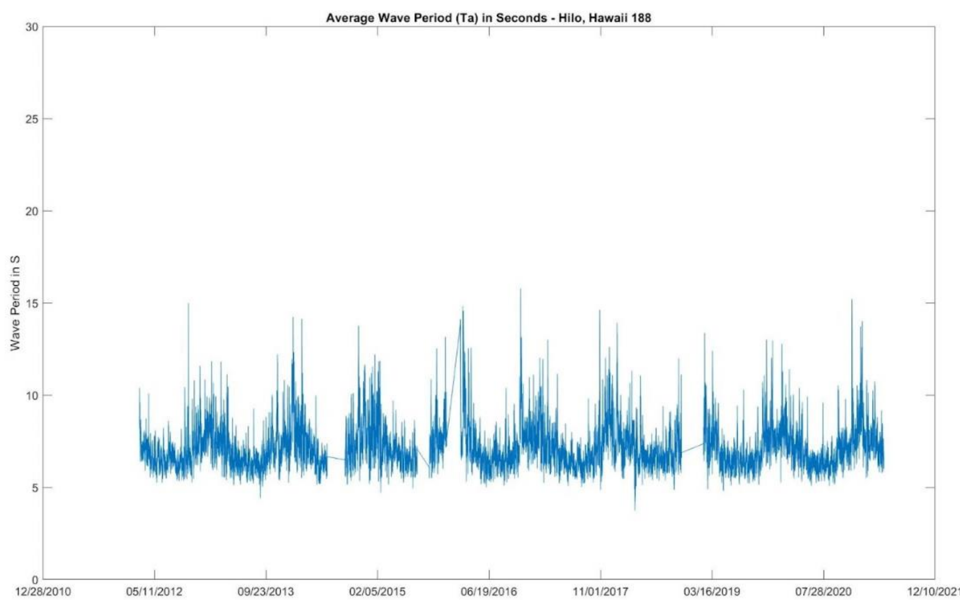

Figure 23: Average wave period (s) vs. time at Hilo Buoy 188

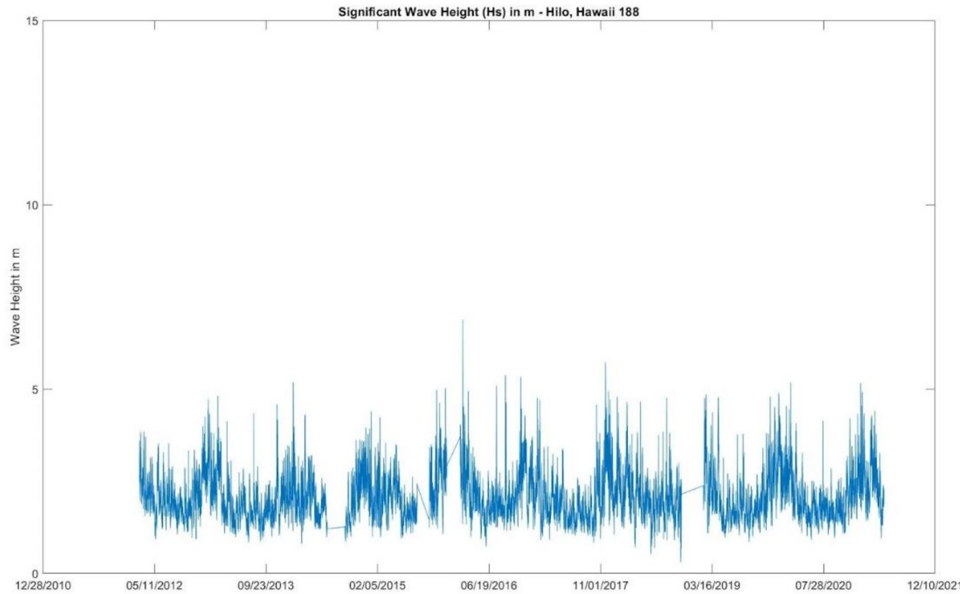

Figure 24: Significant wave height (Hs) (m) vs. time at Hilo Buoy 188

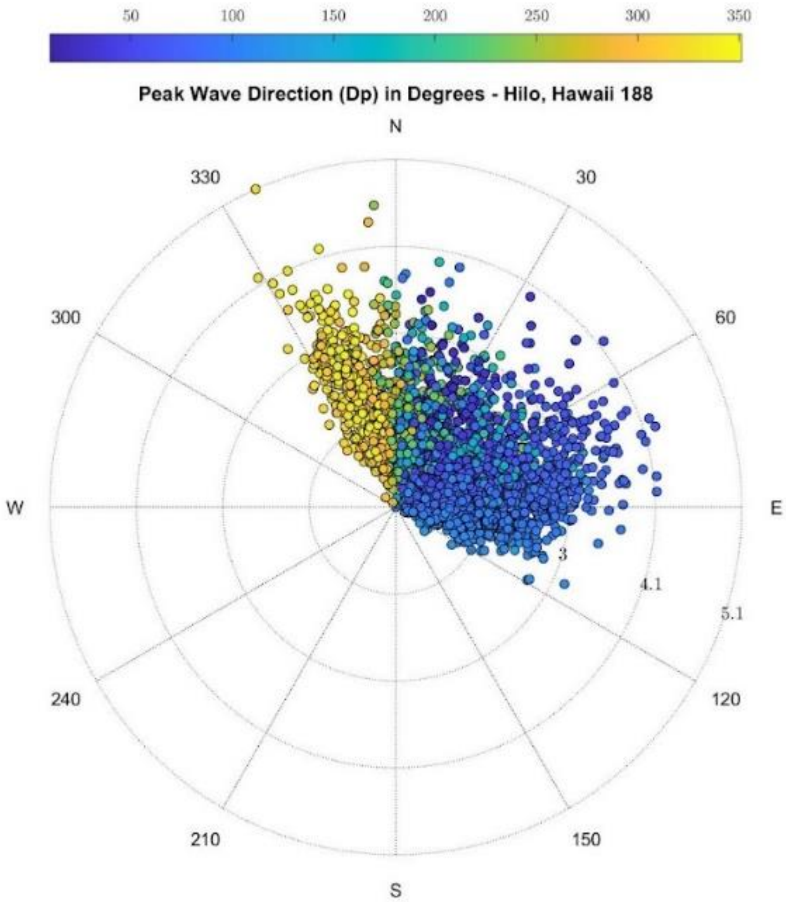

Figure 25: Peak wave direction (°) vs. significant wave height (Hs) (m) at Hilo Buoy 188. Peak wave direction is the direction from which the waves at the dominant period are coming. The units are degrees from true north, increasing clockwise, with north as 0°, east as 90°, south as 180°, and west as 270°.

Kaneohe Waverider Buoy 198

The following figures are the five plots created in MATLAB of total data collected for the Kaneohe Bay, Oʻahu Waverider Buoy (198). Four time series plots of; surface water temperature (°C) (Figure 26), peak wave period (T_p) (Figure 27), average wave period (T_a) (Figure 28), significant wave height (H_s) (Figure 29), and the compass rose plot of peak wave direction (D_p) vs. Significant wave height (H_s) (Figure 30).

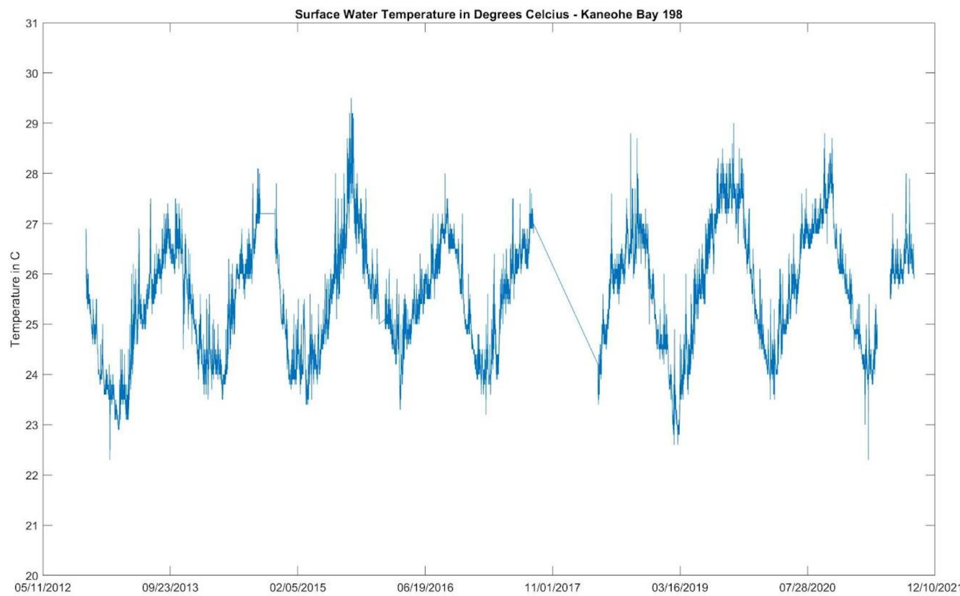

Figure 26: Surface water temperature (°C) vs. time at Kaneohe Buoy 198

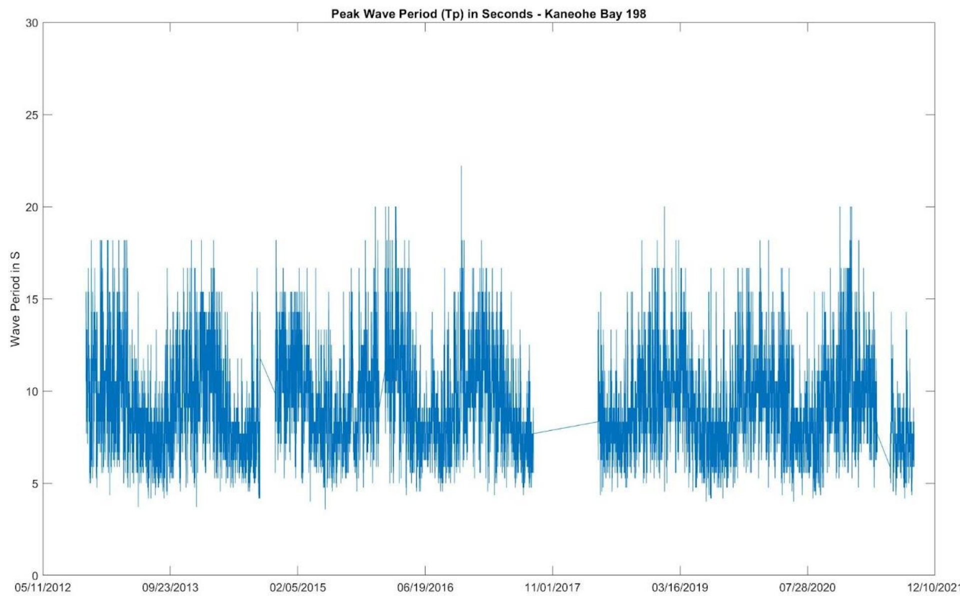

Figure 27: Peak wave period (s) vs. time at Kaneohe Buoy 198

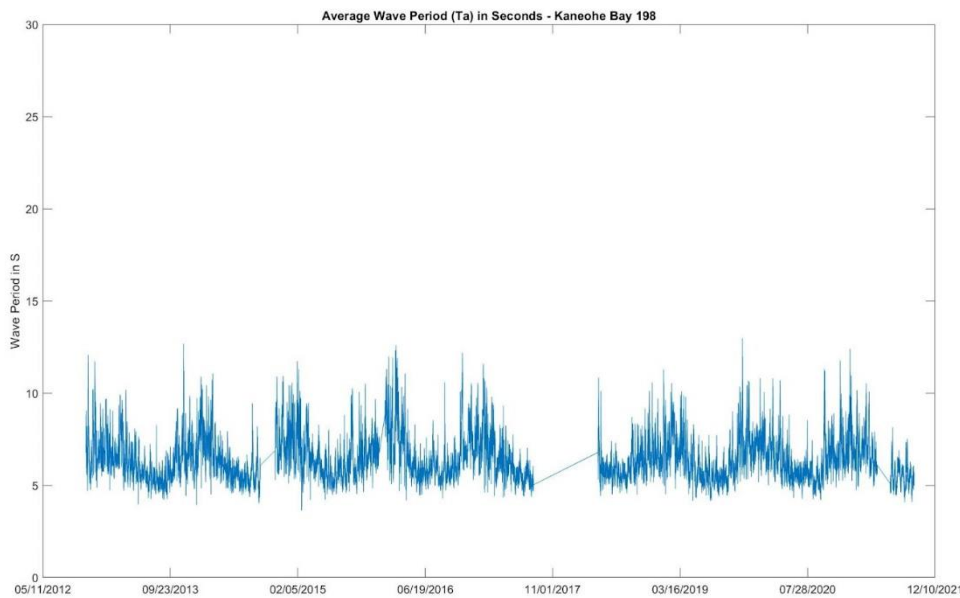

Figure 28: Average wave period (s) vs. time at Kaneohe Buoy 198

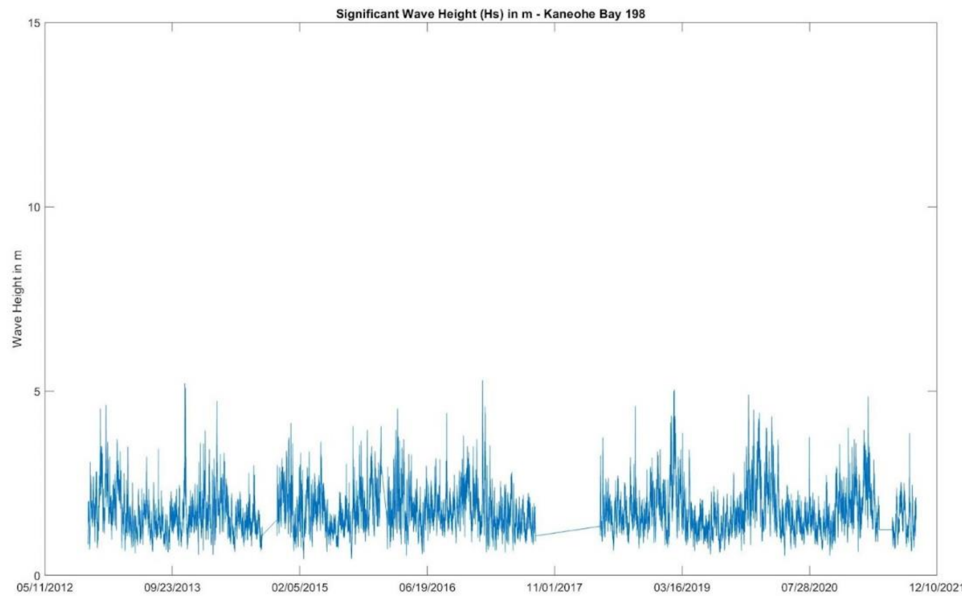

Figure 29: Significant wave height (Hs) (m) vs. time at Kaneohe Buoy 198

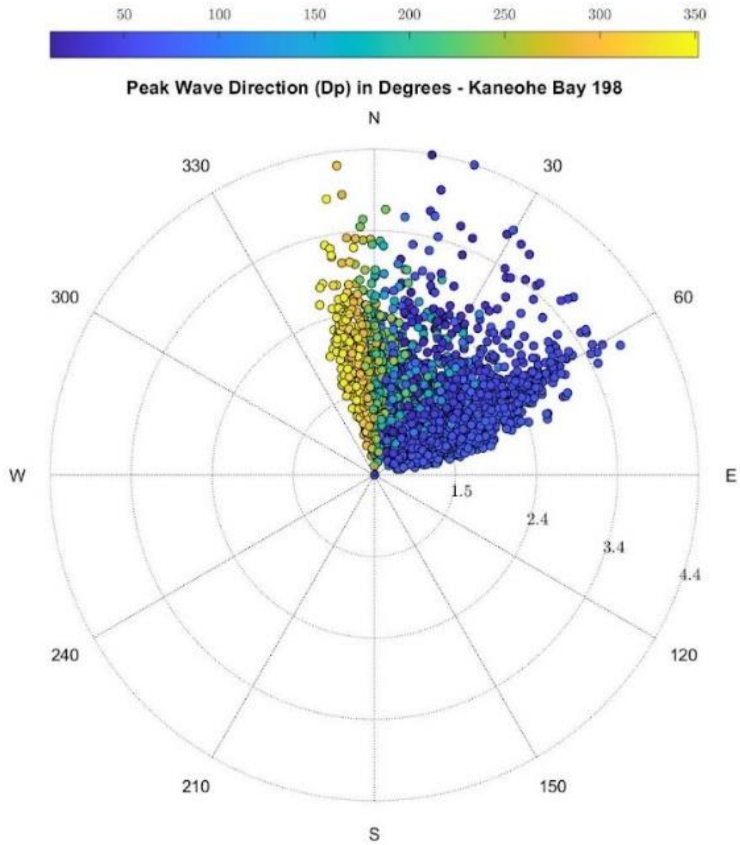

Figure 30: Peak wave direction (°) vs. significant wave height (Hs) (m) at Kaneohe Buoy 198. Peak wave direction is the direction from which the waves at the dominant period are coming. The units are degrees from true north, increasing clockwise, with north as 0°, east as 90°, south as 180°, and west as 270°.

Hanalei Waverider Buoy 202

The following figures are the five plots created in MATLAB of total data collected for the Hanalei, Kauai Waverider Buoy (202). Four time series plots of; surface water temperature (°C) (Figure 31), peak wave period (T_p) (Figure 32), average wave period (T_a) (Figure 33), significant wave height (H_s) (Figure 34), and the compass rose plot of peak wave direction (D_p) vs. Significant wave height (H_s) (Figure 35).

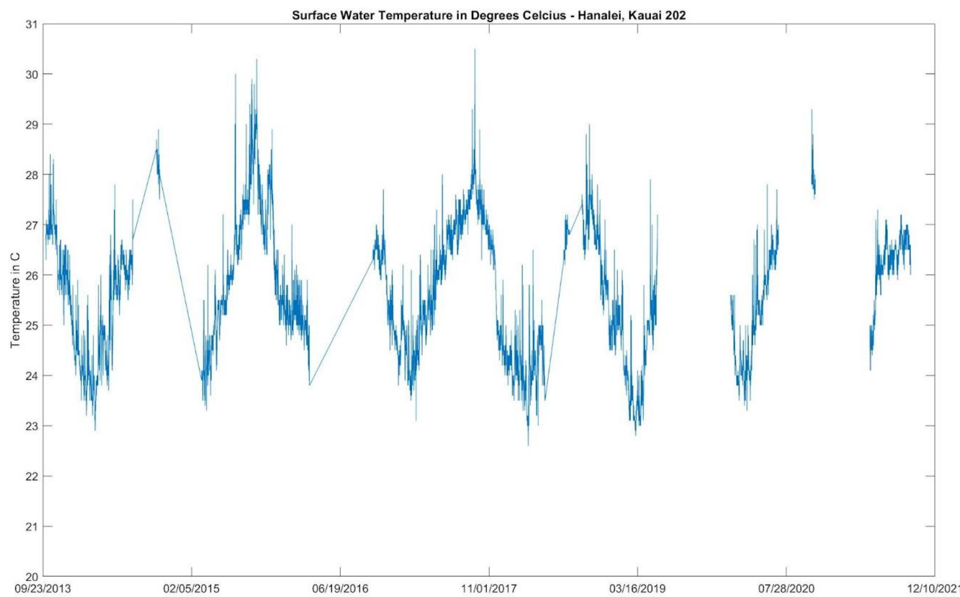

Figure 31: Surface water temperature (°C) vs. time at Hanalei Buoy 202

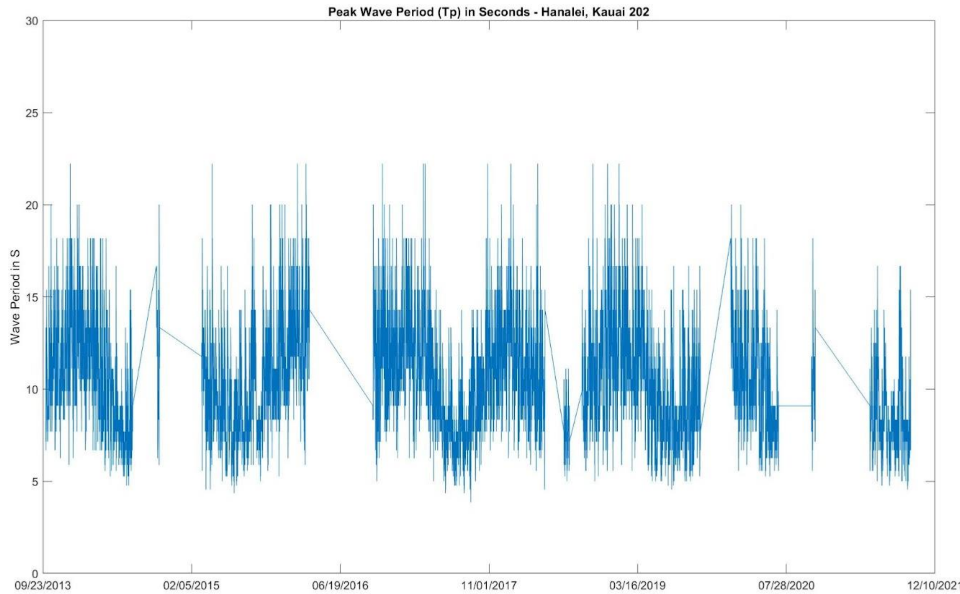

Figure 32: Peak wave period (s) vs. time at Hanalei Buoy 202

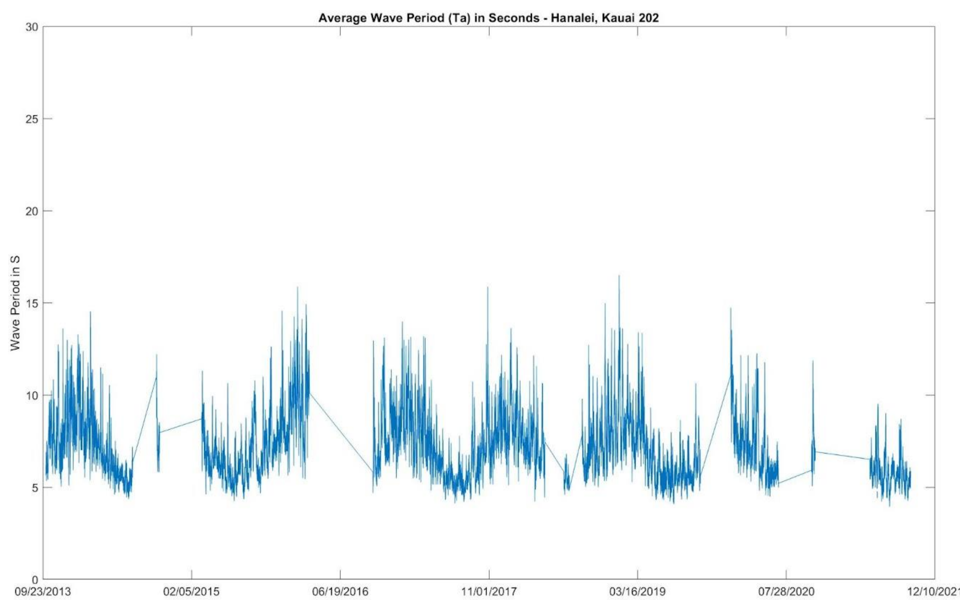

Figure 33: Average wave period (s) vs. time at Hanalei Buoy 202

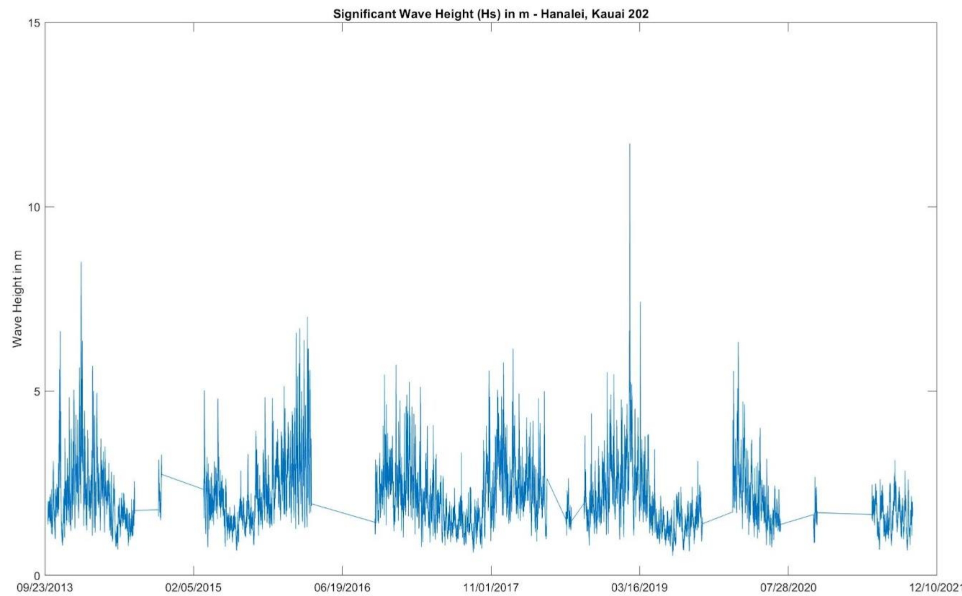

Figure 34: Significant wave height (Hs) (m) vs. time at Hanalei Buoy 202

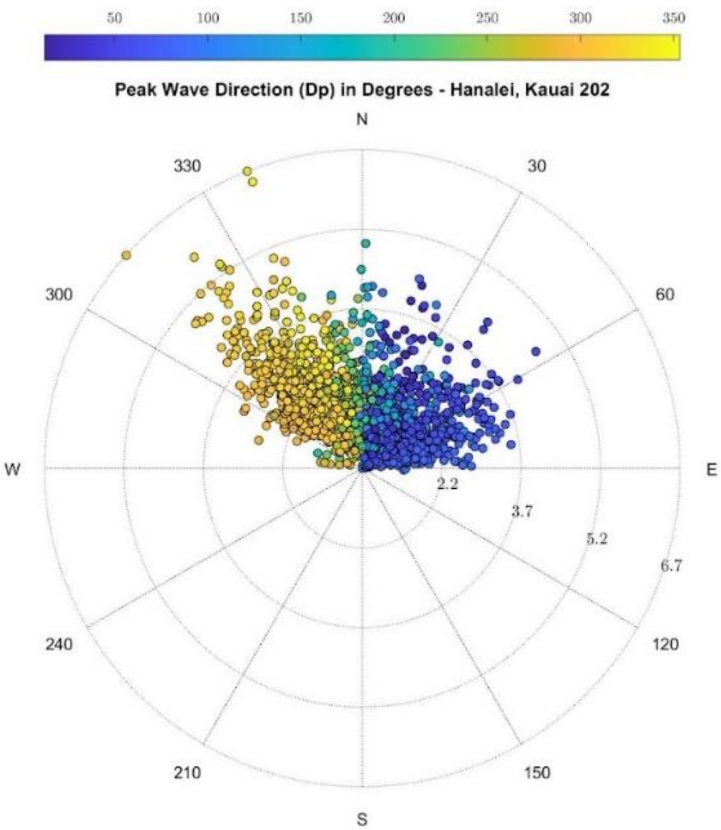

Figure 35: Peak wave direction (°) vs. significant wave height (Hs) (m) at Hanalei Buoy 202. Peak wave direction is the direction from which the waves at the dominant period are coming. The units are degrees from true north, increasing clockwise, with north as 0°, east as 90°, south as 180°, and west as 270°.

Pearl Harbor Waverider Buoy 233

The following figures are the five plots created in MATLAB of total data collected for the Pearl Harbor, Oʻahu Waverider Buoy (233). Four time series plots of; surface water temperature (°C) (Figure 36), peak wave period (T_p) (Figure 37), average wave period (T_a) (Figure 38), significant wave height (H_s) (Figure 39), and the compass rose plot of peak wave direction (D_p) vs. Significant wave height (H_s) (Figure 40).

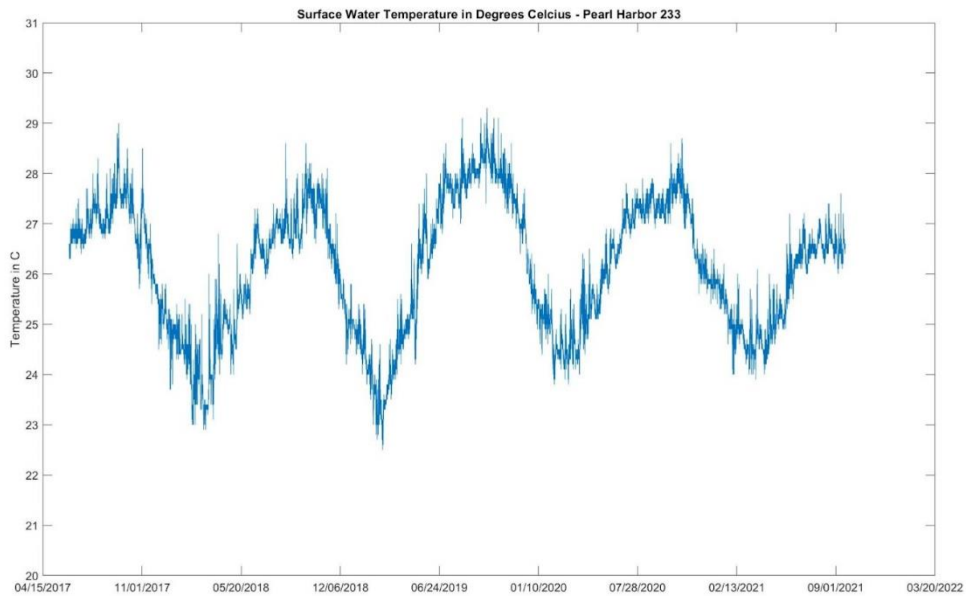

Figure 36: Surface water temperature (°C) vs. time at Pearl Harbor Buoy 233

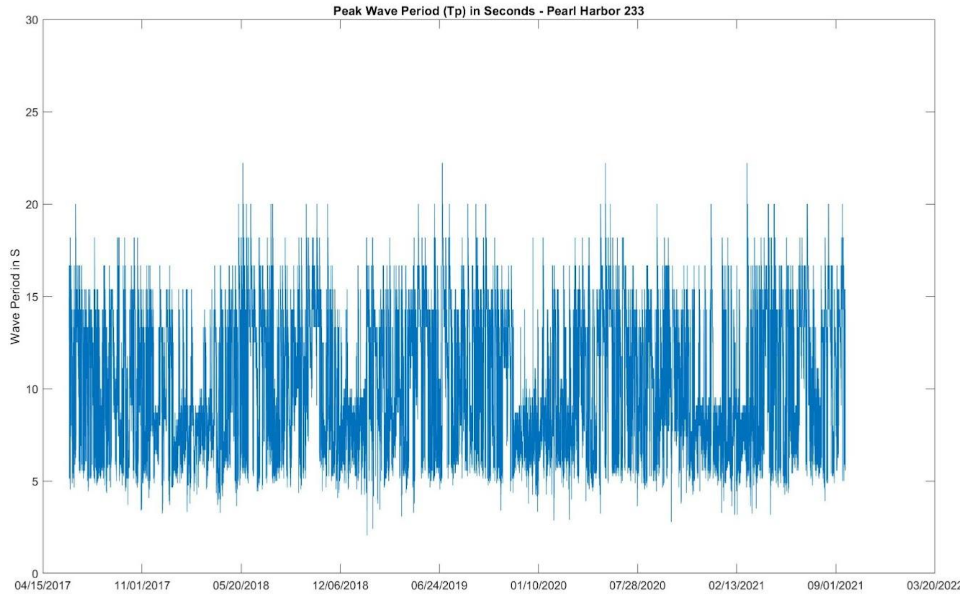

Figure 37: Peak wave period (s) vs. time at Pearl Harbor Buoy 233

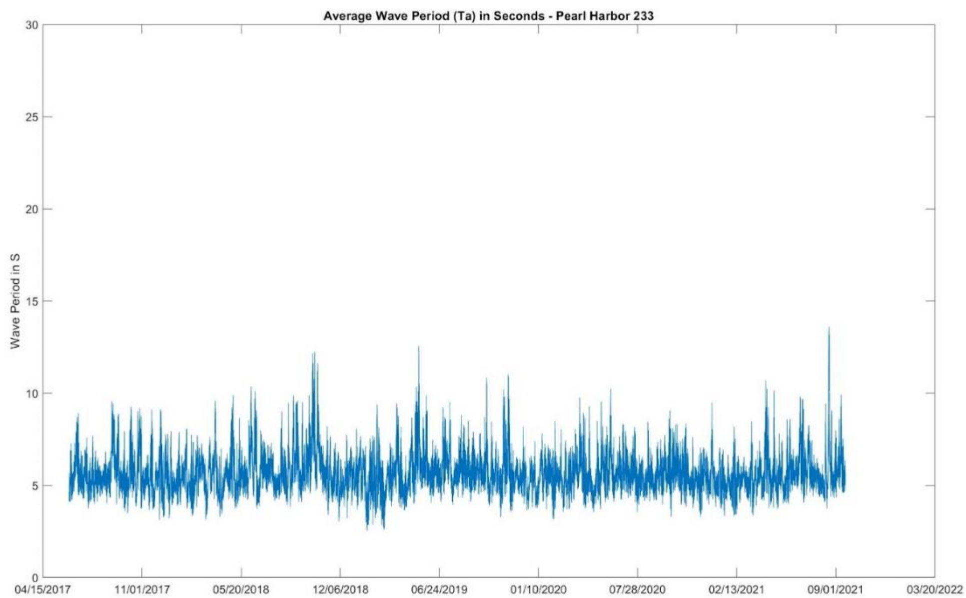

Figure 38: Average wave period (s) vs. time at Pearl Harbor Buoy 233

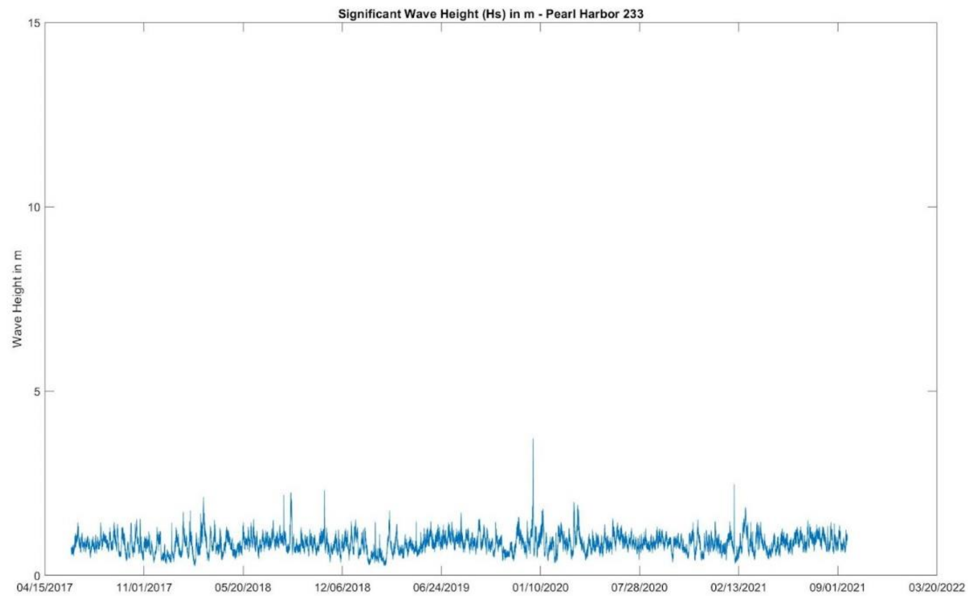

Figure 39: Significant wave height (Hs) (m) vs. time at Pearl Harbor Buoy 233

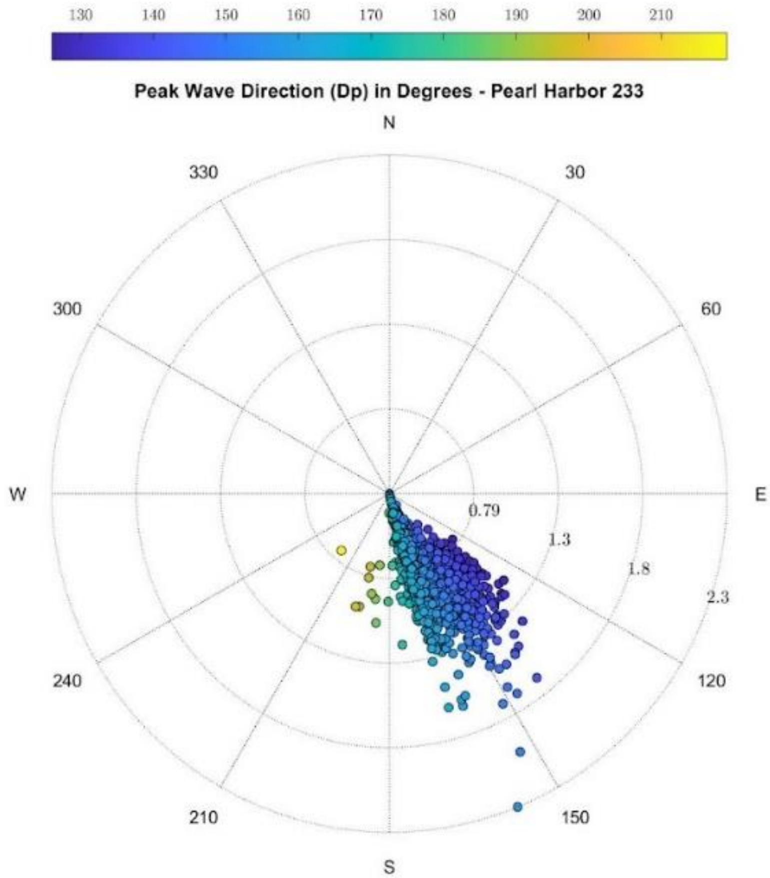

Figure 40: Peak wave direction (°) vs. significant wave height (Hs) (m) at Pearl Harbor Buoy 233. Peak wave direction is the direction from which the waves at the dominant period are coming. The units are degrees from true north, increasing clockwise, with north as 0°, east as 90°, south as 180°, and west as 270°.

Barber's Point Waverider Buoy 238

The following figures are the five plots created in MATLAB of total data collected for the Barber's Point, O'ahu Waverider Buoy (238). Four time series plots of; surface water temperature (°C) (Figure 41), peak wave period (T_p) (Figure 42), average wave period (T_a) (Figure 43), significant wave height (H_s) (Figure 44), and the compass rose plot of peak wave direction (D_p) vs. Significant wave height (H_s) (Figure 45).

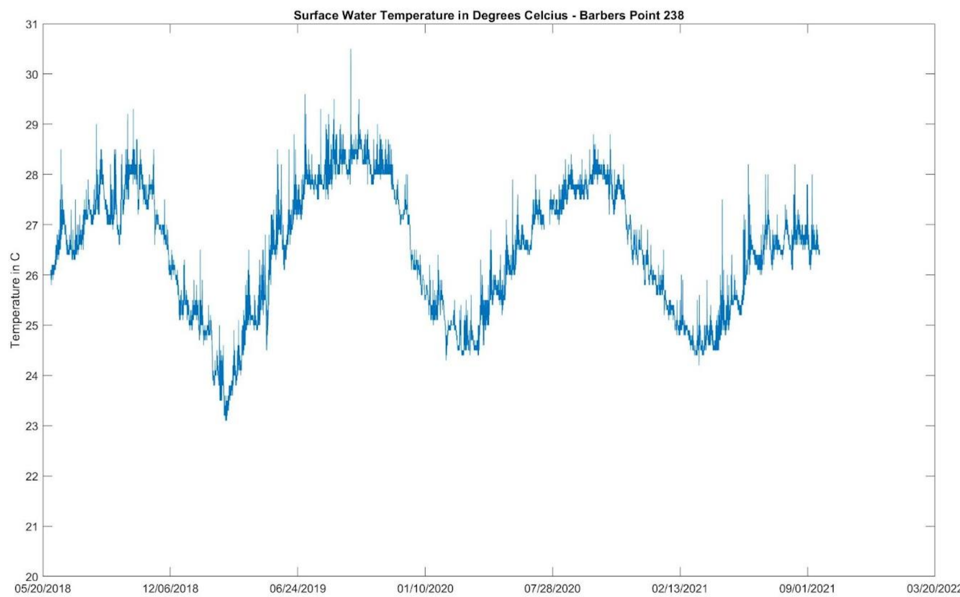

Figure 41: Surface water temperature (°C) vs. time at Barber's Point Buoy 238

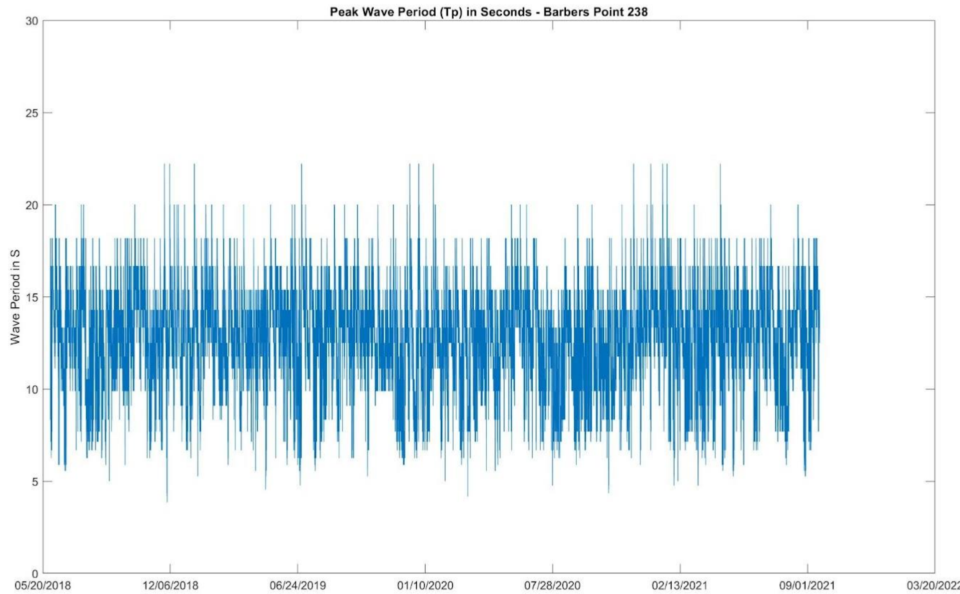

Figure 42: Peak wave period (s) vs. time at Barber's Point Buoy 238

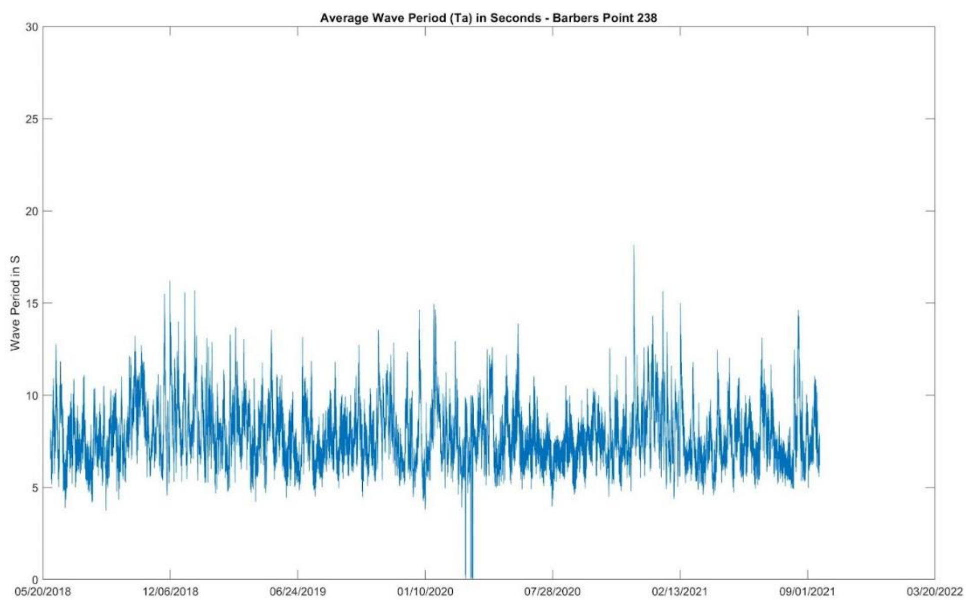

Figure 43: Average wave period (s) vs. time at Barber's Point Buoy 238

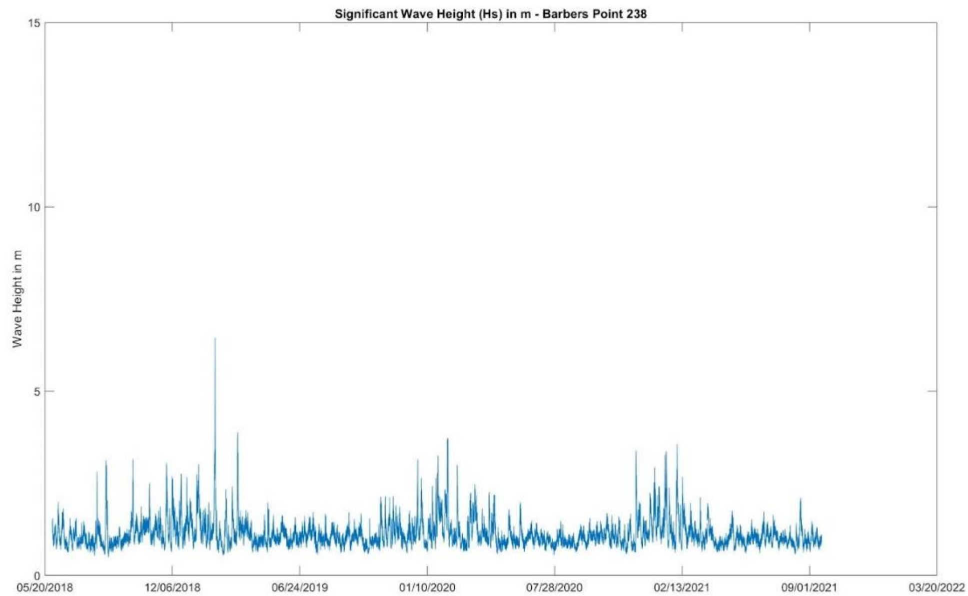

Figure 44: Significant wave height (Hs) (m) vs. time at Barber's Point Buoy 238

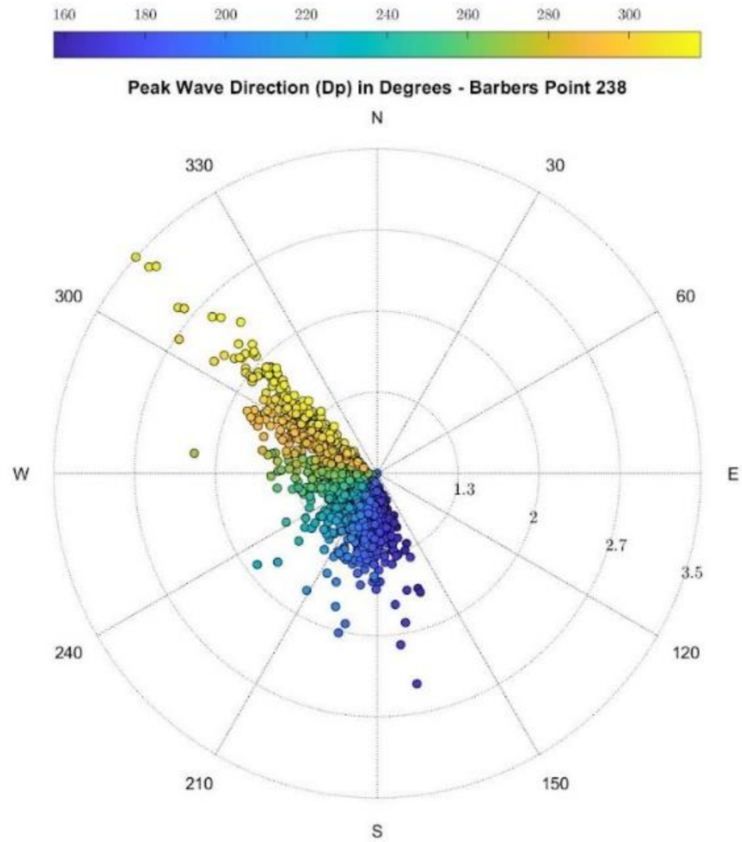

Figure 45: Peak wave direction (°) vs. significant wave height (Hs) (m) at Barber's Point Buoy 238. Peak wave direction is the direction from which the waves at the dominant period are coming. The units are degrees from true north, increasing clockwise, with north as 0°, east as 90°, south as 180°, and west as 270°.

Lanai Southwest Waverider Buoy 239

The following figures are the five plots created in MATLAB of total data collected for the Lanai Southwest Waverider Buoy (239). Four time series plots of; surface water temperature (°C) (Figure 46), peak wave period (T_p) (Figure 47), average wave period (T_a) (Figure 48), significant wave height (H_s) (Figure 49), and the compass rose plot of peak wave direction (D_p) vs. Significant wave height (H_s) (Figure 50).

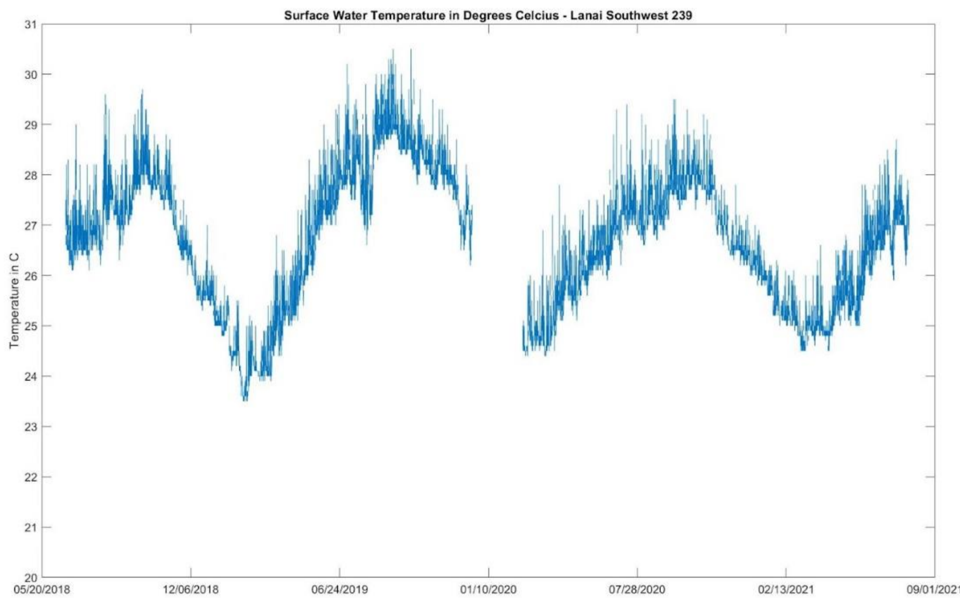

Figure 46: Surface water temperature (°C) vs. time at Lanai Buoy 239

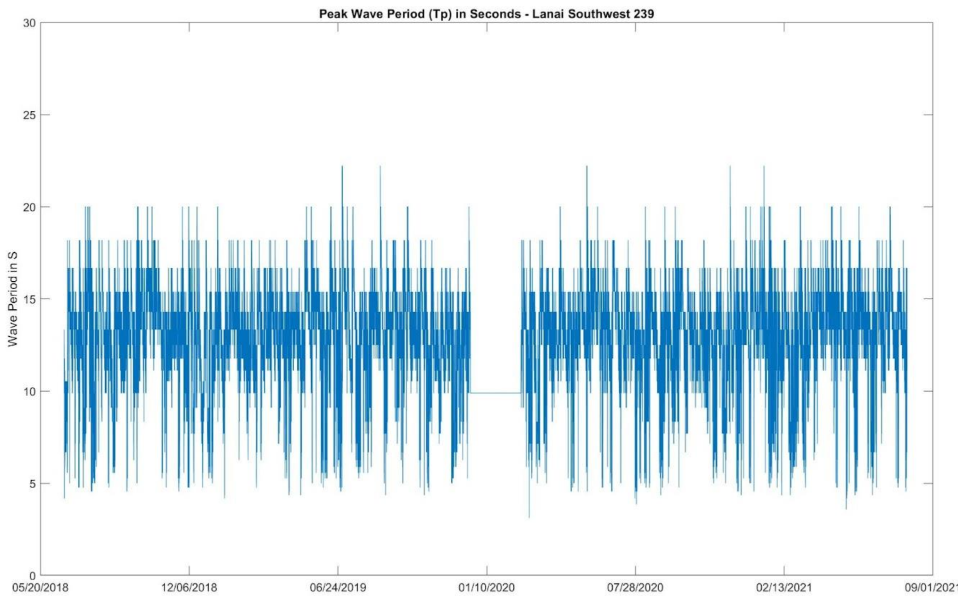

Figure 47: Peak wave period (s) vs. time at Lanai Buoy 239

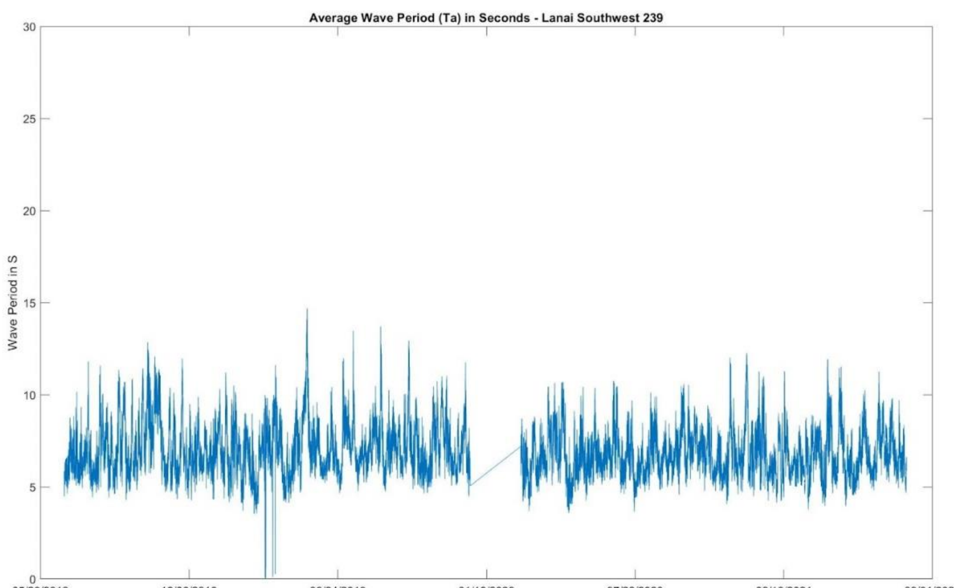

Figure 48: Average wave period (s) vs. time at Lanai Buoy 239

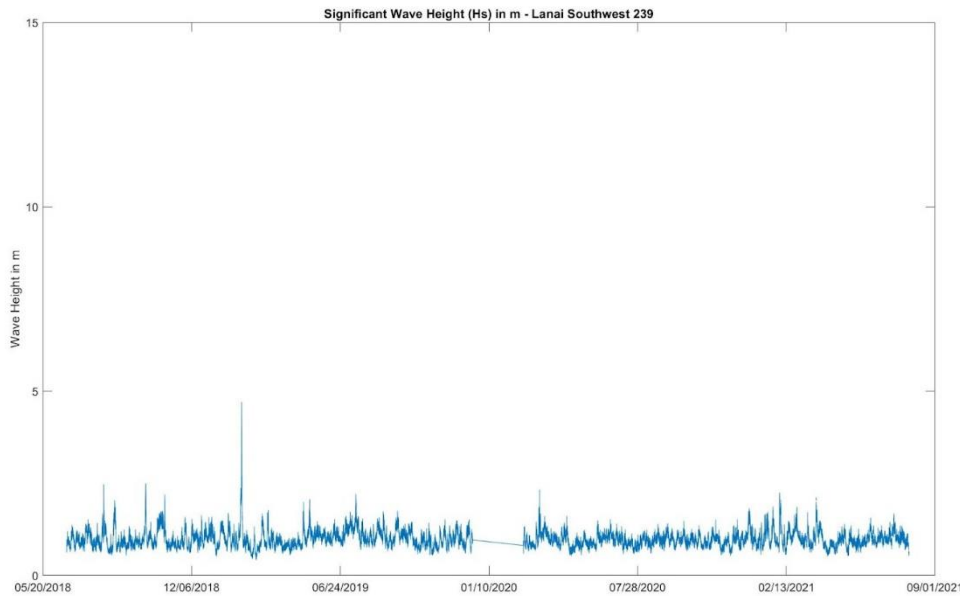

Figure 49: Significant wave height (Hs) (m) vs. time at Lanai Buoy 239

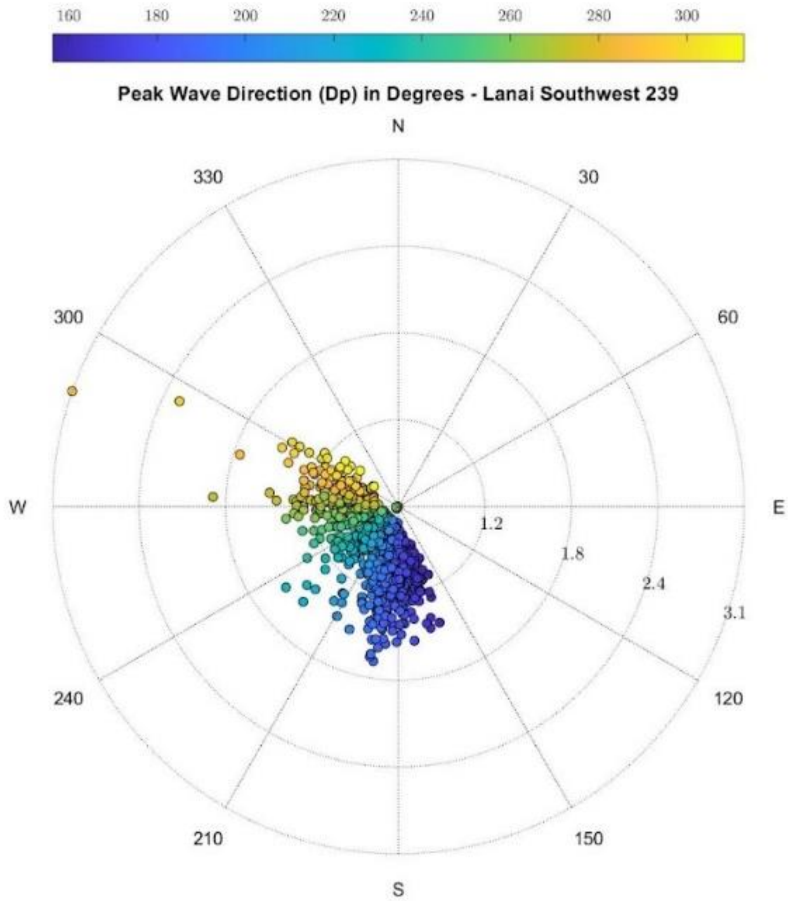

Figure 50: Peak wave direction (°) vs. significant wave height (Hs) (m) at Lanai Buoy 239. Peak wave direction is the direction from which the waves at the dominant period are coming. The units are degrees from true north, increasing clockwise, with north as 0°, east as 90°, south as 180°, and west as 270°.

Parameter Tables

The following section of this thesis shows four tables listing the minimum, maximum, and mean values for each time series parameter for each wavebuoy, along with the range (maximum – minimum) of values for each buoy. Parameters referenced in these tables are sea surface temperature in °C (Table 2), significant wave height in m (Table 3), peak wave period in s (Table 4), and average wave period in s (Table 5).

Table 2: Table of maximum, minimum, and mean temperature recorded in °C for all buoys

Buoy Location	**Maximum Temperature**	**Minimum Temperature**	**Mean Temperature**	**Range (max-min)**
Mokapu	30.20	22.20	25.46	8.00
Waimea	29.50	22.50	25.46	7.00
Pauwela	30.20	22.50	25.36	7.70
Hilo	29.30	21.90	25.67	7.40
Kaneohe	29.50	22.30	25.51	7.20
Hanalei	30.50	22.60	25.57	7.90
Pearl Harbor	29.30	22.50	26.16	6.80
Barber’s Point	30.50	23.10	26.55	7.40
Lanai SW	30.50	23.50	26.72	7.00

Table 3: Table of maximum, minimum, and mean significant wave height recorded in meters for all buoys

Buoy Location	**Maximum Wave Height**	**Minimum Wave Height**	**Mean Wave Height**	**Range (max-min)**
Mokapu	6.46	0.52	1.90	5.94
Waimea	9.09	0.29	1.68	8.80
Pauwela	7.73	0.57	2.07	7.16
Hilo	6.88	0.31	2.05	6.57
Kaneohe	5.29	0.44	1.72	4.85
Hanalei	11.71	0.53	2.14	11.18
Pearl Harbor	3.71	0.25	0.85	3.46
Barber’s Point	6.45	0.50	1.14	5.95
Lanai SW	4.70	0.42	0.99	4.28

Table 4: Table of maximum, minimum, and mean peak wave period recorded in seconds for all buoys

Buoy Location	Maximum Peak Period	Minimum Peak Period	Mean Peak Period	Range (max-min)
Mokapu	25.00	3.57	9.49	21.43
Waimea	25.00	2.38	10.78	22.62
Pauwela	25.00	3.23	10.40	21.77
Hilo	25.00	3.23	10.01	21.77
Kaneohe	22.22	3.57	9.41	18.65
Hanalei	22.22	3.85	10.84	18.37
Pearl Harbor	22.22	2.06	10.19	20.16
Barber’s Point	22.22	3.85	12.96	18.37
Lanai SW	22.22	3.12	13.05	19.1

Table 5: Table of maximum, minimum, and mean average wave period recorded in seconds for all buoys

Buoy Location	Maximum Avg. Period	Minimum Avg. Period	Mean Avg. Period	Range (max-min)
Mokapu	15.37	3.87	6.42	11.50
Waimea	17.31	3.07	7.10	14.24
Pauwela	16.30	3.74	6.87	12.56
Hilo	15.77	3.74	7.17	12.03
Kaneohe	12.97	3.63	6.46	9.34
Hanalei	16.50	4.09	10.84	12.41
Pearl Harbor	12.54	2.55	5.68	9.99
Barber's Point	18.14	0.01	7.90	18.13
Lanai SW	14.68	0.00	6.96	14.68

Yearly Temperature

The following section of this thesis shows nine tables listing the mean temperature for each year of data collection for each buoy (Tables 6 -14) and nine figures of time series plots of mean average temperature per year for each wavebuoy (Figures 51 – 59) .

Table 6: Table of the mean temperature (°C) each year from 2000 to 2021 at Mokapu buoy 098

Year	Temperature
2000	25.90
2001	25.21
2002	25.29
2003	25.62
2004	26.31
2005	25.55
2006	25.23
2007	25.21
2008	25.20
2009	24.89
2010	24.97
2011	25.20
2012	24.56
2013	25.02
2014	25.80
2015	25.98
2016	25.88
2017	25.79

2018	25.40
2019	25.92
2020	26.00
2021	25.22

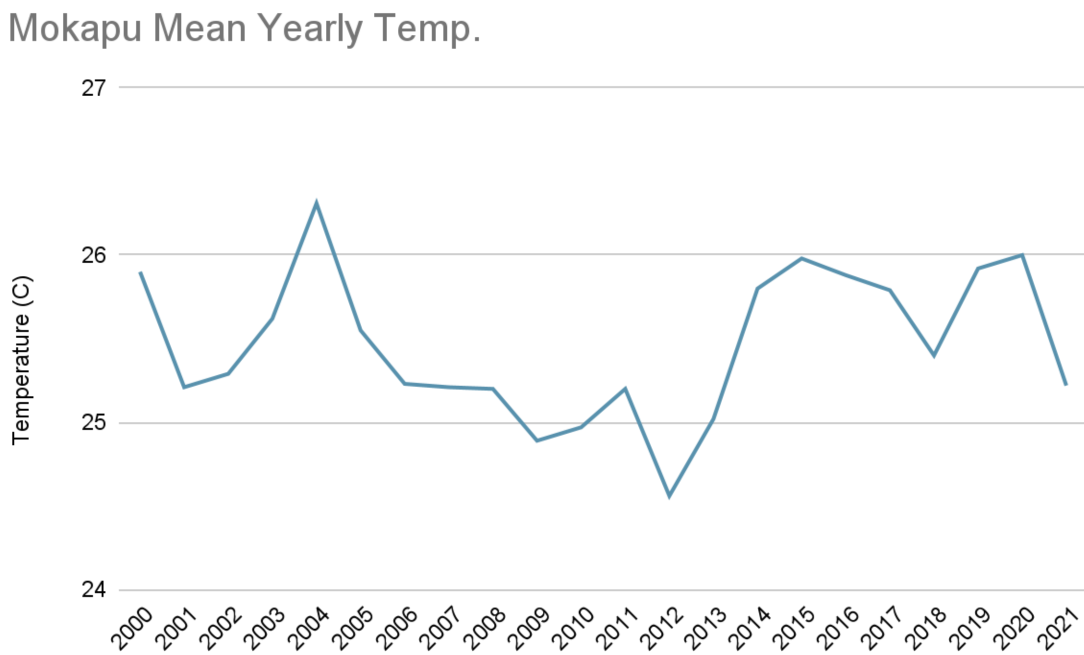

Figure 51: Average temperature (°C) vs. time (year) at Mokapu buoy 098

Table 7: Table of the mean temperature (°C) each year from 2001 to 2021 at Waimea buoy 106

Year	**Temperature**
2001	24.85
2002	25.32
2003	25.21
2004	25.92
2005	25.46
2006	25.99
2007	25.37
2008	25.06
2009	25.06
2010	25.12
2011	25.25
2012	24.7
2013	25.53
2014	25.85
2015	25.78
2016	25.89
2017	NAN
2018	NAN
2019	NAN
2020	25.96
2021	25.58

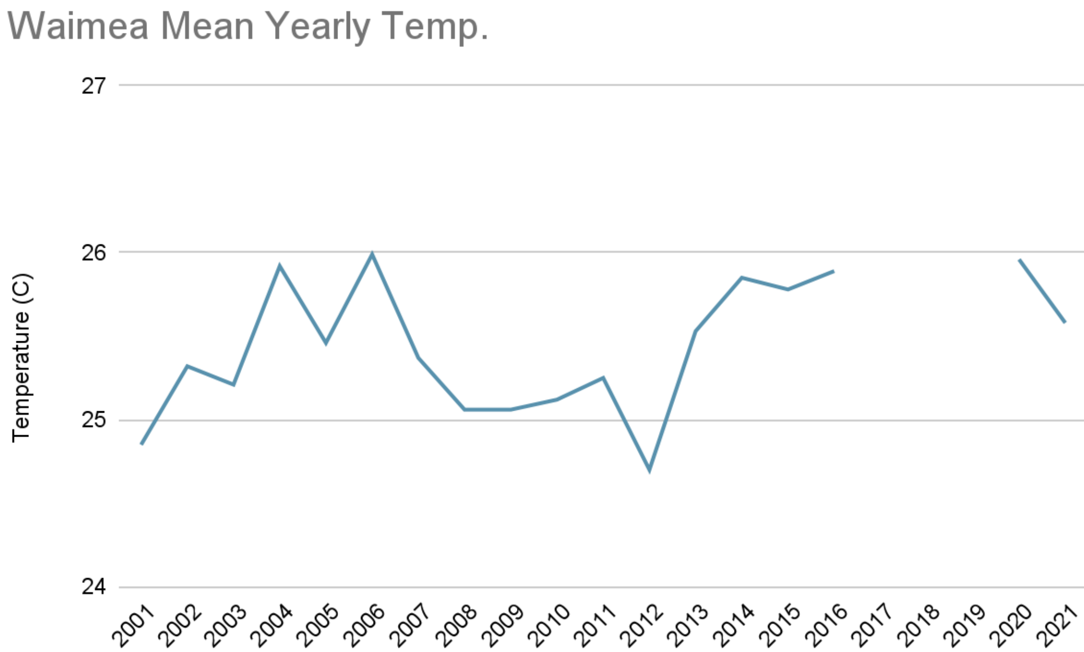

Figure 52: Average temperature (°C) vs. time (year) at Waimea buoy 106

Table 8: Table of the mean temperature (°C) each year from 2011 to 2021 at Pauwela buoy 187

Year	**Temperature**
2011	24.02
2012	24.29
2013	25.3
2014	26.01
2015	25.64
2016	25.64
2017	25.52
2018	25.45
2019	25.33
2020	25.46
2021	25.13

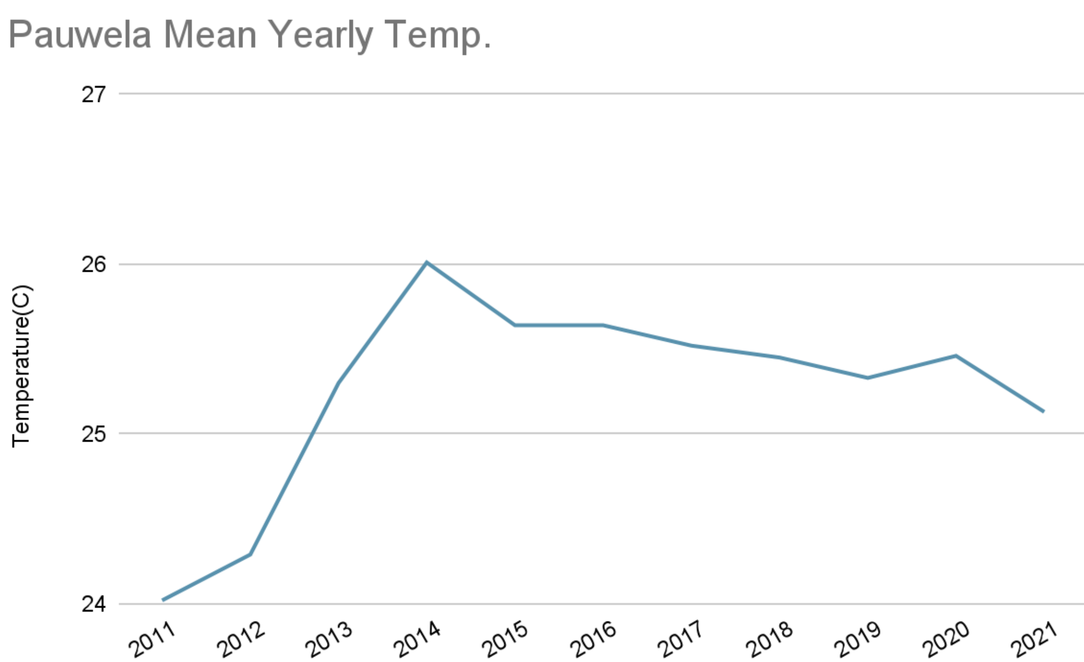

Figure 53: Average temperature (°C) vs. time (year) at Pauwela buoy 187

Table 9: Table of the mean temperature (°C) each year from 2012 to 2021 at Hilo buoy 188

Year	Temperature
2012	24.81
2013	25.35
2014	25.82
2015	25.87
2016	26.03
2017	25.83
2018	25.47
2019	26.24
2020	25.76
2021	24.52

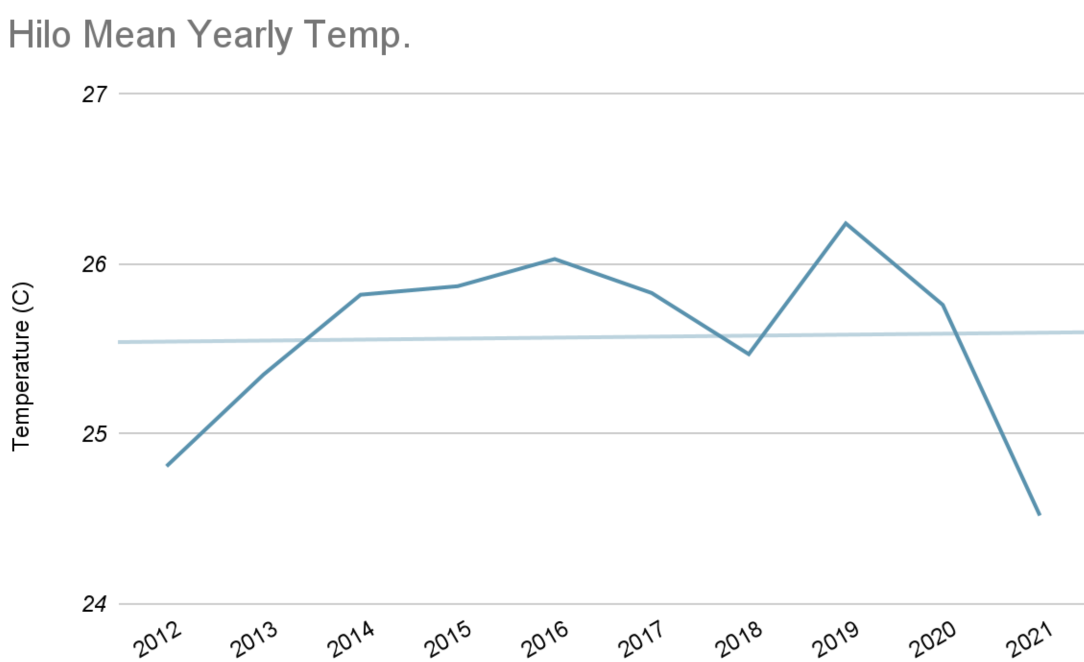

Figure 54: Average temperature (°C) vs. time (year) at Pauwela buoy 188

Table 10: Table of the mean temperature (°C) each year from 2012 to 2021 at Kaneohe buoy 198

Year	**Temperature**
2012	24.84
2013	25.13
2014	25.22
2015	25.54
2016	25.53
2017	25.36
2018	25.86
2019	25.84
2020	25.91
2021	25.32

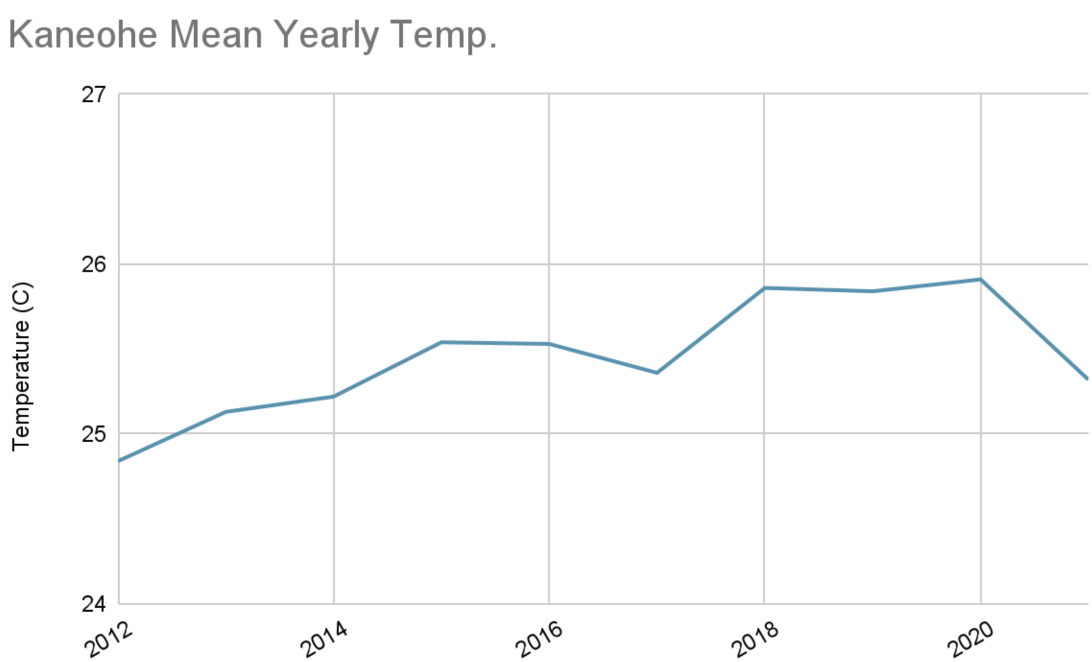

Figure 55: Average temperature (°C) vs. time (year) at Kaneohe buoy 198

Table 11: Table of the mean temperature (°C) each year from 2013 to 2021 at Hanalei Buoy 202

Year	Temperature
2013	26.31
2014	25.06
2015	26.26
2016	25.46
2017	25.96
2018	25.28
2019	24.36
2020	25.32
2021	26.2

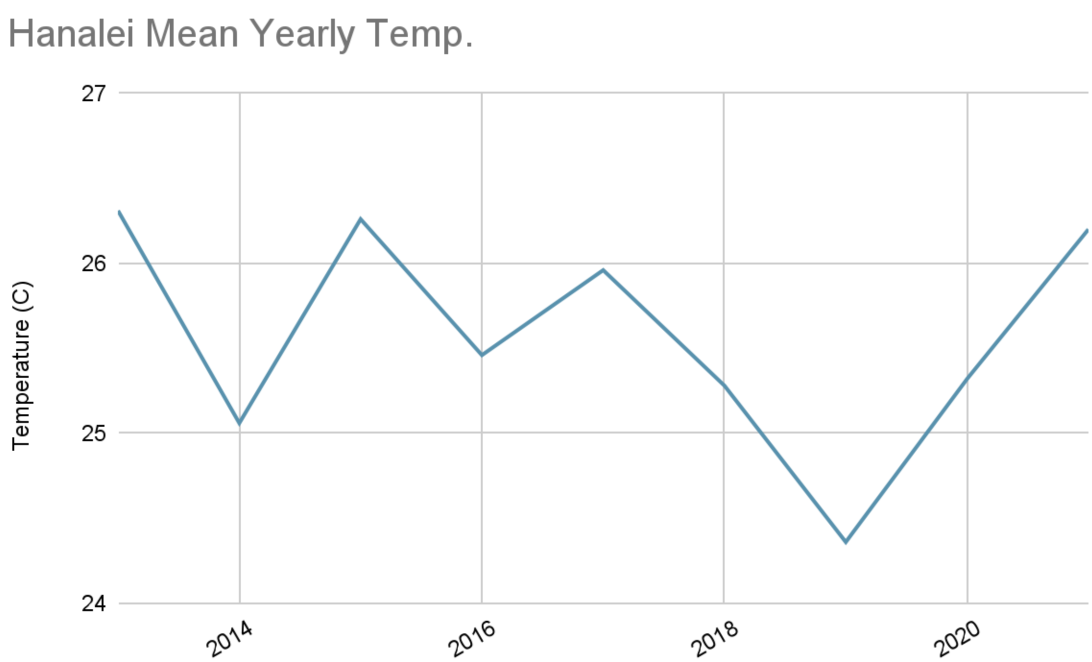

Figure 56: Average temperature (°C) vs. time (year) at Hanalei buoy 202

Table 12: Table of the mean temperature (°C) each year from 2017 to 2021 at Pearl Harbor Buoy 233

Year	**Temperature**
2017	26.75
2018	25.77
2019	26.38
2020	26.2
2021	25.64

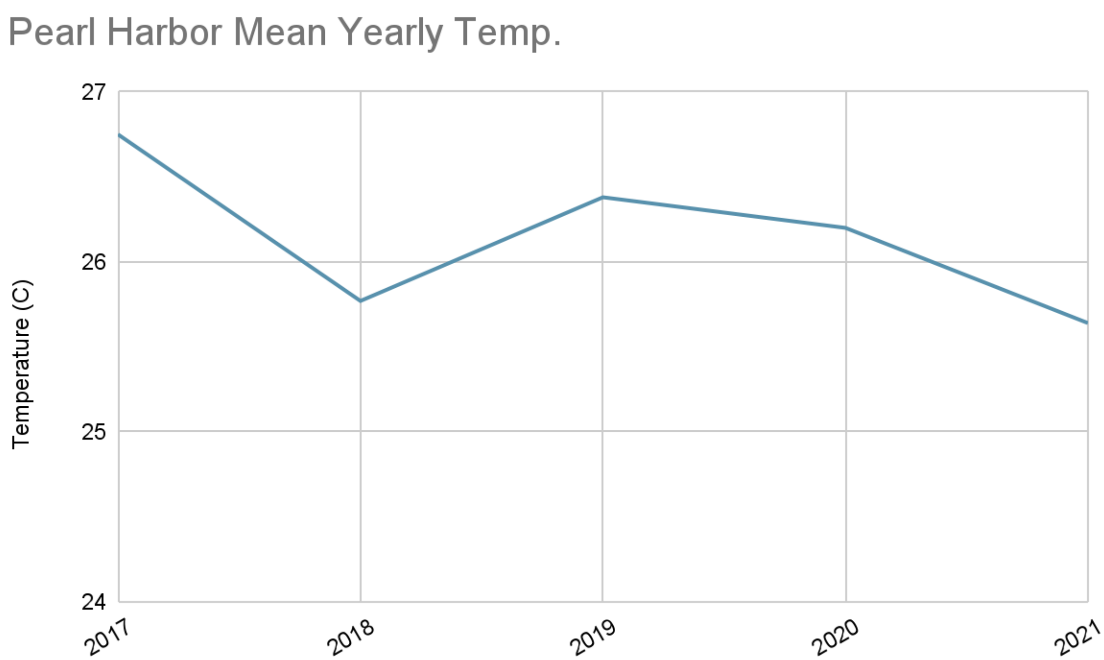

Figure 57: Average temperature (°C) vs. time (year) at Pearl Harbor buoy 233

Table 13: Table of the mean temperature (°C) each year from 2018 to 2021 at Barber's Point Buoy 238

Year	**Temperature**
2018	27.02
2019	26.63
2020	26.45
2021	25.79

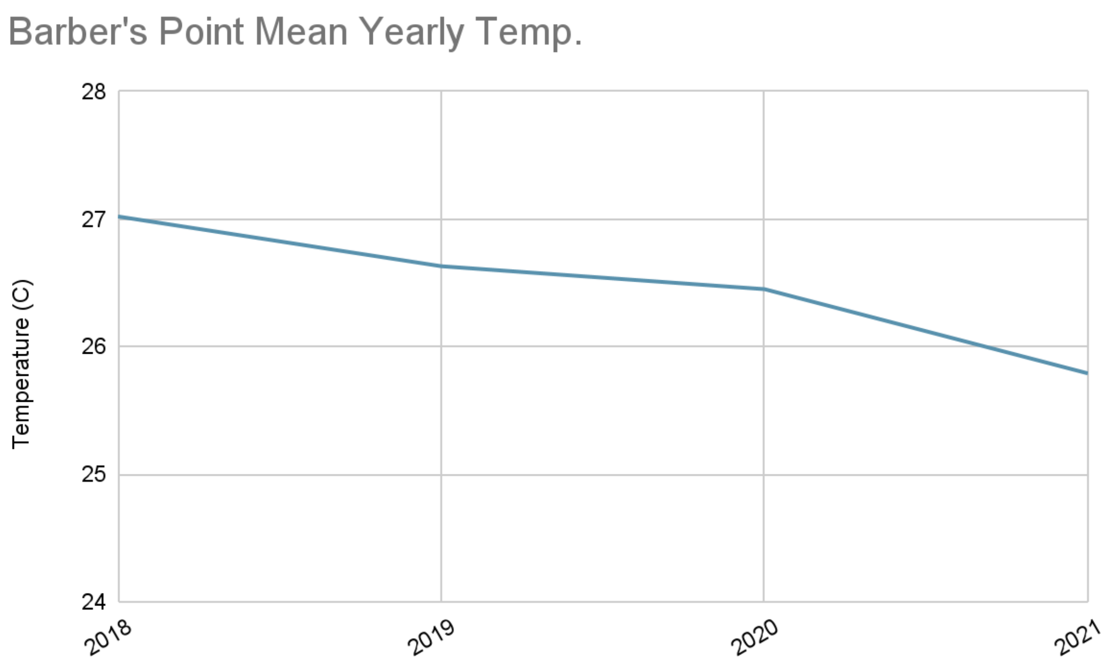

Figure 58: Average temperature (°C) vs. time (year) at Barber's Point buoy 238

Table 14: Table of the mean temperature (°C) each year from 2018 to 2021 at Lanai Buoy 239

Year	Temperature
2018	27.07
2019	26.85
2020	26.62
2021	25.80

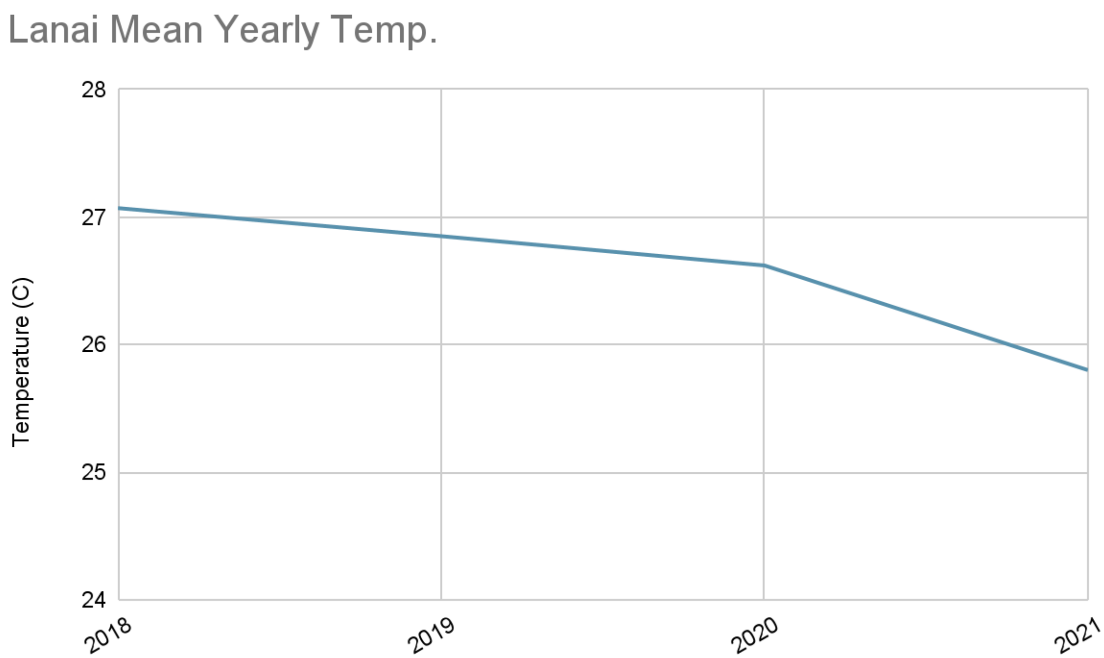

Figure 59: Average temperature (°C) vs. time (year) at Lanai buoy 239

Maximums

The following section of this thesis shows three tables listing the maximum value and corresponding data of sea surface temperature in °C (Table 15), significant wave height in m (Table 16), and average wave period in s (Table 17) for each wavebuoy. These are followed by a table listing the average wave height in m per season (Kau and Hoʻoilo) for each wavebuoy (Table 18). The final table of this section lists the average wave height in m of each wavebuoy during ENSO events (Table 19).

Table 15: Table of maximum sea surface temperature (°C) and corresponding dates for each buoy

Buoy Location	Maximum Temperature	Date
Mokapu	30.20	9/9/2015
Waimea	29.50	9/11/2015
Pauwela	30.20	9/10/2015
Hilo	29.30	8/30/2019
Kaneohe	29.50	9/2/2015
Hanalei	30.50	9/14/2017
Pearl Harbor	29.30	9/27/2019
Barber’s Point	30.50	9/15/2019
Lanai Southwest	30.50	9/3/2019

Table 16: Table of maximum significant wave height (m) and corresponding dates for each buoy

Buoy Location	**Maximum Wave Height**	**Date**
Mokapu	6.46	12/14/2001
Waimea	9.09	2/11/2019
Pauwela	7.73	2/11/2019
Hilo	6.88	9/5/2019
Kaneohe	5.29	1/22/2017
Hanalei	11.71	2/10/2019
Pearl Harbor	3.71	12/25/2019
Barber's Point	6.45	2/11/2019
Lanai Southwest	4.70	2/11/2019

Table 17: Table of maximum recorded average wave period (s) and corresponding dates for each buoy

Buoy Location	**Maximum Avg. Period**	**Date**
Mokapu	15.37	10/10/2012
Waimea	17.31	12/2/2020
Pauwela	16.30	2/25/2015
Hilo	15.77	9/2/2019
Kaneohe	12.97	11/11/2019
Hanalei	16.50	1/12/2019
Pearl Harbor	12.54	5/19/2019
Barber's Point	18.14	12/2/2020
Lanai Southwest	14.68	5/13/2019

Table 18: Table of average seasonal wave height (m) for each buoy

Buoy Location	Kau (May-October)	Ho`oilo (November-April)
Mokapu	1.71	2.08
Waimea	1.27	2.09
Pauwela	1.72	2.41
Hilo	1.78	2.35
Kaneohe	1.50	1.93
Hanalei	1.64	2.55
Pearl Harbor	0.89	0.82
Barber's Point	1.04	1.19
Lanai Southwest	0.99	0.97

Table 19: Table of average wave height (m) during El Niño and La Niña events (ENSO events calculated using the NOAA National Weather Service Climate Prediction Center)

Buoy Location	El Niño	La Niña
Mokapu	1.88	1.92
Waimea	1.68	1.52
Pauwela	2.12	2.02
Hilo	2.09	2.12
Kaneohe	1.74	1.69
Hanalei	2.21	1.99
Pearl Harbor	2.16	1.09
Barber's Point	1.16	1.09
Lanai Southwest	0.98	0.97

Seasonal Wave Height

The following section of this thesis shows nine time series plots of mean monthly significant wave height in m for each wavebuoy (Figures 60 – 68).

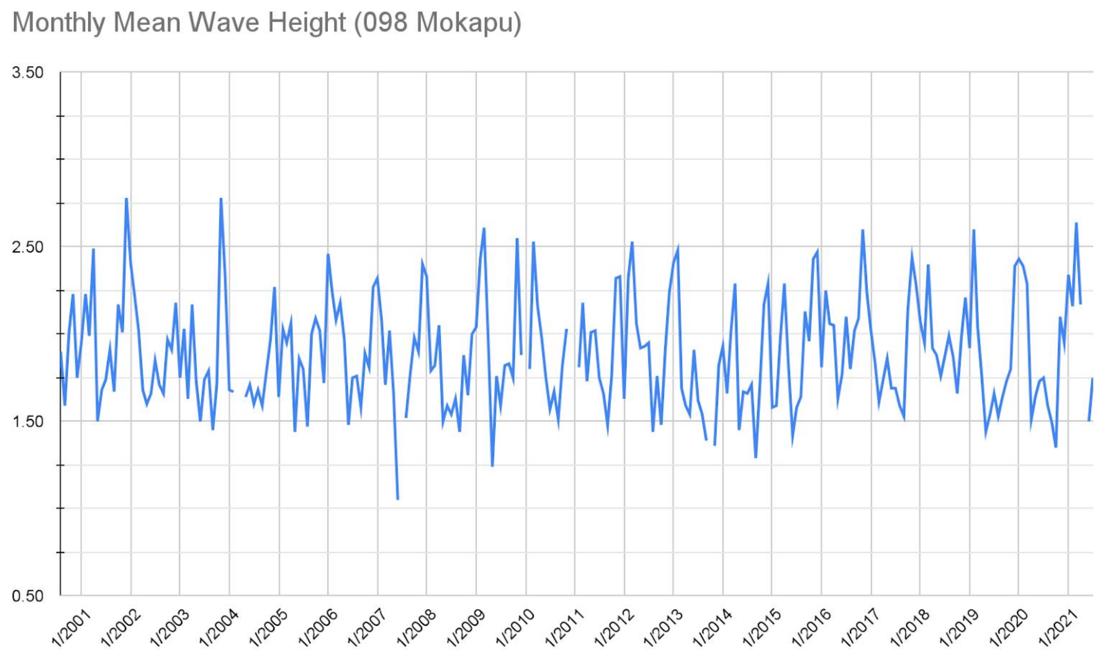

Figure 60: Average significant wave height (H_s) (m) vs. time (month) at Mokapu buoy 098

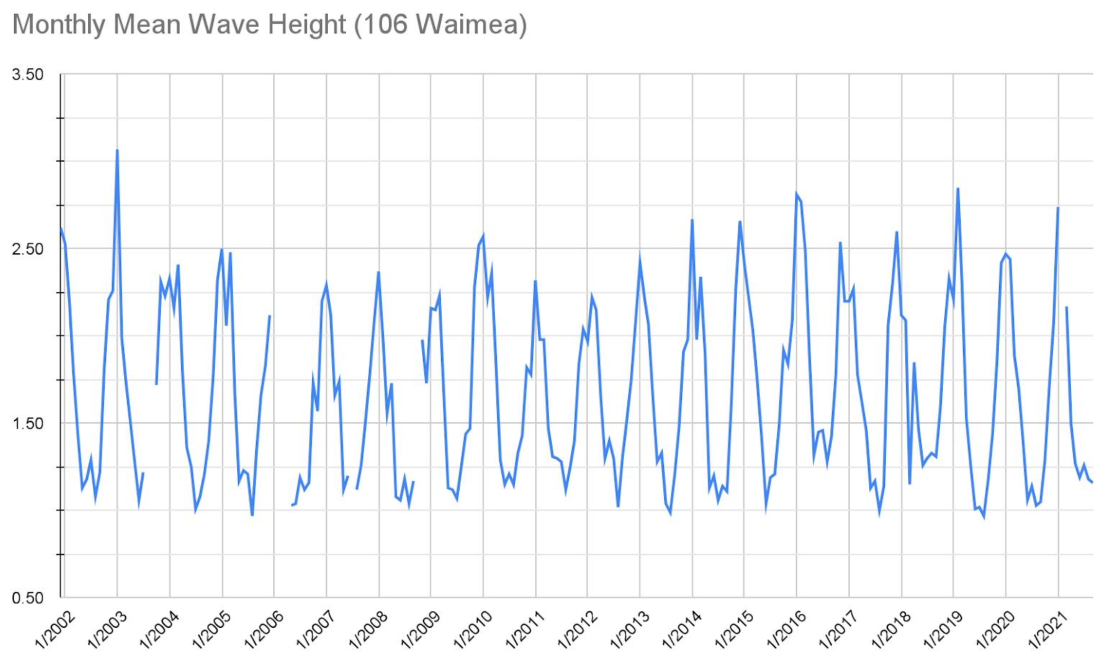

Figure 61: Average significant wave height (H_s) (m) vs. time (month) at Waimea buoy 106

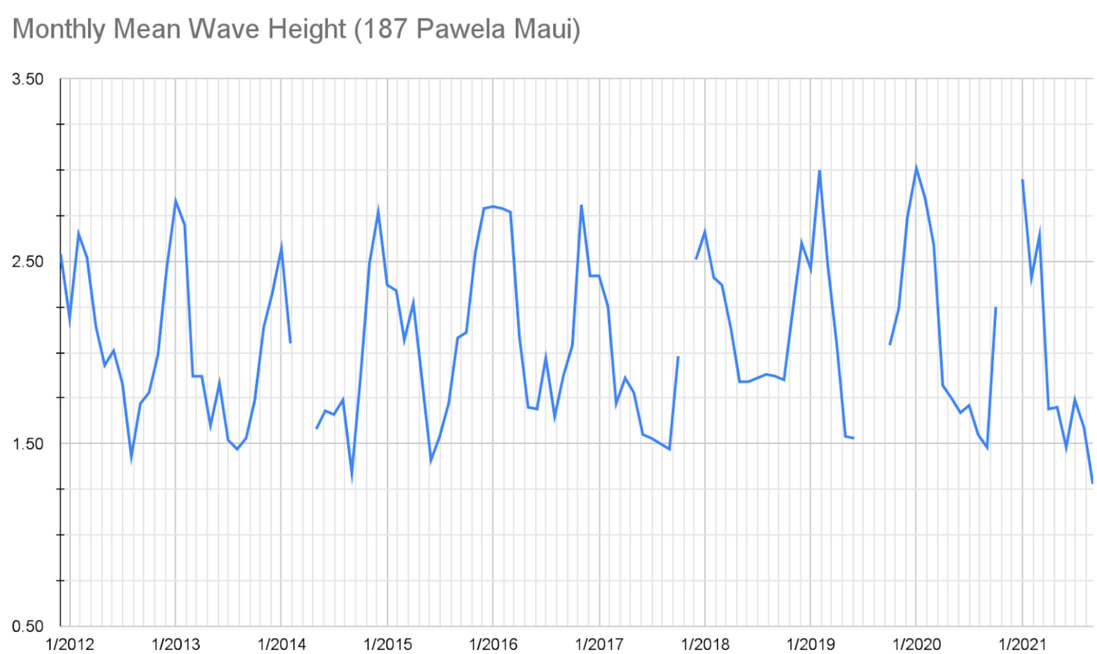

Figure 62: Average significant wave height (H_s) (m) vs. time (month) at Pauwela buoy 187

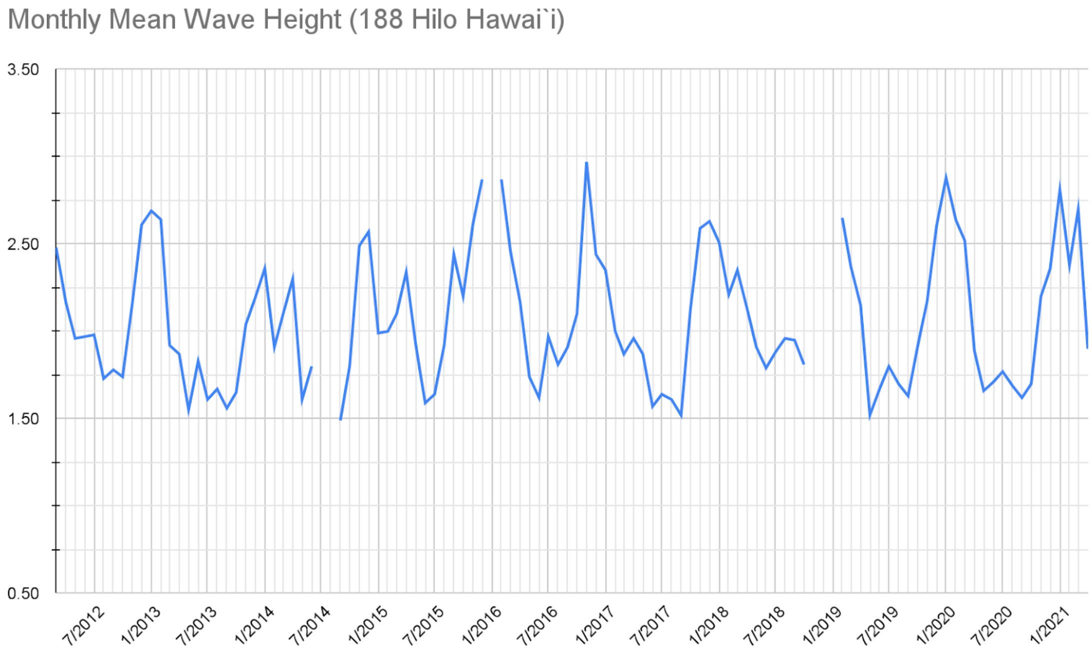

Figure 63: Average significant wave height (H_s) (m) vs. time (month) at Hilo buoy 188

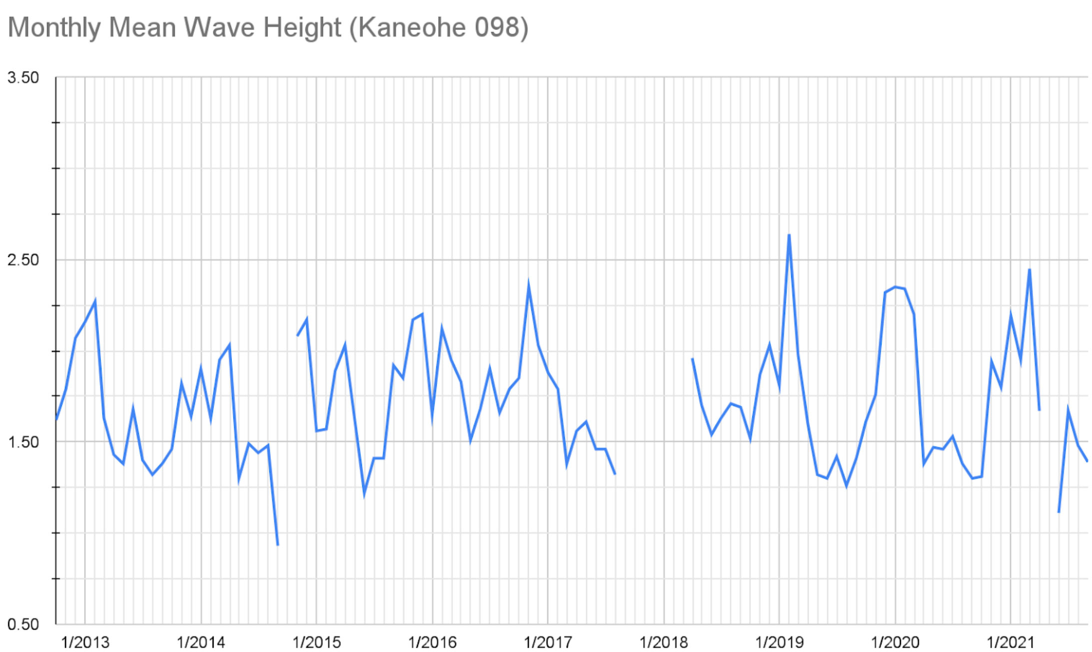

Figure 64: Average significant wave height (H_s) (m) vs. time (month) at Kaneohe buoy 198

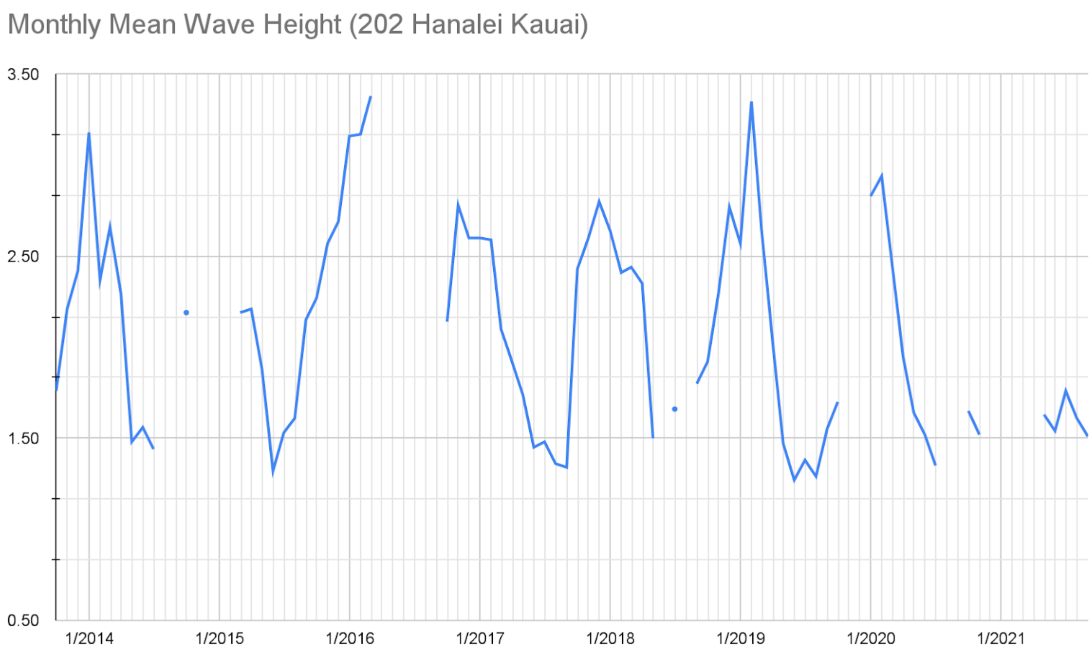

Figure 65: Average significant wave height (H_s) (m) vs. time (month) at Hanalei buoy 202

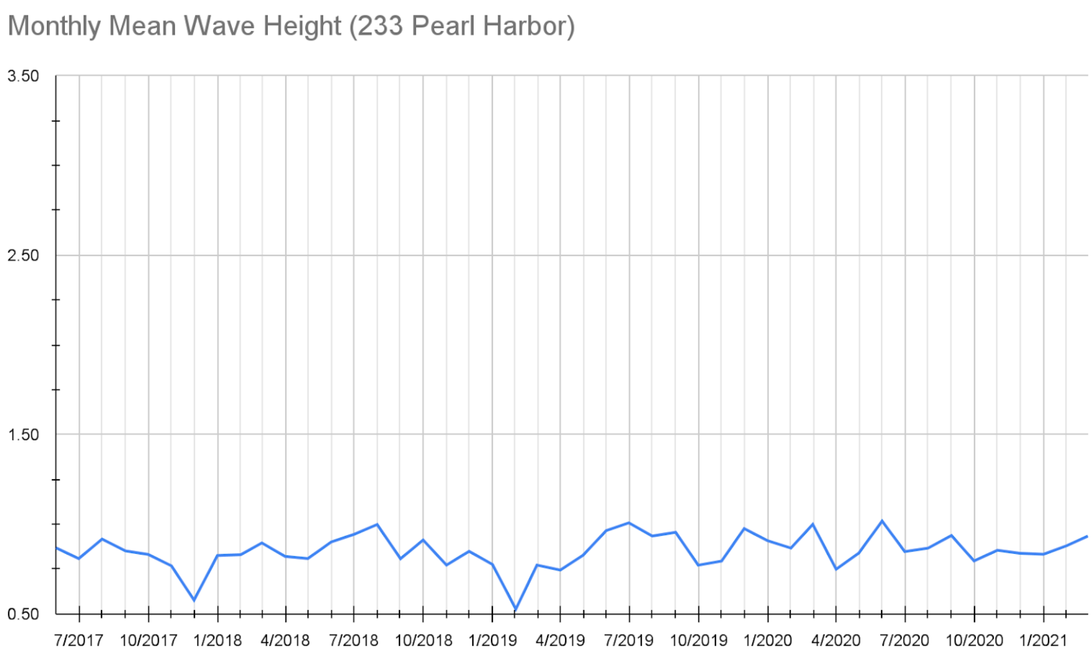

Figure 66: Average significant wave height (H_s) (m) vs. time (month) at Pearl Harbor buoy 233

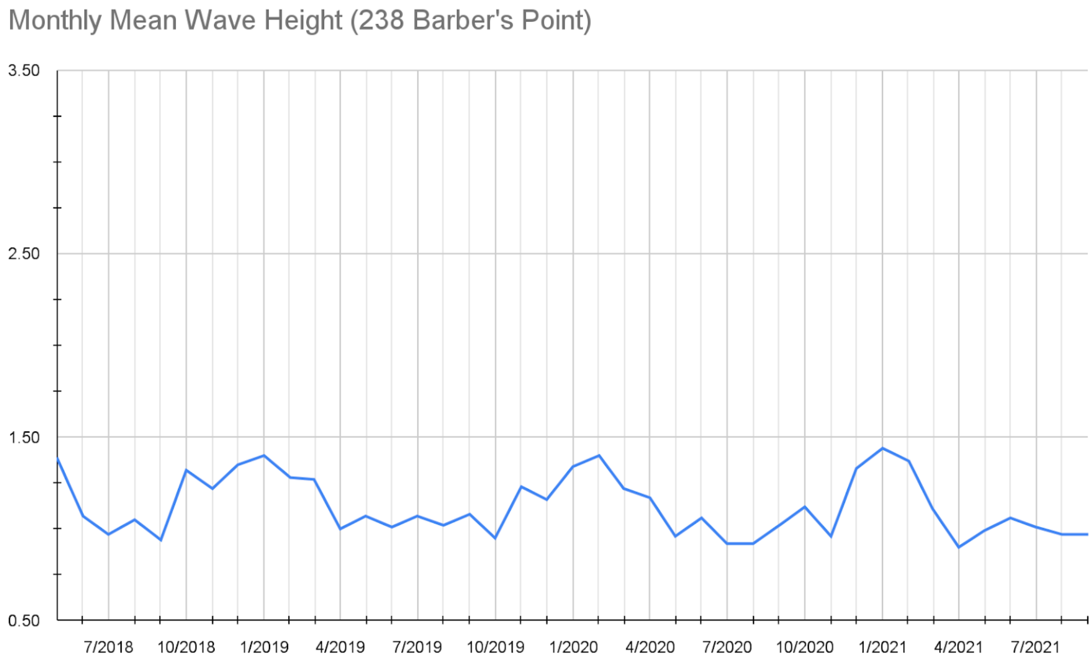

Figure 67: Average significant wave height (H_s) (m) vs. time (month) at Barber's Point buoy 238

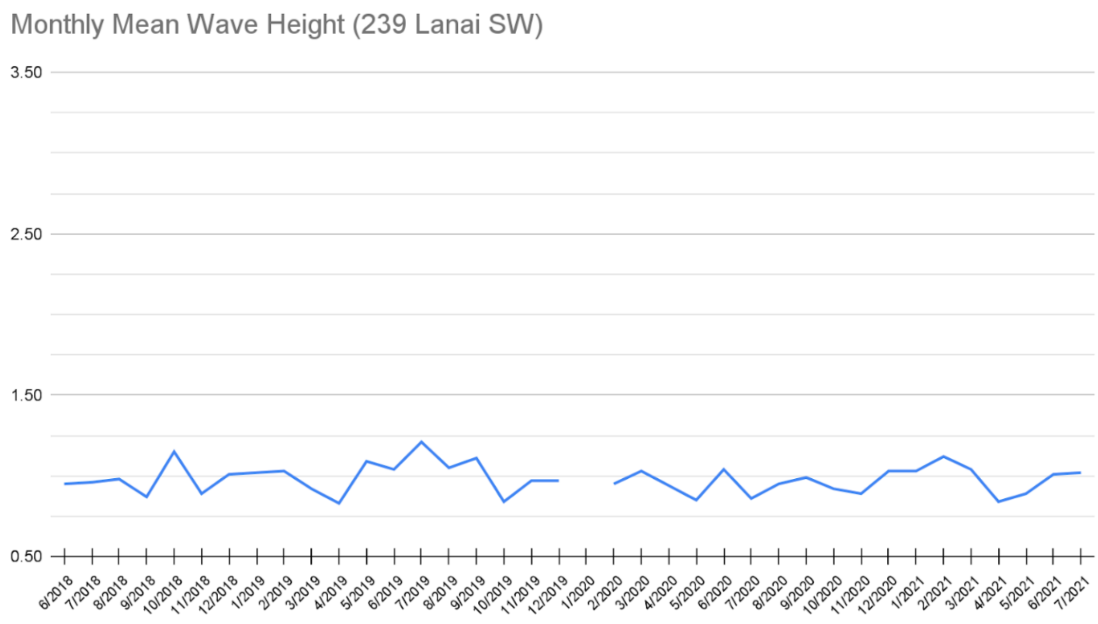

Figure 68: Average significant wave height (H_s) (m) vs. time (month) at Lanai buoy 239

Seasonal Wave Direction

The following section of this thesis shows eighteen histogram plots of wave direction vs. wave frequency per each season (Kau and Ho‘oilo) for each wavebuoy (Figures 69 – 86).

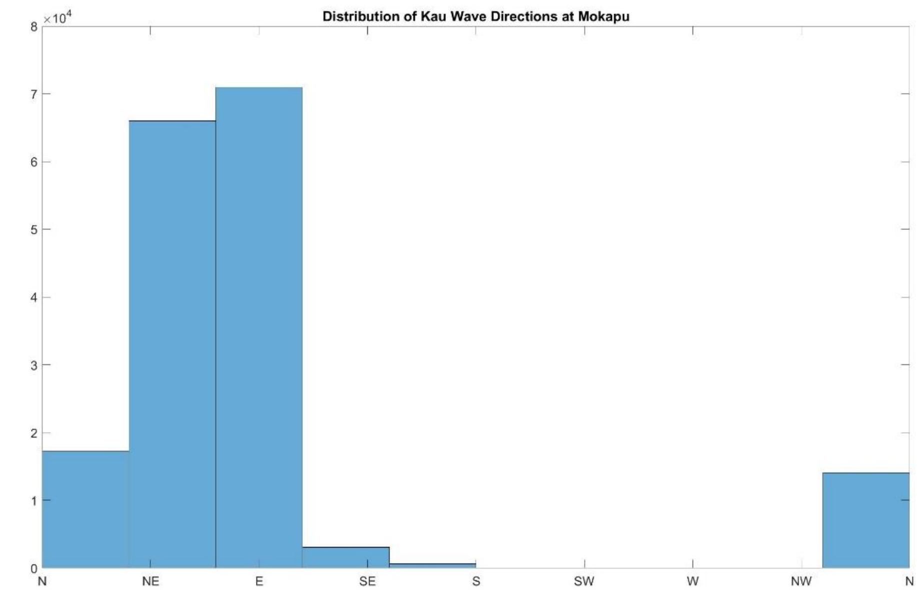

Figure 69: Histogram of wave direction vs. frequency (D_p) during Kau at Mokapu waverider buoy 098

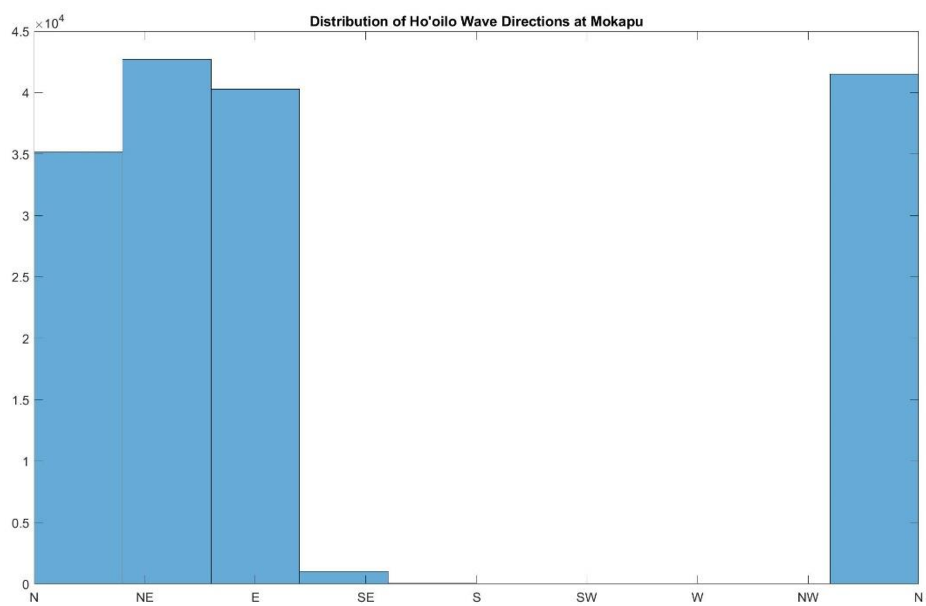

Figure 70: Histogram of wave direction vs. frequency (D_p) during Ho`oilo at Mokapu waverider buoy 098

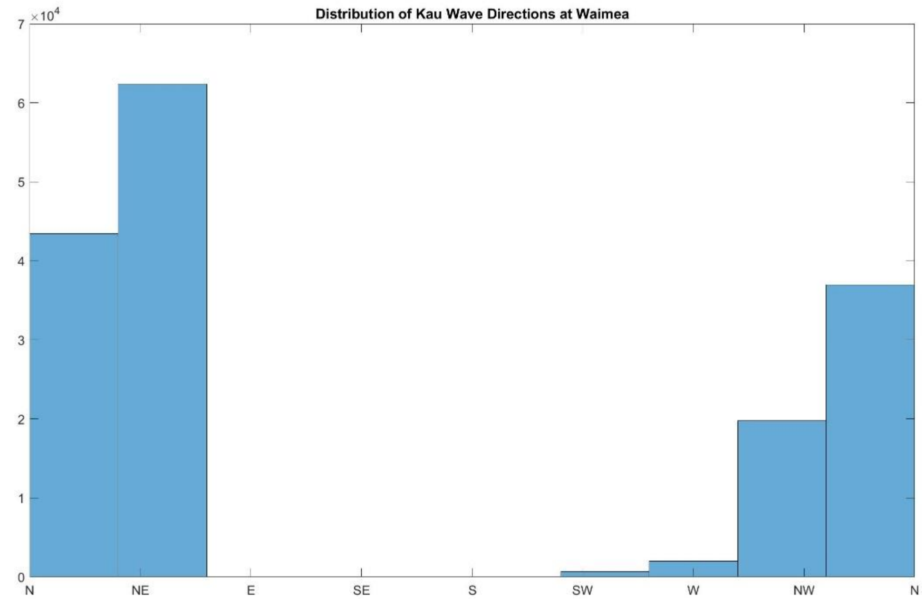

Figure 71: Histogram of wave direction vs. frequency (D_p) during Kau at Waimea waverider buoy 106

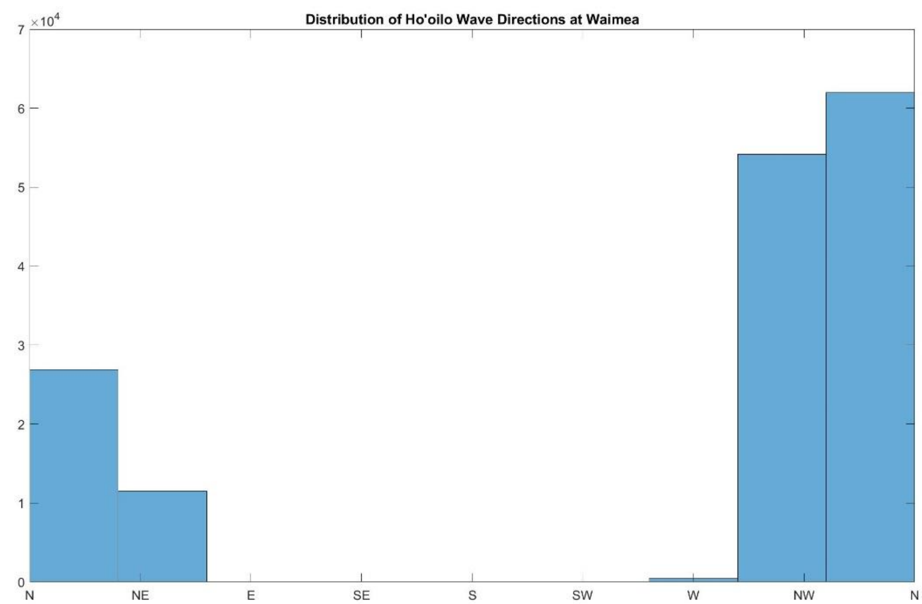

Figure 72: Histogram of wave direction vs. frequency (D_p) during Ho`oilo at Mokapu waverider buoy 106

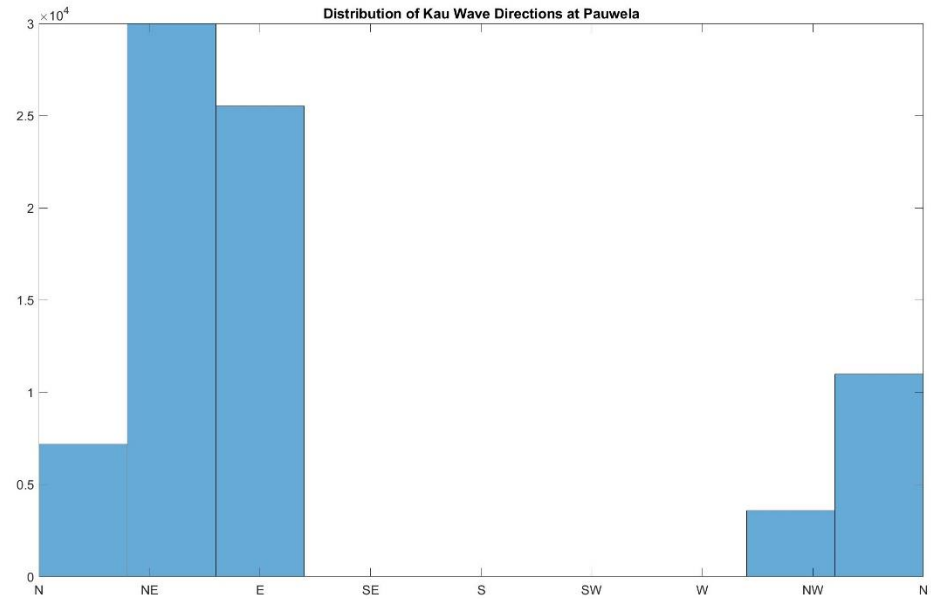

Figure 73: Histogram of wave direction vs. frequency (D_p) during Kau at Pauwela waverider buoy 187

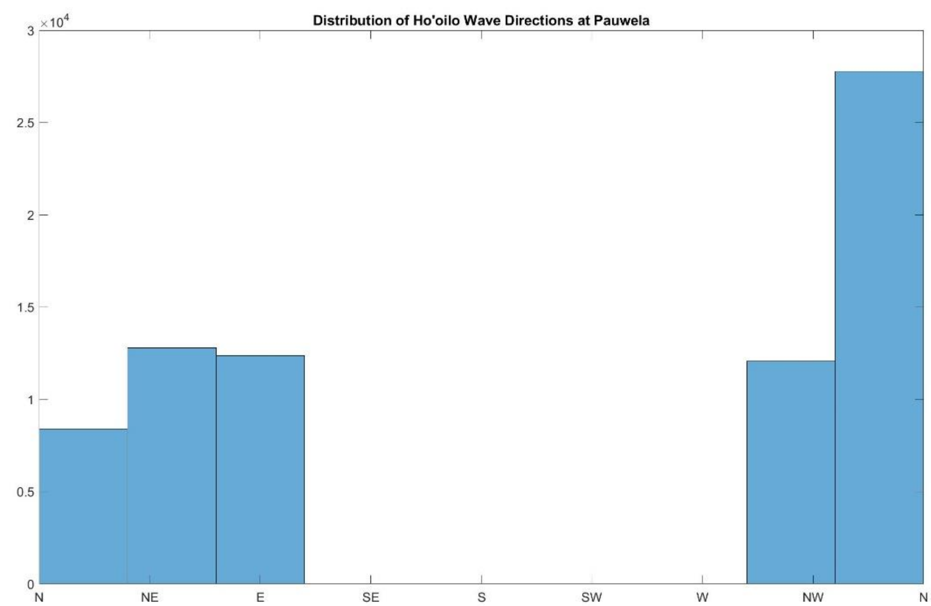

Figure 74: Histogram of wave direction vs. frequency (D_p) during Ho`oilo at Pauwela waverider buoy 187

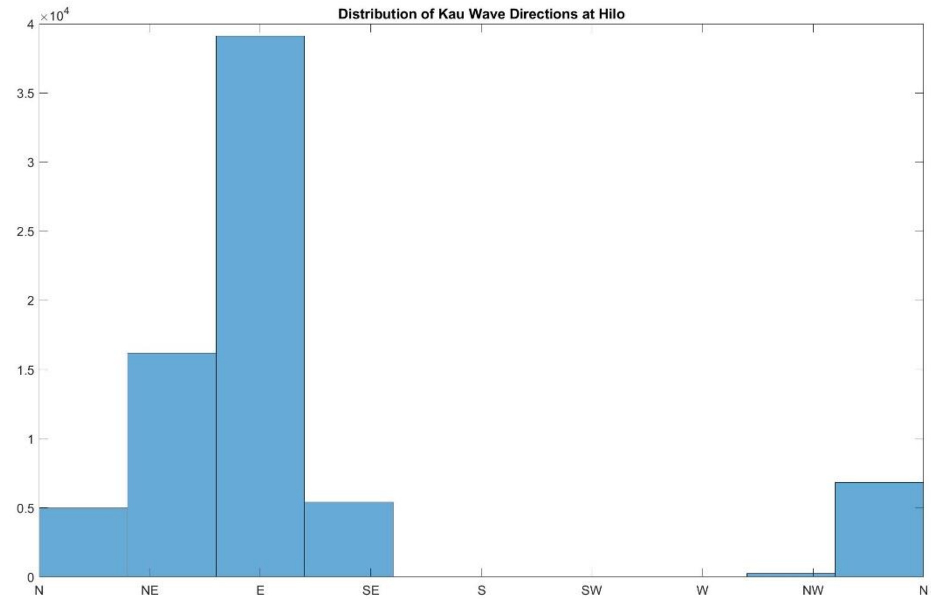

Figure 75: Histogram of wave direction vs. frequency (D_p) during Kau at Hilo waverider buoy 188

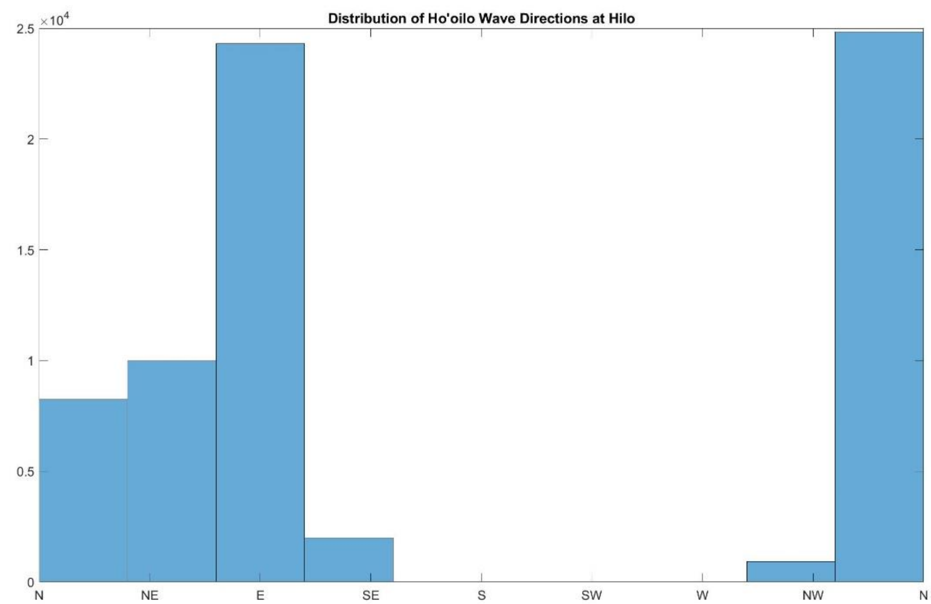

Figure 76: Histogram of wave direction vs. frequency (D_p) during Ho`oilo at Hilo waverider buoy 188

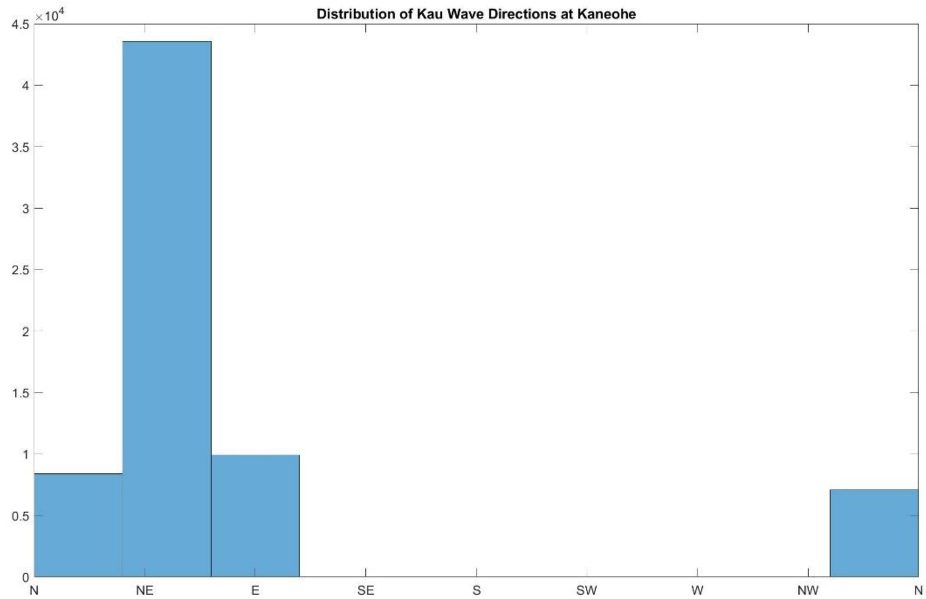

Figure 77: Histogram of wave direction vs. frequency (D_p) during Kau at Kaneohe waverider buoy 198

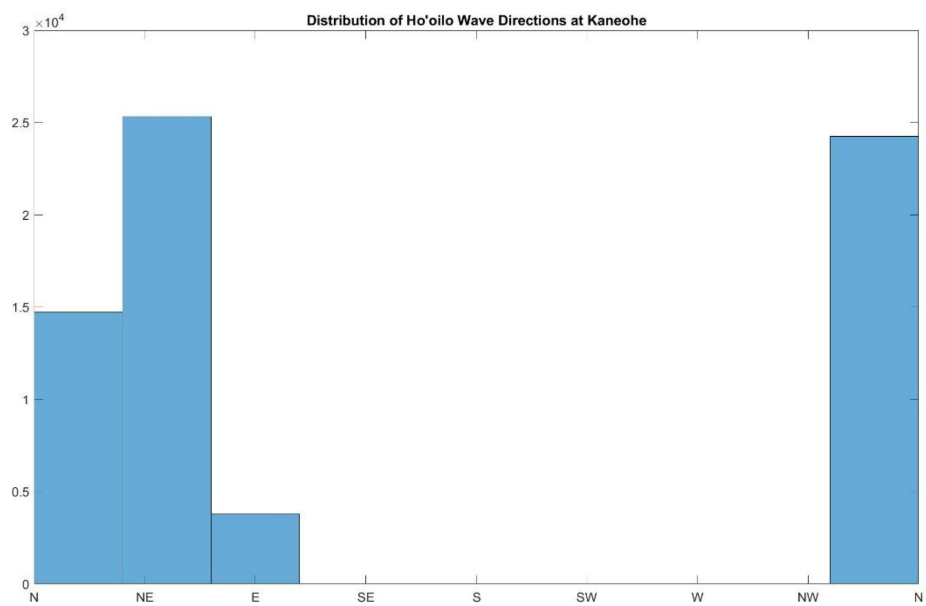

Figure 78: Histogram of wave direction vs. frequency (D_p) during Ho`oilo at Kaneohe waverider buoy 198

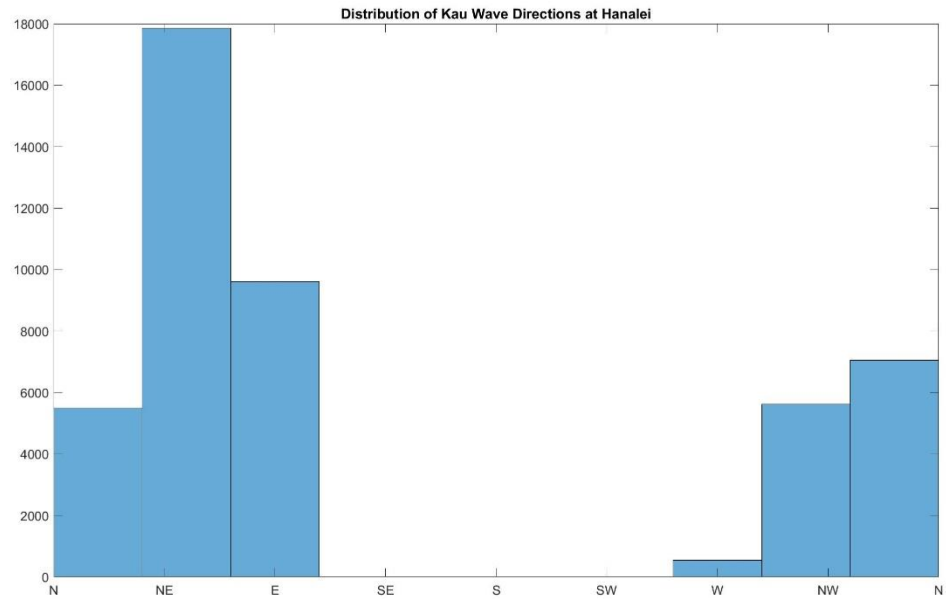

Figure 79: Histogram of wave direction vs. frequency (D_p) during Kau at Hanalei waverider buoy 202

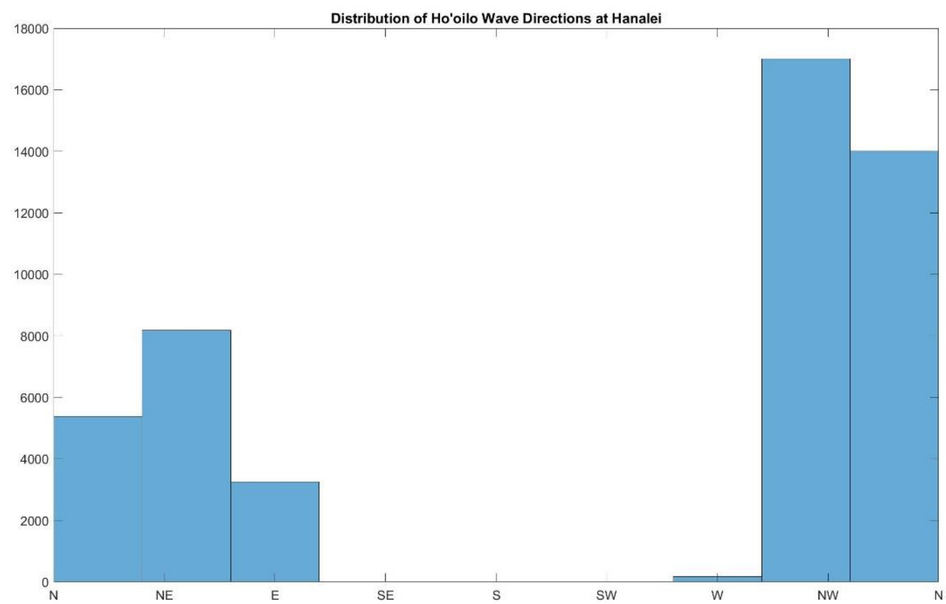

Figure 80: Histogram of wave direction vs. frequency (D_p) during Ho`oilo at Hanalei waverider buoy 202

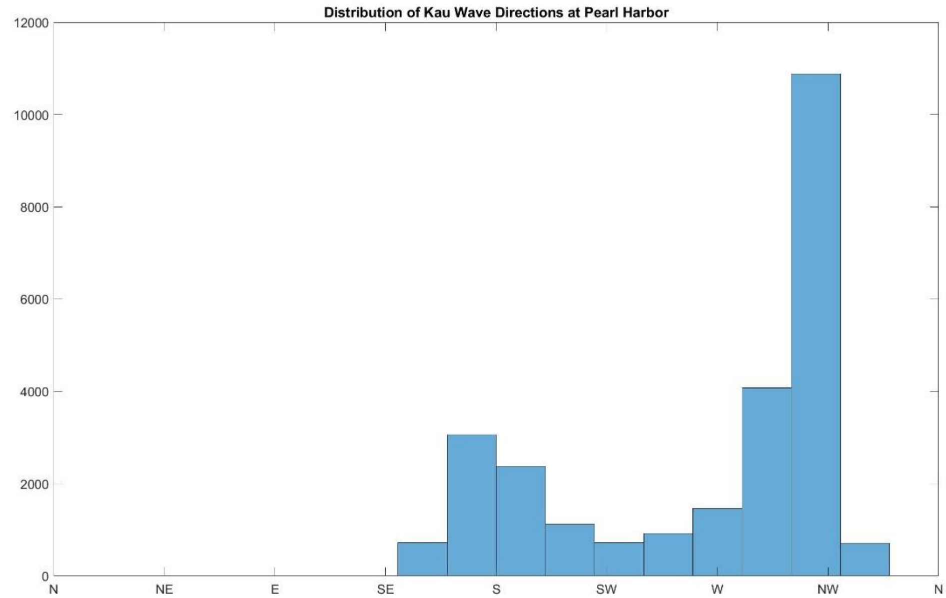

Figure 81: Histogram of wave direction vs. frequency (D_p) during Kau at Pearl Harbor waverider buoy 233

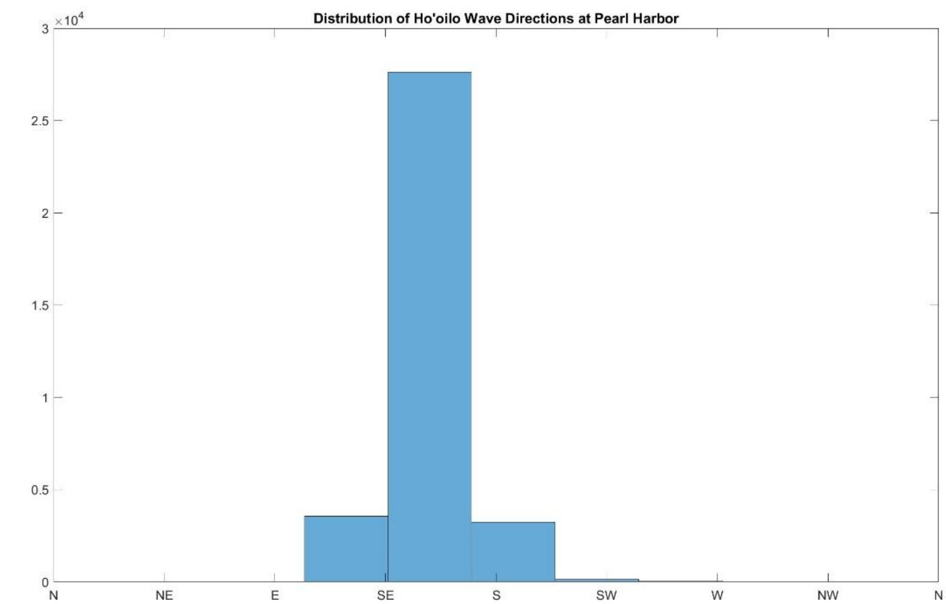

Figure 82: Histogram of wave direction vs. frequency (D_p) during Ho`oilo at Pearl Harbor waverider buoy 233

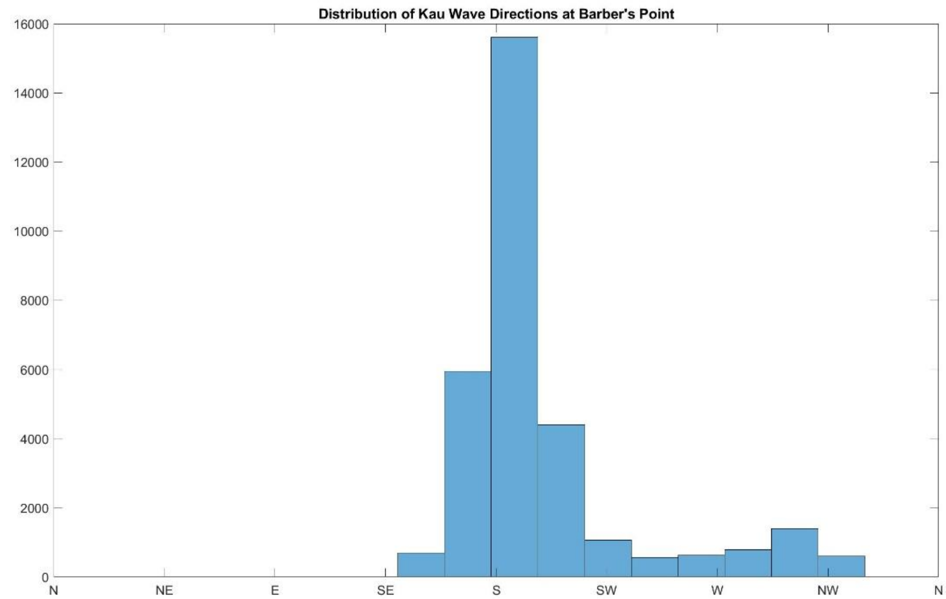

Figure 83: Histogram of wave direction vs. frequency (D_p) during Kau at Barber's Point waverider buoy 238

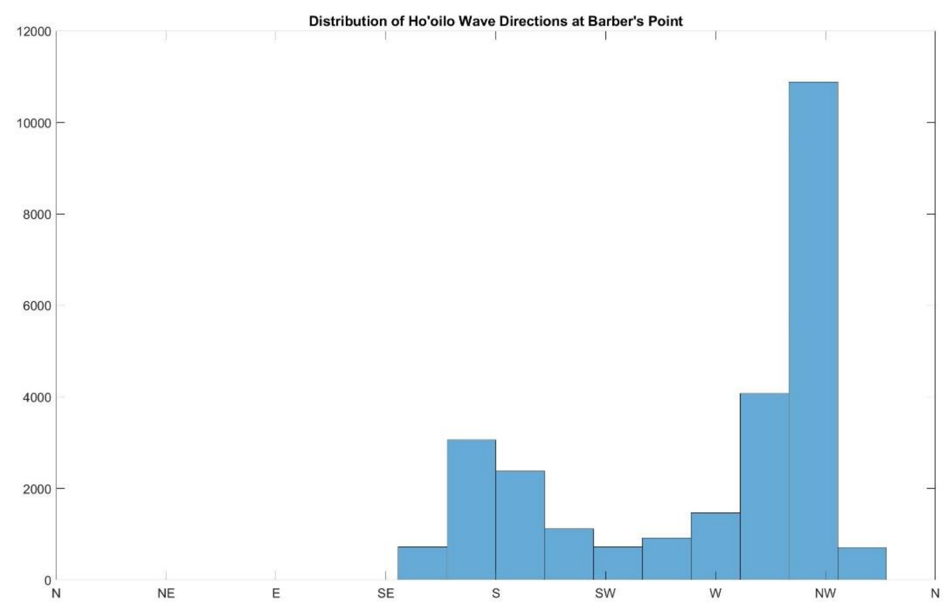

Figure 84: Histogram of wave direction vs. frequency (D_p) during Ho`oilo at Barber's Point waverider buoy 238

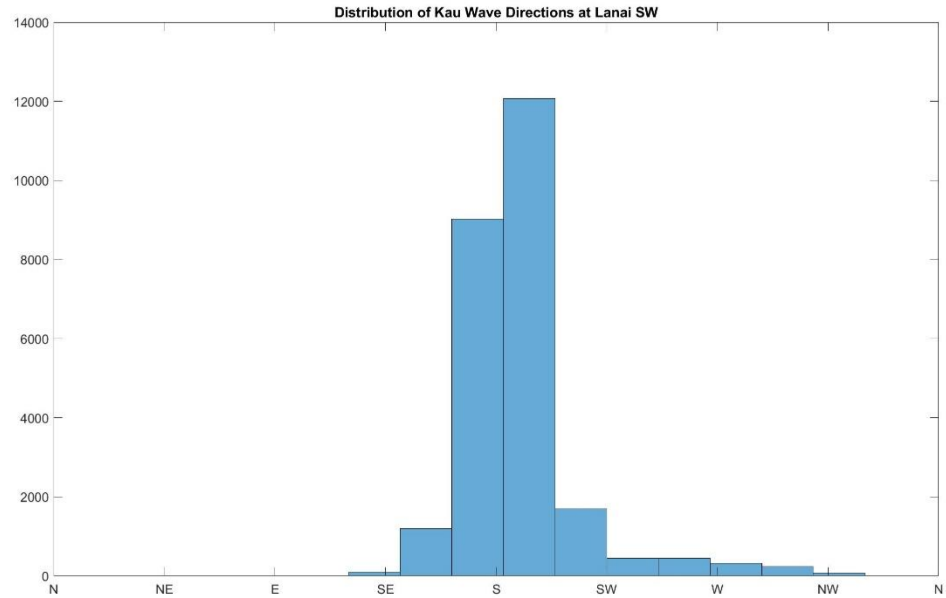

Figure 85: Histogram of wave direction vs. frequency (D_p) during Kau at Lanai waverider buoy 239

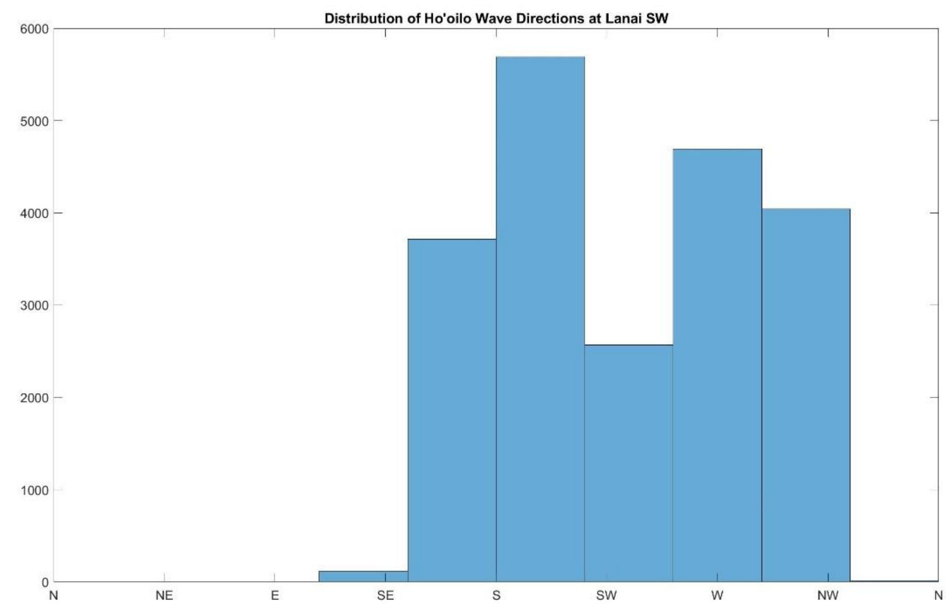

Figure 86: Histogram of wave direction vs. frequency (D_p) during Ho`oilo at Lanai waverider buoy 239

Waverider Buoy Data Summaries

The following section of this thesis will summarize all data parameters of total data collected for each of the nine wavebuoys.

Mokapu 098

Data collection at the Mokapu buoy began on August 9, 2000. Twenty-one years of data, between August 9, 2000, and July 17, 2021, are examined in this contribution.

Surface water temperature at the Mokapu location ranged from 22.20 to 30.20 °C, with a mean temperature of 25.46 °C (Table 2). Significant wave height ranged from 0.52 to 6.46 m, with a mean wave height of 1.90 m (Table 3). Peak wave period ranged from 3.57 to 25.00 s, with a mean period of 9.49 s (Table 4). Average wave period ranged from 3.87 to 15.37 s, with a mean period of 6.42 s (Table 5).

The highest recorded temperature of 30.20 °C, occurred on September 9, 2015 (Table 15). The highest recorded wave height of 6.46 m, occurred on December 14, 2001 (Table 16).

Monthly mean wave height shows that waves trended higher during Ho`oilo (between November and April), and lower during Kau (between May and October) (Figure 60). Mean wave height during Ho`oilo months was 2.08 m, and mean wave height during Kau months was 1.71m (Table 18).

The longest recorded average wave period recorded of 15.37 s, occurred on October 10, 2012 (Table 17).

Over the twenty-one years of measurements, peak wave direction ranged from 350 - 150^{o}, or from a northern to southeasterly direction (Figure 10). There was little seasonal difference in wave direction overall, ranging from the south-southeast to the northwest during both seasons. However, during Kau, the majority of waves occurred from the northeast to the east, and during Ho`oilo, the majority of waves had a slightly wider range, occurring from the north to the east (Figures 69 and 70).

Waimea 106

Data collection at the Waimea buoy began on December 16, 2001. Twenty years of data, between December 9, 2001, and September 18, 2021, are examined in this contribution.

Surface water temperature at the Waimea location ranged from 22.50 to 29.50 °C, with a mean temperature of 25.46 °C (Table 2). Significant wave height ranged from 0.29 to 9.09 m, with a mean wave height of 1.68 m (Table 3). Peak wave period ranged from 2.38 to 25.00 s, with a mean period of 10.78 s (Table 4). Average wave period ranged from 3.07 to 17.31 s, with a mean period of 7.10 s (Table 5).

The highest recorded temperature of 29.50 °C occurred on September 11, 2015 (Table 15). Highest recorded wave height of 9.09 m occurred on February 11, 2019 (Table 16).

Monthly mean wave height shows that waves trended higher during Ho`oilo (November to April), and lower during Kau (May to October) (Figure 61). Mean wave height during Ho`oilo months was 2.09 m, and mean wave height during Kau months was 1.27 m (Table 18).

The longest recorded average wave period of 17.31 s occurred on December 2, 2020 (Table 17).

Over the twenty years of measurements, peak wave direction ranged from 270 - 40^{o}, or from the west to northeasterly direction (Figure 15). There was little seasonal difference in wave direction overall, ranging from the northeast to the west-southwest during both seasons. However, during Kau, the majority of waves had a slightly wider range compared to Ho`oilo, with the majority of waves occurring from the northeast to the north (Figure 71). During Ho`oilo, the majority of waves occurred from the north to the northwest (Figure 72).

Pauwela 187

Data collection at the Pawela buoy began on December 3, 2011. Ten years of data, between December 3, 2011, and September 15, 2021, are examined in this contribution. Surface water temperature at the Pawela ranged from 22.50 to 30.20 °C,

with a mean temperature of 25.36 °C (Table 2). Significant wave height ranged from 0.57 to 7.73 m, with a mean wave height of 3.23 m (Table 3).
Peak wave period ranged from 3.23 to 25.00 s, with a mean period of 10.40 s (Table 4). Average wave period ranged from 3.74 to 16.30 s, with a mean period of 6.87 s (Table 5).

The highest recorded temperature of 30.20 °C occurred on September 10, 2015 (Table 15). Highest recorded wave height of 7.73 m occurred on February 11, 2019 (Table 16).

Monthly mean wave height shows that waves trended higher during Ho`oilo (November to April), and lower during Kau (May to October) (Figure 62). Mean wave height during Ho`oilo was 2.41 m, and mean wave height during Kau was 1.72 m (Table 18).

The longest recorded average wave period of 16.30 s occurred on February 25, 2015 (Table 17).

Over the ten years of measurements, peak wave direction ranged from 315 - 100^{o}, or from the northwest to easterly direction (Figure 20). There was little seasonal difference in wave direction overall, ranging from the east to the northwest during both seasons. However, during Kau, the majority of waves occurred from the northeast to the east, and during Ho`oilo, the majority of waves occurred from the northwest (Figures 73 and 74).

Hilo 188

Data collection at the Hilo location began on March 4, 2012. Nine years of data, between March 4, 2012 and April 24, 2021 are examined in this contribution.

Surface water temperature at the Hilo location ranged from 21.90 to 29.30 °C, with a mean temperature of 25.67 °C (Table 2). Significant wave height ranged from 0.31 to 6.88 m, with a mean wave height of 2.05 m (Table 3). Peak wave period ranged from 3.23 to 25.00 s, with a mean period of 10.01 s (Table 4). Average wave period ranged from 3.74 to 15.77 s, with a mean period of 7.17 s (Table 5).

The highest recorded temperature of 29.30 °C occurred on August 30, 2019 (Table 15). Highest recorded wave height of 6.88 m occurred on September 5, 2019 (Table 16).

Monthly mean wave height shows that waves trended higher during Ho`oilo (November to April), and lower during Kau (May to October) (Figure 63). Mean wave height during Ho`oilo months was 2.35 m, and mean wave height during Kau months was 1.78 m (Table 18).

The longest recorded average wave period of 15.66 s occurred on September 2, 2019 (Table 17).

Over the nine years of measurements, peak wave direction ranged from 325 - 120^{o}, or from the northwest to southeasterly direction (Figure 25). There was little seasonal difference in wave direction overall, ranging from the northwest to the southeast during both seasons. However, during Kau, the majority of waves occurred from the east, and during Ho`oilo, the majority of waves occurred from the east and the north-northwest (Figures 75 and 76).

Kaneohe 198

Data collection at the Kaneohe location began on October 26, 2012. Nine years of data, between October 26, 2012 and September 18, 2021 are examined in this contribution.

Surface water temperature at the Kaneohe location ranged from 22.30 to 29.50 °C, with a mean temperature of 25.51 °C (Table 2). Significant wave height ranged from 0.44 to 5.29 m, with a mean wave height of 1.72 m (Table 3). Peak wave period ranged from 3.57 to 22.22 s, with a mean period of 9.41 s (Table 4). Average wave period ranged from 3.57 to 12.97 s with a mean period of 6.46 s (Table 5).

The highest recorded temperature of 29.50 °C occurred on September 2, 2015 (Table 15). Highest recorded wave height occurred of 5.29 m mon January 22, 2017 (Table 16).

Monthly mean wave height shows that waves trended higher during Ho`oilo (November to April), and lower during Kau (May to October) (Figure 64). Mean wave height during Ho`oilo months was 1.93 m, and mean wave height during Kau months was 1.50 m (Table 18).

The longest recorded average wave period of 12.97 s occurred on November 11, 2019 (Table 17).

Over the nine years of measurements, peak wave direction ranged from 340 - 75^o, or from the north northwest to northeasterly direction (Figure 30). There was little seasonal difference in wave direction overall, ranging from the north to the east during both seasons. However, during Kau, the majority of waves occurred from the northeast, and during Ho`oilo, the majority of waves had a slightly wider range, occurring from the north to the northeast (Figures 77 and 78).

Hanalei 202

Data collection at the Hanalei location began on October 2, 2013. Eight years of data, between October 2, 2013 and September 18, 2021 are examined in this contribution.

Surface water temperature at the Hanalei location ranged from 22.60 to 30.50 °C, with a mean temperature of 25.57 °C (Table 2). Significant wave height ranged from 0.53 to 11.71 m, with a mean wave height of 2.14 (Table 3). Peak wave period ranged from 3.85 to 22.22 s, with a mean period of 10.84 s (Table 4). Average wave period ranged from 4.09 to 16.5 s, with a mean period of 7.30 s (Table 5).

The highest recorded temperature of 30.50 °C occurred on September 14, 2017 (Table 15). Highest recorded wave height of 11.71 m occurred on February 10, 2019 (Table 16).

Monthly mean wave height shows that waves trended higher during Ho`oilo (November to April), and lower during Kau (May to October) (Figure 62). Mean wave height during Ho`oilo months was 2.55 m, and mean wave height during Kau months was 1.64 m (Table 18).

The longest recorded average wave period of 16.50 s occurred on January 12, 2019 (Table 17).

Over the eight years of measurements, peak wave direction ranged from 270 - 90^o, or from the west to easterly direction (Figure 35). There was little seasonal difference in wave direction overall, ranging from the west to the east during both seasons. However, during Kau, the majority of waves occurred from the east to the northeast, and during Ho`oilo, the majority of waves occurred from the north to the northwest (Figure 79 and 80).

Pearl Harbor 233

Data collection at the Pearl Harbor location began on June 6, 2017. Four years of data, between June 6, 2017 and September 19, 2021 are examined in this contribution.

Surface water temperature at the Pearl Harbor location ranged from 22.5 °C to 29.30 °C, with a mean temperature of 26.16 °C (Table 2). Significant wave height ranged from 0.25 to 3.71 m, with a mean wave height of 0.85 m (Table 3). Peak wave period ranged from 2.06 to 22.22 s, with a mean period of 10.19 s (Table 4). Average wave period ranged from 2.55 to 12.54 s, with a mean period of 5.68 s (Table 5).

The highest recorded temperature of 29.30 °C occurred on September 27, 2019 (Table 15).Highest recorded wave height occurred of 3.71 m on December 25, 2019 (Table 16).

Monthly mean wave height shows no discernable seasonal variability, with a mean wave height of 0.85 m (Figure 63). Mean wave height during Ho`oilo months was 0.89 m, and mean wave height during Kau months was 0.82 m (Table 18).

The longest recorded average wave period of 12.54 s occurred on May 19, 2019 (Table 17).

Over the four years of measurements, peak wave direction ranged from 125 - 225^{o}, or from the southeast to southwesterly direction (Figure 40). There was a large difference in wave directions between the Kau and Ho`oilo seasons. During Kau, waves occurred from a wide range of directions, from the northwest to the southeast, with the majority of waves occurring from the northwest (Figure 81). During Ho`oilo, waves ranged from the east-southeast to the south, with the majority of waves occurring from the southeast (Figure 82).

Barber's Point 238

Data collection at the Barber's Point location began on May 31, 2018. Three years of data, between May 31, 2018 and September 19, 2021 are examined in this contribution.

Surface water temperature at the Barber's Point location ranged from 23.10 to 30.50 °C, with a mean temperature of 26.55 °C (Table 2). Significant wave height ranged from 0.50 to 6.45 m, with a mean wave height of 1.14 m (Table 3). Peak wave period ranged from 3.85 to 22.22 s, with a mean period of 12.96 (Table 4). Average wave period ranged from 0.01 to 18.14 s, with a mean period of 7.90 s (Table 5).

The highest recorded temperature of 30.50 °C occurred on September 15, 2019 (Table 15). Highest recorded wave height of 6.45 m occurred on February 11, 2019 (Table 16).

Monthly mean wave height shows that waves trended higher during Ho`oilo (November to April), and lower during Kau (May to October) (Figure 67). Mean wave height during Ho`oilo months was 1.93 m, and mean wave height during Kau months was 1.50 m (Table 18).

The longest recorded average wave period of 18.14 occurred on December 2, 2020 (Table 17).

Over the three years of measurements, peak wave direction ranged from 160 - 320^{o}, or from the southeast to northwesterly direction (Figure 45). There was little seasonal difference in wave direction overall, ranging from the southeast to the northwest during both seasons. However, during Kau, the majority of waves occurred from the south, and during Ho`oilo, the majority of waves occurred from the northwest (Figures 83 and 84).

Lanai Southwest 239

Data collection at the Lanai southwest location began on June 21, 2018. Three years of data, between June 21, 2018 and July 27, 2021 are examined in this contribution.

Surface water temperature at the Lanai southwest location ranged from 23.50 to 30.50 °C, with a mean temperature of 26.72 °C (Table 2). Significant wave height ranged from 0.42 to 4.7 m, with a mean wave height of 0.99 m (Table 3). Peak wave period ranged from 3.12 to 22.22 s, with a mean period of 13.05 s (Table 4). Average wave period ranged from 0 to 14.68 s, with a mean period of 6.96 s (Table 5).

The highest recorded temperature of 30.50 °C occurred on September 3, 2019 (Table 15). Highest recorded wave height of 4.70 m occurred on February 11, 2019 (Table 16).

Monthly mean wave height shows no discernable seasonal variability, with a mean wave height of 0.98 m (Figure 65). Mean wave height during Ho`oilo months was .097 m, and mean wave height during Kau months was 0.99 m (Table 18).

The longest recorded average wave period of 14.68 s occurred on May 13, 2019 (Table 17).

Over the three years of measurements, peak wave direction ranged from 160 - 315^{o}, or from the southeast to northwesterly direction (Figure 50). There was little seasonal difference in wave direction overall, ranging from the southeast to the northwest during both seasons. However, during Kau, the majority of waves occurred from the south, and during Ho`oilo, the majority of the waves were more evenly distributed from the south to the northwest (Figures 85 and 86).

Temperature

The two buoys with the largest amount of data collected (Mokapu and Waimea) recorded similar trends in sea surface temperature (Figure 6, Figure 11). Yearly average temperatures first trended higher from 2001 to 2004/2006 (Figures 51 and 52). Yearly average temperatures then trended lower until 2012, where both buoys recorded the lowest yearly average temperature. The average yearly temperature at Mokapu in 2012 was 24.56 °C (Table 6), and the average yearly temperature at Waimea in 2012 was 24.70 °C (Table 7). first trended higher from 2000 - 2004. Temperatures then trended lower from 2004 - 2012.

The Mokapu, Waimea, Pauwela, Hilo, and Kaneohe buoys all record an upward trend in average yearly sea surface temperature between approximately 2011 - 2015 (Figures 48 – 55).

The Mokapu, Waimea, Pauwela, and Kaneohe buoys all recorded a maximum sea surface temperature within the first two weeks of September of 2015 (Table 15). It is interesting to note that all of these buoys are located on the north shores of their respective islands of O’ahu and Maui (Figure 4) The Hilo, Pearl Harbor, Barber’s Point, and Lanai buoys all recorded a maximum sea surface temperature between late August and September of 2019, although these buoys do not show elevated temperatures for the entire year of 2015 (Table 15).

Significant Wave Height

The Waimea, Pauwela, Kaneohe, Hanalei, Pearl Harbor, Barber's Point, and Lanai buoys all recorded a maximum wave height in 2019 (Table 16). The Waimea, Pauwela, Barber's Point, and Lanai buoys all recorded their maximum wave height on February 11, 2019 (Table 16).

The Mokapu and Hilo buoys had slightly higher average wave height during La Niña than El Niño (Table 19).

The Waimea, Pauwela, Kaneohe, Hanalei, Pearl Harbor, Barber's Point, and Lanai buoys had slightly higher average wave height during El Niño than La Niña (Table 19).

Peak Wave Direction

The north shore wavebuoys (Mokapu, Waimea, Pauwela, Hilo, Kaneohe, and Hanalei) had waves incoming from similar directions all year. However, these buoys did show a seasonal shift of direction for the majority of waves, occurring more frequently from the north and the northeast during the Kau as opposed to Ho`oilo (Figures 69 – 80).

The south shore wavebuoys (Pearl Harbor, Barber's Point, and Lanai Southwest) show a large difference in wave directions between the Kau and Ho`oilo seasons (Figures 81 – 86). At the Pearl Harbor buoy during Kau, waves occurred from a wide range of directions, from the northwest to the southeast, with the majority of waves occurring from the northwest (Figure 81). During Ho`oilo, waves ranged from the east-southeast to the south, with the majority of waves occurring from the southeast (Figure 82). The Barber's point buoy had waves incoming from similar directions all year, however showed waves occurring more frequently from the south during Kau, and occurring more frequently from the northwest during Hoʻoilo (Figures 83 and 84). The Lanai Southwest buoy had waves incoming from similar directions all year, however showed waves occurring more frequently from the south southwest during Kau than during Hoʻoilo (Figures 85 and 86).

Wave Period

The Hilo, Kaneohe, Hanalei, Pearl Harbor, and Lanai buoys all recorded a maximum recorded average wave period in 2019, although these dates do not correspond with the maximum recorded wave height for their respective buoys (Table 17).

DISCUSSION

Temperature

The Mokapu, Waimea, Pauwela, and Kaneohe buoys (all of which are deployed on the northern side of their respective islands (O'ahu and Maui) [Figure 3]) recorded a maximum sea surface temperature within the first two weeks of September of 2015. There are two potential related causes for elevated temperature readings across multiple wavebuoy stations. The first potential cause is that these trends in sea surface temperature coincide with the El Niño event of 2015-2016.

The 2015-2016 El Niño can be best understood by looking at sea surface temperatures (SSTs) at the NINO 3.4 index. NINO 3.4 is a region in the central equatorial Pacific (coordinates 5N-5S, 170W-120W) in between the NINO 3 and 4 indices, respectively, commonly used as a measure of the overall strength of an El Niño–Southern Oscillation (ENSO) event (Figure 87). The NINO 3.4 index uses a 5-month running mean, and ENSO events are defined when SSTs in the region exceed +/-0.4°C of the regional mean for a period of six months or longer (Shea 2018). The 2015-2016 El Niño broke SST warming records in the central Pacific, indicated by the NINO 3.4 index. At its peak in November 2015, the NINO 3.4 SST anomaly reached 3.0°C, breaking the previous record of 2.8°C set in January of 1983 (Stockdale et al. 2017).

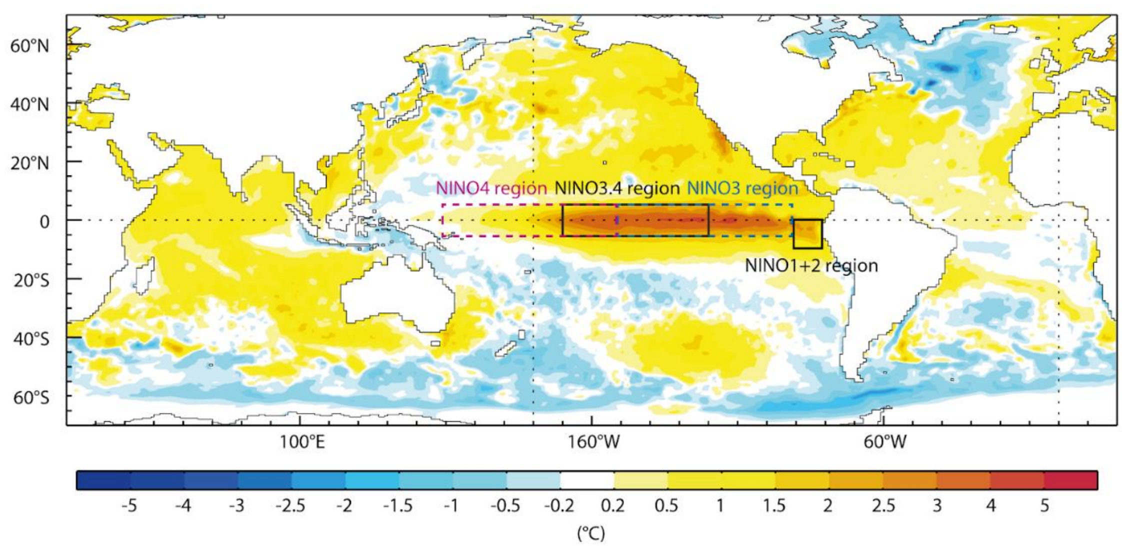

Figure 87: Map showing the Niño 1, 2, 3, 4, and 3.4 regions (figure from Stockdale et al. 2017)

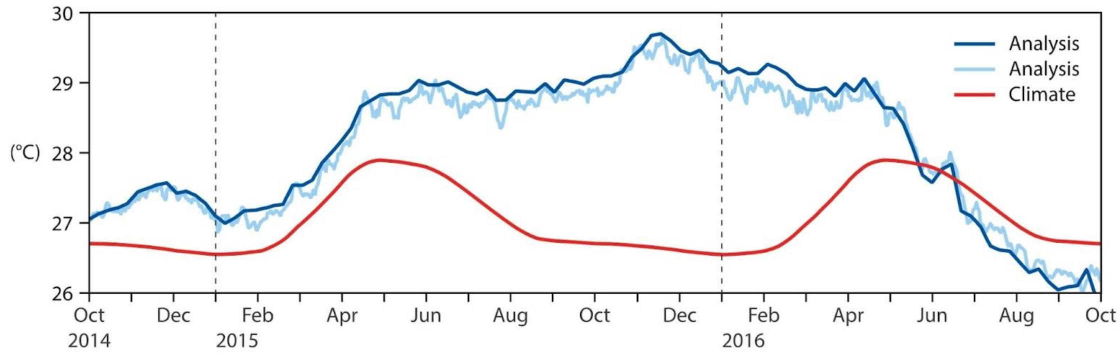

Figure 88: Time evolution of observed SSTs from October 2014 to October 2016 using two different analyses (blue lines). The SST NINO 3.4 mean seasonal cycle is represented by the red line. The difference between the red and blue lines is the SST anomaly (figure from Stockdale et al. 2017)

The second potential cause of the wavebuoys' elevated temperatures is a phenomenon called a marine heat wave (MHW). 2015 was known to have multiple MHWs, which have been defined as a period of at least six consecutive days with SSTs exceeding the 90th percentile of the local long-term climatology. While it cannot be determined that there is a singular cause for MHWs, be it global climate change or an ENSO event, according to a report by Hoboday et al. (2018), increased average temperatures do increase the likelihood of MHW events to occur. Therefore the multiple MHWs that occurred in 2015 are likely associated with the 2015-2016 El Niño.

In seeking to more accurately define and categorize MHWs, a report was done of ten commonly known MHWs across all seasons, four of which occurred between 2015-2016, based on data from the NOAA High-Resolution SST report (OISST V2) (Hoboday et al. 2018). MHWs were broken into four categories: Category I, or moderate, classified by SSTs 1-2 times above the climatological 90th percentile of historical regional temperatures. Category II, or strong, classified by SSTs 2-3 times above the climatological 90th percentile. Category III, or severe, classified by SSTs 3-4 times above the climatological 90th percentile. Category IV, or extreme, classified by SSTs greater than 4 times above the climatological 90th percentile (Hoboday et al 2018).

The most notable MHW that occurred during 2015 was the northeast Pacific Heatwave, more commonly known as "The Blob", ranked as a Category III, or severe, heatwave at its peak (Hoboday et al. 2018). This MHW is notable not only due to its severity but also the extent of time that it lasted: 711 days (Hoboday et al. 2018). The biological impacts of the Blob are still being studied, this MHW led to a reduction in phytoplankton availability and facilitated changes in zooplankton and marine invertebrate populations along the North American west coast (Cavole et al. 2016).

It should also be noted that surface air temperature in Hawaiʻi was ~1.5°C higher than the climatological mean from July to October 2015 (Zhu, Li 2017). Using a definition reported by Fischer and Schär (2010) where a heatwave is defined as a period of at least six consecutive days with maximum temperatures exceeding the local 90th percentile of the control period (1961-1990), in a report by Zhu and Li (2017) it was found that there were 98 exceptional local heatwave days occurring within that same period of time. 2015 was the hottest summer in Hawaiʻi since records began in 1948, both in absolute temperature and in the number of heatwave days.

The Hilo, Pearl Harbor, Barber's Point, and Lanai southwest buoys all recorded a maximum sea surface temperature between late August and September of 2019 (Table 15). This does not appear to correlate with any significant ENSO event, as the NINO 3.4 SSTs did not exceed anomalies greater than 0.4°C higher than the regional mean within these months (NOAA).

Wave Height

The Waimea, Pauwela, Barber's Point, and Lanai buoys all recorded a maximum wave height on February 11, 2019 (Table 16). This can be attributed to a large weather system that affected areas from northwest America all the way to the Hawaiian Islands (Erdman 2019). The National Weather Service reported 18 m waves north of Kauai and Oahu at the height of the storm, with significant wave heights reaching 12 m, along with wind gusts of up to 110 kph in some areas. The storm system was believed to be caused by a shift in the jet stream across the central and eastern Pacific Ocean (Di Liberto 2019).

The Mokapu, Waimea, Pauwela, Hilo, Kaneohe, and Hanalei buoys are all deployed on the northern side of their respective islands (O'ahu, Maui, Kauai, and

Hawai‘i) (Figure 4). Waves on the north-facing shores of islands in Hawai‘i are known to be very large during the winter months of Ho`oilo, particularly in December and January, as a result of Northern Pacific winter storms generating large ocean swells that move south toward the Hawaiian Islands, breaking on north-facing shores (Fletcher et al. 2007) (Figures 60 – 65, Table 18).

Over the entire data collection period, Hanalei, Kauai had the largest average wave height during the Ho`oilo seasons (Table 18). The Hanalei buoy also had the largest range of all wave heights recorded (Table 3).

The Lanai, Barber’s Point, and Pearl Harbor buoys are deployed on the south and southwestern coasts of their respective islands (O’ahu and Lanai) (Figure 4). While it was expected that the data from these buoys would show higher average waves during Kau, that was not necessarily reflected in the respective graphs and tables (Figures 66 – 68, Table 18). Waves approaching from the south are known to be larger during the summer months of Kau, particularly in July and August, as a result of Southern Hemisphere winter storms generating large swells that move northwest toward the Hawai`ian Islands, breaking on south and southeast-facing shores (Fletcher et al. 2007). However, the Barber’s Point buoy recorded slightly higher average monthly wave heights during Ho`oilo than during Kau, and the average seasonal wave height was 0.15 m higher during Ho`oilo than during Kau (Figure 67, Table 18).

The average seasonal wave heights were slightly higher during Kau than during Ho‘oilo at the Lanai and Pearl Harbor buoys, with Pearl Harbor showing a difference of 0.07 m, and Lanai showing a difference of 0.02, respectively (Figures 66 and 68, Table 18).

It is important to note that the Pearl Harbor buoy is deployed at the entrance to the Pearl Harbor channel, at a distance from shore of approximately 2 kilometers. This location is at such a depth that the data shown does not necessarily represent the actual wave activity of the southern shores of O’ahu (Figure 4). When looking at wave height (total and monthly) and wave direction data (Figures 39, 66, and 40), there is little to no variation in data at the Pearl Harbor buoy compared to all other buoy locations in Hawai‘i. It is likely that this buoy is located close enough to shore that Higher amplitude swell has already broken offshore and the remaining short period, low amplitude waves are being steered by the channel.

There was a distinctive difference in seasonal wave direction at Pearl Harbor compared to all other buoys. During the Ho`oilo, waves at the Pearl Harbor buoy occurred almost exclusively from the southeast, but during Kau, waves occurred from the southeast to the northwest, but primarily from the northwest (Figures 81 and 82). It is possible that due to the increased southern swell during the summer months of Kau, that the waves are refracting back from the sides of the Pearl Harbor channel.

The Lanai Southwest buoy, which shows very little variability in total and seasonal wave height, may also be due to its location relative to the island. While it is apparent that waves during Kau are more concentrated from a southern direction compared to during Ho`oilo (Figures 85 and 86), it is possible that summer southern swell is weakened by the time the waves reach the Lanai buoy.

CONCLUSIONS

Global climate change has and will continue to cause sea level rise and increase the severity of events such as storms resulting in larger waves in the Pacific. Understanding waves and how they behave on a regional scale is highly valuable to the people of Hawai‘i looking to understand how future climate events will impact their shorelines, and communities living on them, in the future.

Data from the PacIOOS wavebuoys are useful in informing the public in real time about wave conditions, whether it be for safety or for recreational purposes. Moreover, these data are critical for those looking to understand how waves have looked around the Hawaiian Islands in the past, and how they might change in the future.

PacIOOS wavebuoys may also serve a purpose in augmenting existing global-scale satellite ocean data. The NOAA Coral Reef Watch Satellites (CRW1) are an excellent example. The CRW satellites monitor ocean temperatures globally using remote sensing to predict mass coral bleaching events (NOAA 2021). However, the accuracy of these satellite temperature readings is unreliable along coastlines of land masses. The nearshore temperature data from the PacIOOS wavebuoys can provide data with a higher level of accuracy than CRW satellite data is able to along nearshore ocean regions.

It can be argued that some buoys, particularly the Pearl Harbor and Lanai Southwest buoys, are currently not at optimal locations to accurately record waves and their behavior at their respective shores. PacIOOS could benefit from either moving the buoys to a more optimal location, or adding more buoys along southern shores of multiple islands to increase the scale of information being cataloged at southern Hawaiian shores.

The analysis shows that the data collected by PacIOOS wavebuoys to date can reflect significant climate events and storms. Continuing to observe and catalog these data will allow us to predict future wave activity in various climate and storm events, and allow the public to be informed on how waves will impact their daily activities. Ultimately, the value of these data will only increase with time as more data are collected and more patterns emerge.

LIST OF REFRENCES

Cavole, L. M., Demko, A. M., Diner, R. E., Giddings, A., Koester, I., Pagniello, C. M. L. S., Paulsen, M.-L., Ramirez-Valdez, A., Schwenck, S. M., Yen, N. K., Zill, M. E., & Franks, P. J. S. (2016). Biological Impacts of the 2013–2015 Warm-Water Anomaly in the Northeast Pacific: Winners, Losers, and the Future. *Oceanography*, *29*(2), 273–285.

Datawell BV oceanographic instruments. (2009). *Datawell Waverider Reference Manual WR-SG DWR-MkIII DWR-G*.

Dennis Shea (September 2018) Climate Data NINO SST INDICES (NINO 1+2, 3, 3.4, 4; ONI AND TNI) (accessed 22 September 2021)

Erdman, Jonathan. (2019, February 14). Hawaii Storm Might Have Set the State's All-Time Record Low; Snow Fell on Maui, Too. *The Weather Channel.*

Fletcher, C. H., Dunn, R. A., & Frazer, L. N. (2007). The Predictive Accuracy of Shoreline Change Rate Methods and Alongshore Beach Variation on Maui, Hawai‘i. Journal of Coastal Research, 231, 87–105. https://doi.org/10.2112/05-0521.1

Fletcher, C., Rooney, J., Barbee, M., Lim, S.-C., & Richmond, B. (2003). Mapping Shoreline Change Using Digital Orthophotogrammetry on Maui, Hawai‘i. Journal of Coastal Research, 106–124.

Herring, S. C., Hoell, A., Hoerling, M. P., Kossin, J. P., Schreck, C. J., & Stott, P. A. (2016). EXPLAINING EXTREME EVENTS OF 2015 FROM A CLIMATE PERSPECTIVE. *Bulletin of the American Meteorological Society*, *97*(12), Si-S145.

Hobday, A. J., Oliver, E. C. J., Gupta, A. S., Benthuysen, J. A., Burrows, M. T., Donat, M. G., Holbrook, N. J., Moore, P. J., Thomsen, M. S., Wernberg, T., & Smale, D. A. (2018). Categorizing and Naming MARINE HEATWAVES. *Oceanography, 31*(2), 162–173.

Jason K. Levy. (2009). Managing the Catastrophic Impacts of Sea Level Rise in Hawaii. Water Resources IMPACT, 11(1), 18–22.

NOAA (2001) NOAA’s Climate Prediction Center (accessed 22 September 2021)

NOAA (2021) NOAA Satellite and Information Service Coral Reef Watch (accessed 12 November 2021)

Tim Stockdale, Magdalena Balmaseda, Laura Ferranti (April 2017) The 2015/2016 El Niño and beyond (accessed 22 September 2021)

Tom Di Liberto (2019) Wild weather on the West Coast in February 2019. NOAA Climate.gov

Zhu, Z., & Li, T. (2017). The Record-Breaking Hot Summer in 2015 over Hawai‘i and Its Physical Causes. *Journal of Climate*, *30*(11), 4253–4266.